Study Program for
Canadian Domestic Communications Satellite

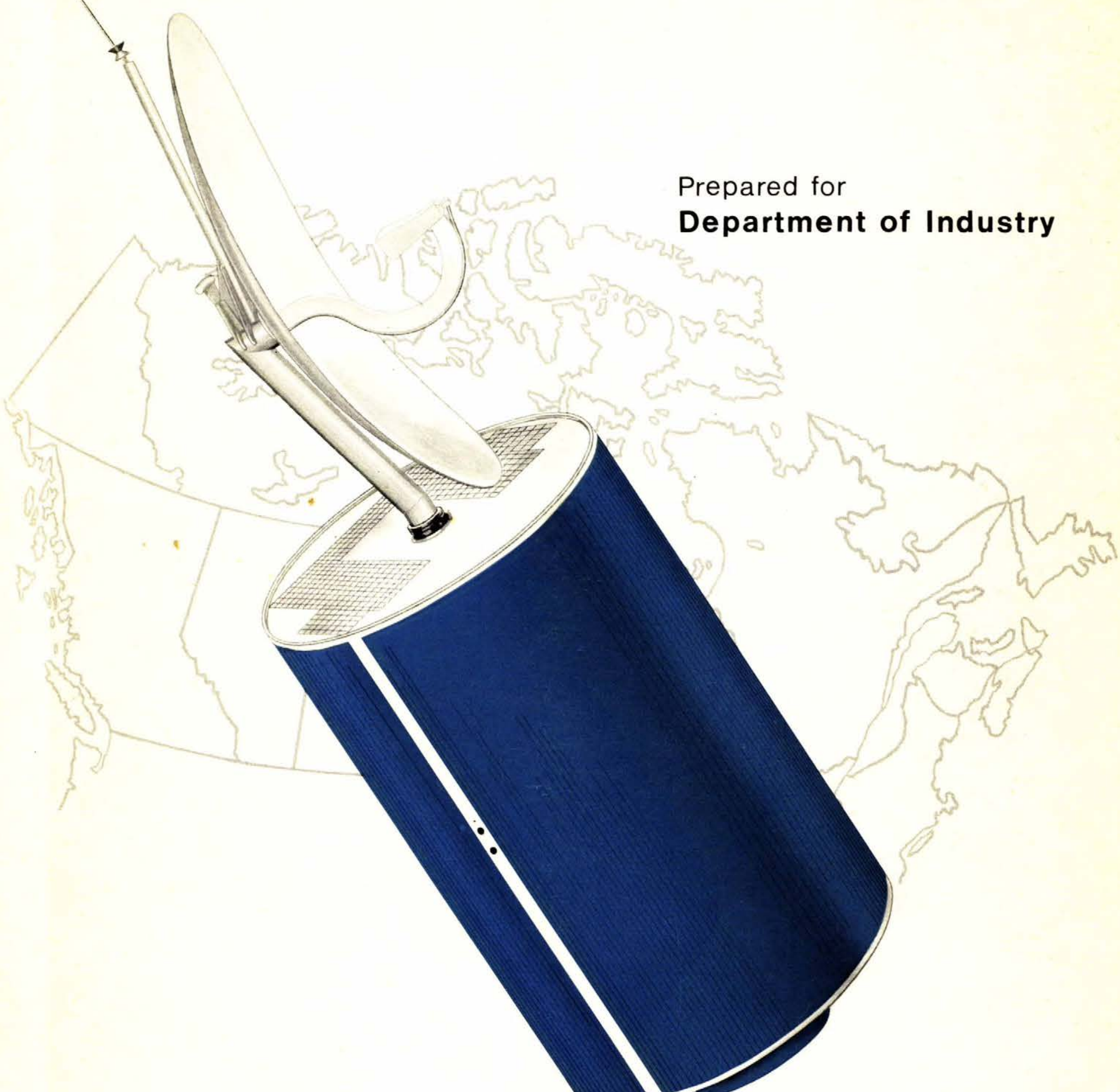

Prepared for
Department of Industry

Final Report
Volume Two - Part Two-Spacecraft Design-
Mechanical & Support

RCA Space Systems

Copy No. 48

STUDY PROGRAM

for the

DESIGN, DEVELOPMENT AND SUPPLY

of a

DOMESTIC SATELLITE COMMUNICATIONS SYSTEM

FINAL REPORT
VOLUME 2b, SPACECRAFT DESIGN, MECHANICAL

Prepared for

DEPARTMENT OF INDUSTRY

by

RCA LIMITED, Space Systems
1001 Lenoir Street, Montreal

PROPOSITION No. 2220-1

NOVEMBER 25th, 1968

PREFACE

This report is submitted by RCA Limited to the Department of Industry in compliance with Section 4.2 of the Statement of Work forming part of D.O.I. Contract, File No. IRA. 9122-03-4.

The report is in six volumes, namely:

Volume 1	Design Considerations
Volume 2(a)	Spacecraft Design - Electrical
Volume 2(b)	Spacecraft Design - Mechanical
Volume 3	Technical Appendices
Volume 4	Program Plan
Volume 5	Program Costs

The information contained in the report is supplied to Her Majesty for use solely in connection with the design, development, manufacture, operation, repair, maintenance and testing of a Canadian Domestic Satellite Communication System.

II 9:

APOGEE MOTOR

9. APOGEE MOTOR SUBSYSTEM

The apogee motor is used to provide the velocity increment necessary to inject the satellite into a circular, equatorial orbit at the apogee of the transfer ellipse. It is fired by ground command at the optimum time in the mission sequence so that the satellite will achieve the desired drift orbit. Figure 9-1 presents a preliminary summary specification for the apogee motor requirements.

9.1 DESCRIPTION OF MOTOR

The Thiokol Chemical Corp. has been tentatively selected as the apogee motor supplier. Figure 9-2 shows the design concept of the motor, which will be developed to provide optimum physical and performance characteristics.

9.1.1 Physical Characteristics

The motor consists of a spherical case, a high expansion ratio contoured nozzle, a high-energy polybutadiene propellant, and a space-qualified Pyrogen igniter and safe-arm device.

9.1.1.1 Case and Nozzle Assembly

The motor case material is 6Al-4V titanium. Provisions are included for mounting the igniter and safe-arm device to an adapter on the head end and installation of the nozzle assembly to an aluminum closure at the aft end of the motor. Gengard type V-44 rubber insulation is provided internally to prevent excessive case temperatures during motor firing and heat soak-back conditions. The motor case is designed for a factor of safety of 1.25, with a maximum expected operating pressure (MEOP) of 466 psia.

The nozzle assembly is a high expansion ratio (48:1), contoured, composite carbon, plastic and titanium structure. The nominal weight of the nozzle assembly is 14 pounds, and the overall length is 22.1 inches of which 20.7 inches are external to the rocket motor chamber. The nozzle uses a "Graph-I-Tite G-90" carbon-throat insert, a graphite cloth phenolic throat backup structure, a 6-Al-4V titanium attachment ring and a carbon cloth phenolic rosette exit cone. The aft titanium closure-to-exit cone joint is secured with a glass filament phenolic overwrap. An integral, graphite roving phenolic ring is provided at the nozzle exit plane as a rounding hoop and protector for the aft edge of the carbon cloth phenolic rosette exit cone.

FIGURE 9 - 1 SUMMARY SPECIFICATION APOGEE MOTOR

FUNCTION:

Provides the satellite with a velocity increment necessary to achieve a circular, equatorial orbit at the apogee of the transfer ellipse.

PERFORMANCE AND OPERATIONAL REQUIREMENTS:

Total impulse: Nominal vacuum total impulse is to be such that a velocity increment of 6040 ft/sec $\pm$1% is imparted to the satellite.

Thrust level: Maximum instantaneous thrust not to exceed a value which would impose a 10 g acceleration load on the satellite.

Satellite nominal spin speed:

Firing temperature range: +30 to +90°F

Storability: Capability for three years storage in any attitude while exposed to temperatures of +20 to +120°F at a relative humidity of not greater than 65%.

MOTOR PERFORMANCE: *

Temperature (°F)	+30	+70	+90
Maximum thrust (lb.):	3680	3860	3960
Maximum chamber pressure (psia):	-34	-55	-66
Maximum Total Impulse (lb - sec.):	140,070	140,326	140,487
Specific Impulse (sec.):	294.9	295.5	295.8
Burn time (sec.):	43.0	41.0	40.0

PHYSICAL CHARACTERISTICS: *

Propellant type: TP - 4 - 3135

Configuration: Spherical case with unsubmerged nozzle

Case material: Titanium

Nozzle:

Exit cone material: Plastic

Throat material: Graphite

Exit cone area: 230 in^2

Throat area: 5.89 in^2

Expansion ratio: 48

Weight:

Total motor:	502.95 lb.
Inert:	50.65 lb.
Propellant:	452.3 lb.
Burn-out:	49.10 lb.
Mass Fraction:	.900

Overall length: 50.80 in.

Case diameter: 24.79 in.

Ignition system: Pyrogen igniter with redundant squibs, electro-mechanical safe and arm device qualified for TE-M-364 motor.

*Motor performance and physical characteristics based on Thiokol revised proposal EP333A-68, dated 9/23/68

RELIABILITY:

________________ to survive launch and meet all performance requirements while subject of a space environment.

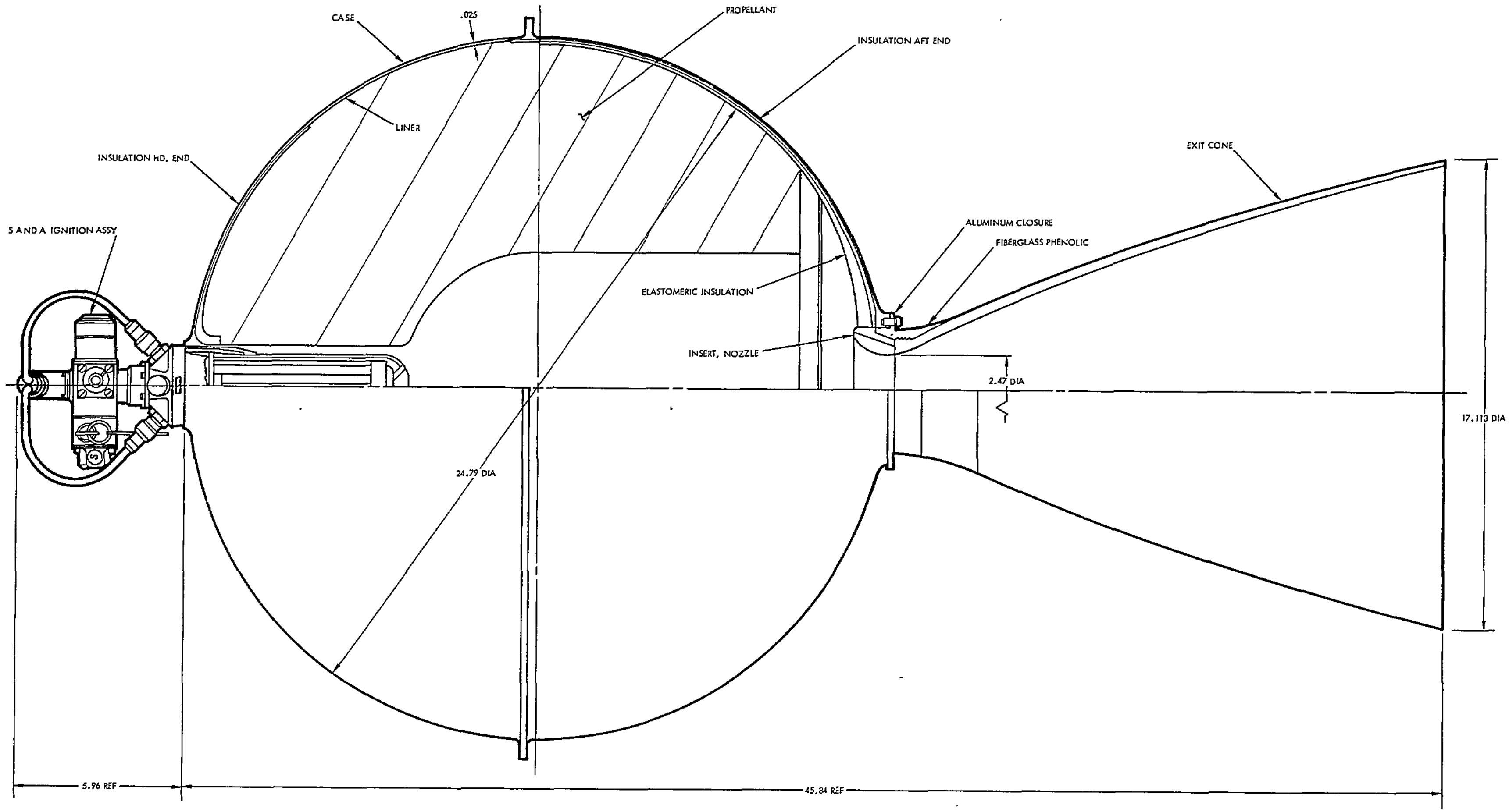

Figure 9–2 Thiokol Chemical Corporation Apogee Motor Design. Mod. 6, Concept C.

9.1.1.2 Propellant and Grain Configuration

The propellant selected by Thiokol is designated TP-H-3135, an 88% total solids carboxy-terminated polybutadiene propellant which contains 16% aluminum, 72% ammonium perchlorate and 12% HC polymer-curing agent. The chemical and mechanical properties of this propellant are well formulated, and are derived from propellants of similar composition with an extensive history of space applications. The following is a summary of the measured ballistic properties of the TP-H-3135 propellant:

Specific Impulse* (lbf-sec/lbm)	296.0
Density (lbm/in.^{3})	0.0641
Characteristic Velocity (ft/sec)	5150
Burn Rate Equation (60°F)	$0.226(P/500)^{0.306}$
π_k (%/°F from +10%)	0.09

The grain configuration is a scaled-down version of the existing Thiokol TE-M-364 motor grain, which was used for the Surveyor Retro program.

9.1.1.3 Ignition System

The space-proven Delta and Surveyor TE-P-358 Pyrogen igniter and safe-arm unit assures reliable, reproductive motor ignition characteristics in a hard vacuum environment. The aluminum Pyrogen case contains a propellant (TP-H-3062) cartridge which supplies the heat and pressure required for ignition. A pyrotechnic charge of boron potassium nitrate pellets, which can be ignited by one or both of two electric squibs,is used to ignite the Pyrogen propellent. The aluminum Pyrogen case is insulated externally to prevent its being consumed during motor operation.

The electromechanical S/A device consists of a dc torque motor that moves a mechanical shutter and an electrical switch to provide the SAFE feature. When the device is in the SAFE position, accidental squib ignition will not ignite any other part of the ignition train or the rocket motor. This device has been fully qualified and flight tested from both the Eastern and Western Test Ranges. The S/A device is composed of an upper assembly containing the electromechanical drive train and switch gear, and the lower housing assembly which contains the blocking rotor, squib, ignition train, and mounting flange. Nominal operating voltage is 27 volts dc, which serves to operate the device successfully at temperatures as low as -175°F and as high as +200°F at pressures as low as 10 microns. The electric squibs, which are mounted in the S/A device, are designed to positively prevent ignition of the motor in the event one (or both) of the squibs is accidentally ignited. These squibs (Hi-Shear PC-37) have a minimum 1-ampere, 1-watt, no-fire capability. Normal firing current is 5 amperes per squib which is applied for 25 milliseconds to ensure ignition.

*Reference conditions are P_c=500 psia, vacuum, 50:1 expansion ratio

9.1.2 Motor Performance

The Thiokol motor provides a +3 sigma maximum total impulse capability of 140,326 lb-sec at a firing temperature of +70°F. Thiokol has indicated that, because of their capability to accurately control the total propellant weight for each motor, the total impulse reproducibility will be not greater that + 1%. Also, the +3 sigma maximum thrust level (3960 lb at + 90°F) is such that an axial acceleration not exceeding 6g's will be imparted to the satellite during motor burn. Figures 9-3, 9-4 and 9-5 show the variation of thrust, chamber pressure and acceleration with burn time for the motor.

9.2 DESIGN, PERFORMANCE AND OPERATIONAL CONSIDERATIONS

It is important that careful consideration be given to all physical performance and operational factors which could affect the ability of the motor to reliably perform its intended function. Recognition and resolution of potential problems during the contract negotiation and early design and development phases of the program will provide assurance of meeting program goals consistent with schedule and economic limitations. Some of these considerations for the apogee motor program are indicated in the following paragraphs.

9.2.1 Physical Considerations

Interfaces. Mechanical, electrical and thermal interfaces of the motor with the satellite require firm definition. One area of particular concern is the attachment surface design to permit installation and alignment of the motor, and to ensure structural integrity when exposed to the vibration and acceleration load environment imposed by the boost vehicle.

Structural Integrity. The motor must be designed to assure the structural integrity of the case and nozzle during and after firing. Separation of parts or pieces from the motor, burn-through or rupture of the case, nozzle or seals, or boil-off of condensibles resulting from exposure of plastic materials to excessive temperatures are examples of structural failures. Also, it is important that the distribution and thickness of internal insulation be adequate to protect the motor case from excessive temperatures during post-fire soakback. Other design features should be carefully examined during Design Reviews and verified by a comprehensive motor development test program.

Mass Properties. The motor total weight should be a minimum consistent with the launch vehicle capability and motor structural integrity characteristics. Also, minimum burnout weight is desired, to minimize the quantity of hydrazine required for stationkeeping manuevers.

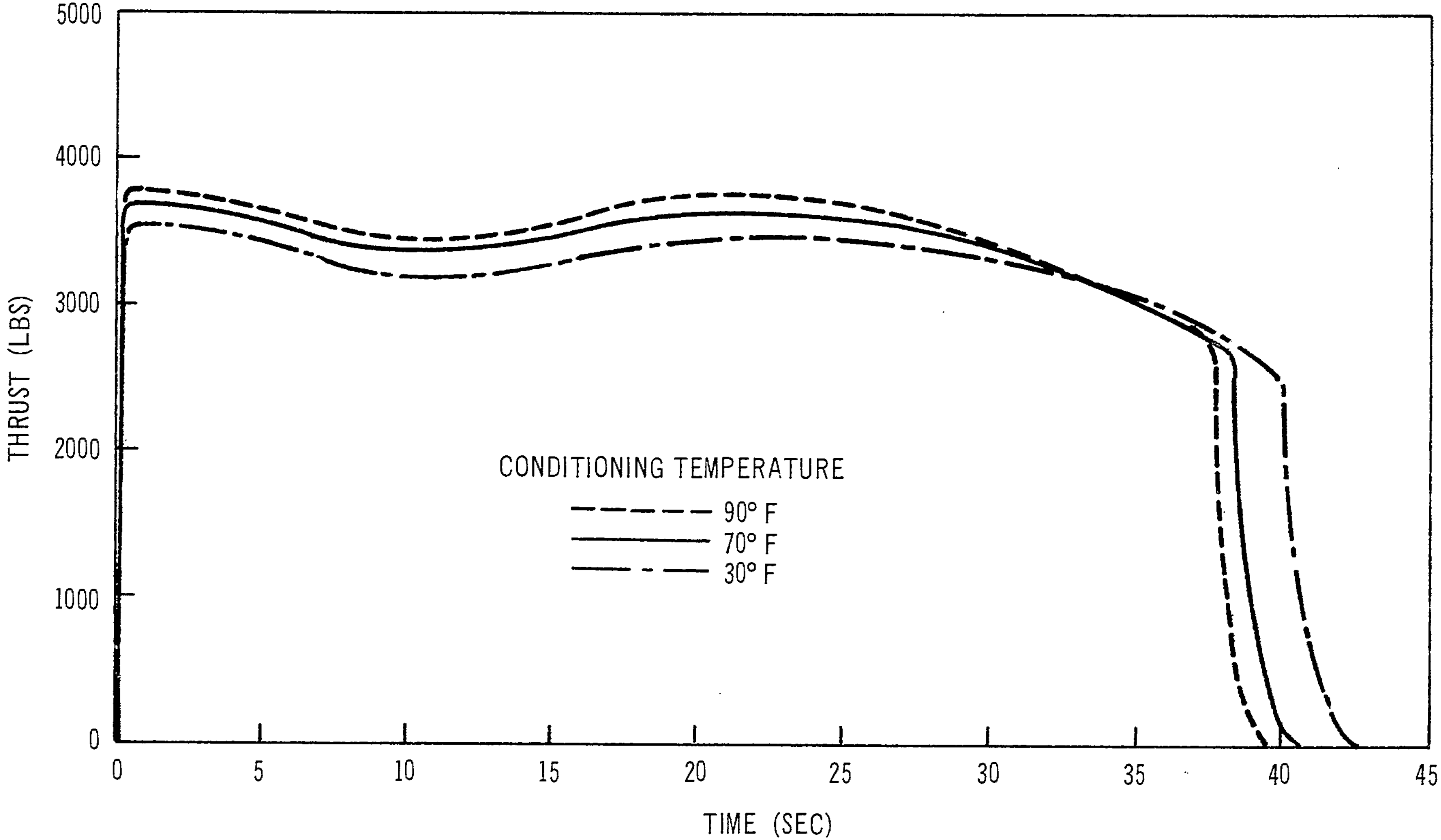

Figure 9–3 Thrust versus Time

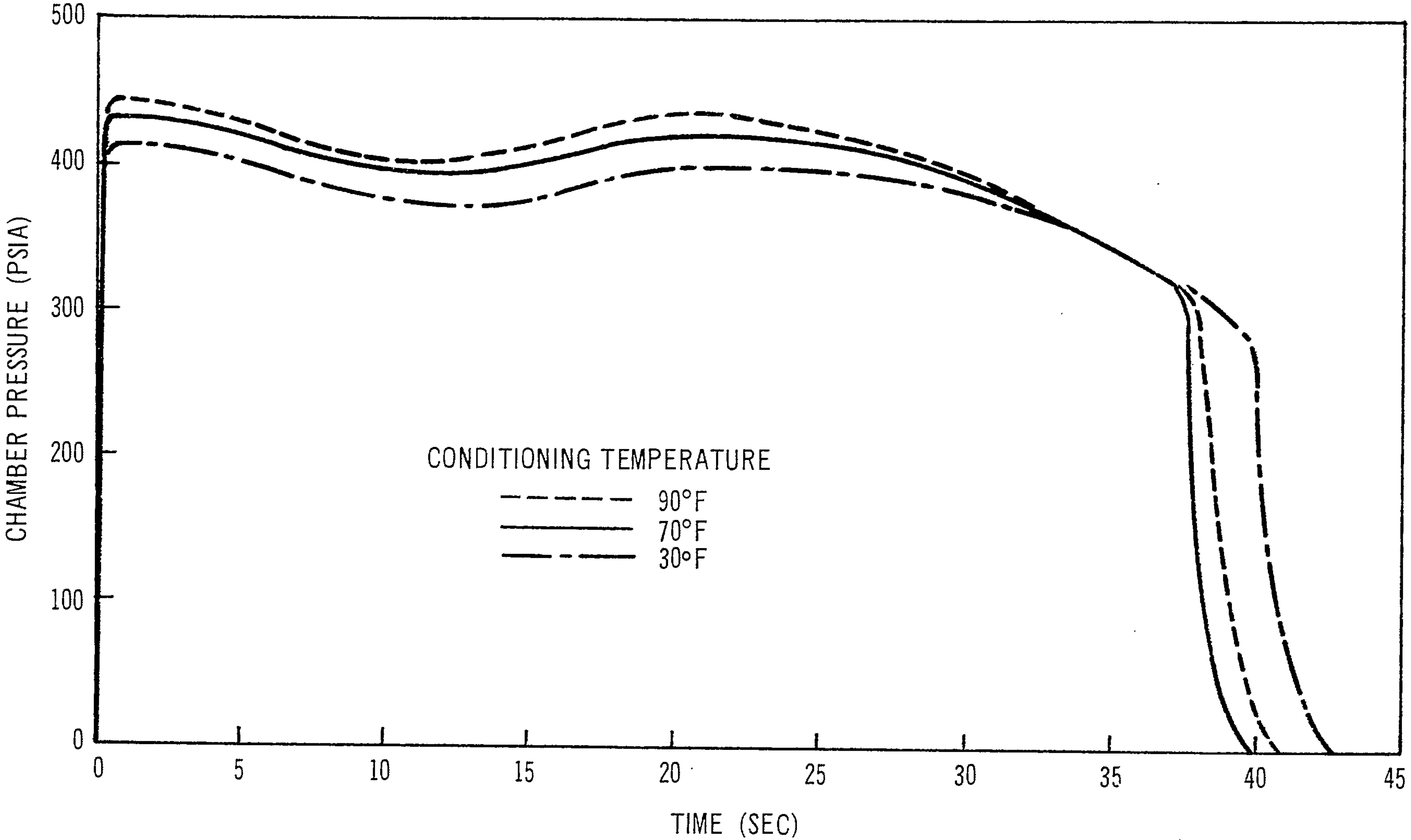

Figure 9–4 Chamber Pressure versus Time

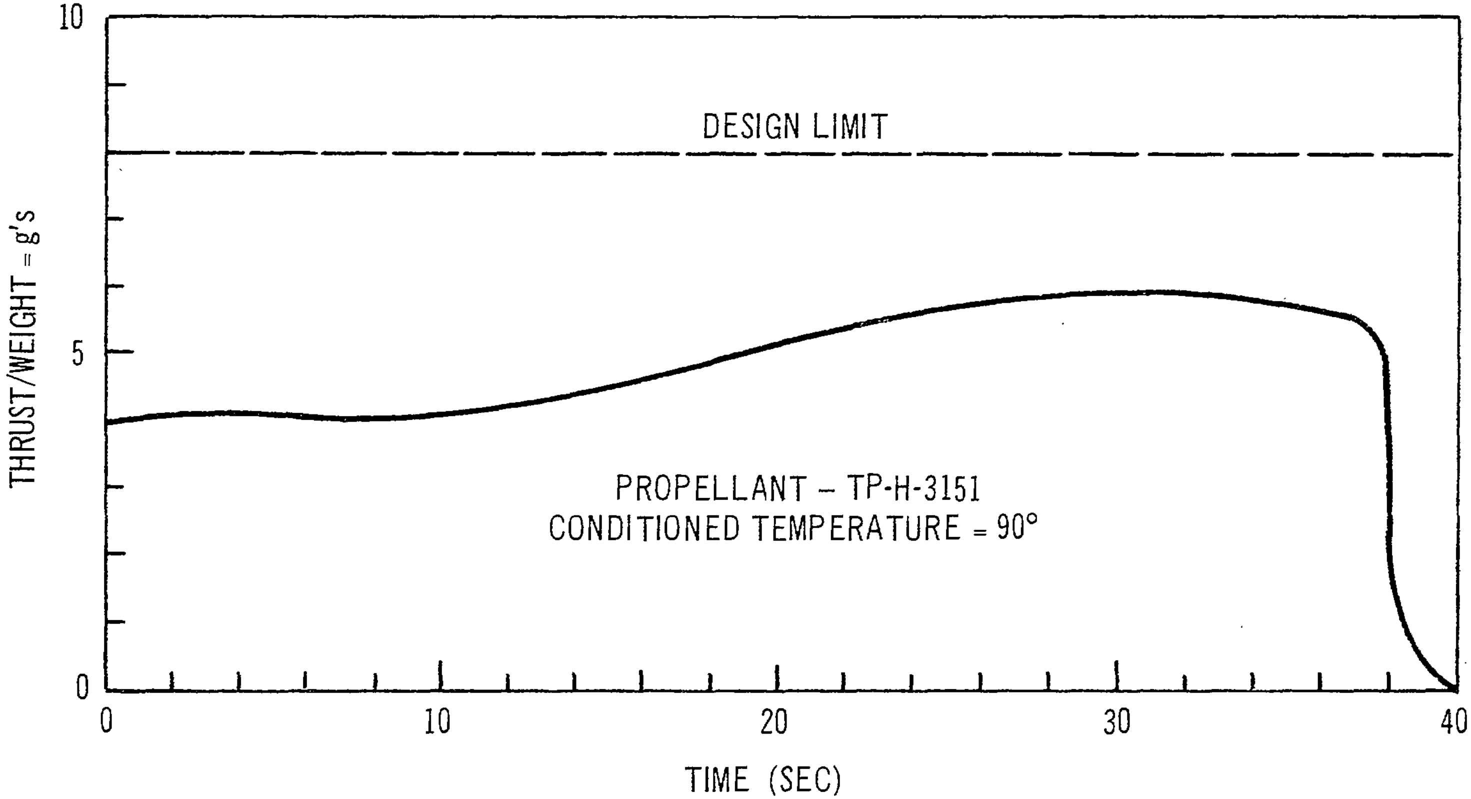

Figure 9–5 Maximum Longitudinal Acceleration (g's) versus Time

Therefore, the motor should be designed for as high a mass fraction and specific impulse as practicable. Other mass properties of interest include moments-of-inertia, centre-of-gravity, and static and dynamic balance before propellant loading, with loaded propellant and after motor firing. Thiokol has indicated that, for the proposed design, the 3 sigma variation of total motor weight will be equal to or less than 0.33%.

- Configuration. An interface-envelope control drawing showing details of all motor-to-satellite physical interfaces serves to assure compliance with physical requirements.

- Miscellaneous Items. Other items requiring consideration during the early phases of motor design include: a nozzle closure (or throat plug) to protect the motor during transportation, storage and handling, telemetry instrumentation to provide a positive indication of motor firing or to monitor motor temperatures prior to firing, and possibly, bonding straps to provide electromagnetic compatibility between the motor and satellite structure.

9.2.2 Performance Considerations

- Total impulse. The motor total impulse accuracy must be such that the velocity increment imparted to the satellite may be reliably predicted. If not, an excessive quantity of hydrazine propellant may be required to attain the final satellite position. Also, it may be considered desirable to size the motor case to allow the addition of propellant, should the satellite weight increase. The Intelsat III apogee motor was designed to accommodate a $\pm$ 10% propellant weight variation from the nominal requirement.

- Thrust level. The motor thrust level should not exceed a value which corresponds to the maximum allowable satellite acceleration. If the axial load factor imposed by the launch vehicle is greater than that due to apogee motor firing, the satellite structual design will be based on the more severe launch environment.

- Thrust Alignment. The alignment of the motor axis with the satellite spin axis and orientation of the thrust vector during firing should comply with mission operational constraints. It would be anticipated that the motor construction characteristics and design tolerances will be well within the limits imposed, both prior to and during apogee motor burn. Thiokol has indicated that the angle between the nozzle axis, defined by a line through the controids at the nozzle exit plane and the nozzle throat, and the motor center line will not exceed 0.025°, and that the radial displacement at the nozzle centerline from the motor centerline at any place between the plane of the nozzle throat and the nozzle exit plane will not be greater than 0.010 inch.

- Ignition and Thrust Transients. The motor ignition delay time and thrust transient characteristics must be within allowable satellite operational and structural constraints. It would be expected that motor ignition will take place within milliseconds and the thrust buildup to the maximum initial value will be rapid and smooth.

9.2.3 Operational Considerations

- Prelaunch Environment. The Transport, handling, final assembly storage and checkout characteristics must comply with the specified prelaunch environmental citeria. Normally, the motor will be designed for transport by any common carrier while in its shipping carrier. A typical storage requirement would be for a period of up to three years while exposed to temperatures between +20 and +120°F at a maximum relative humidity of 65 percent.

- Launch Environment. During the launch ascent and transfer orbit period the motor may be exposed to the combined environments of vibration, acceleration loads, shock, temperature cycling, spin and pressure variations from sea level to vacuum. An adequate qualification test program will assure that the motor will reliably withstand exposure to these environments.

- Firing Environment. The motor should be capable of firing while spinning under hard vacuum conditions when conditioned to a temperature between approximately +30 to +90°F. The thermal control system must provide protection against exposing the motor to temperature extremes which could cause premature thrust termination or malfunction because of high stress loads between the propellant and case, and other possible adverse situations.

- Safety. The motor must comply with safety regulations for transportation as governed by the Interstate Commerce Commission, and operations at the AFETR as governed by the Range Safety Manual and other documents. The final decision as to whether a safe and arm device (S & A) will be required for the motor will depend on existing requirements at the time of contract award. It is not recommended that propellants containing beryllium be considered.

- Reliability. The reliability of the motor is critical to the achievement of a successful mission. Therefore, it is desirable that space proven components and materials with a history of reliable performance be used to the greatest extent practical. The ignition system should be provided with redundant initiation and firing circuitry so that motor ignition will occur if only one initiator fires. Implementation of a successful qualification test program, whereby the motor is subjected to environments more severe than those expected during flight will enhance confidence in the reliability of flight motors.

9.3 ALTERNATE DESIGN APPROACHES

Several candidate apogee motor suppliers were requested to furnish information to assure that appropriate consideration be given to current and advanced apogee motor concepts and to enable identification of potential technical and program problem areas which might be encountered for this application. It was indicated that the apogee motor could be either a new motor or a modification of an existing motor. The letter Information Request was based on preliminary mission analysis data, which indicated a velocity increment requirement of 6350 ft/sec and total satellite weights in the transfer orbit of 930 and 1020 lb. Subsequently, it was decided that a ΔV=6040 ft/sec and a satellite weight of 965 lb should be used, which corresponds to the Thor-Delta DSV-3L^2 launch vehicle. Since the motor total impulse required for the combined requirements of ΔV=6350 ft/sec and W_{sat}=930 lb is essentially equal to that required for ΔV=6040 ft/sec and W_{sat}=965 lb, it was concluded that a valid basis exists for comparison of the motor designs submitted on the basis of the original requirement. Table 9-1 presents a summary of the information received from the various candidate motor suppliers, who are all considered capable of successfully performing the design, development testing, qualification and fabrication of apogee motors for this program. A summary of each company's design approach is presented in the following paragraphs.

9.3.1 Aerojet-General Corp.

Aerojet, located in Sacramento, California, presented a design approach based on Intelsat II and III apogee motor technology. Since both Intelsat motors are smaller than that required, Aerojet proposed the development of a new motor. This motor would have a total impulse approximately 34% greater than the Intelsat III motor. The fiberglass case has a semi-elliptical configuration and consists of integral aluminum bosses for attachment of the igniter and nozzle assemblies. Also, an aluminum thrust ring is provided for mounting the motor in the satellite. A silica-loaded nitrile rubber is provided for internal insulation, and a polybutadiene liner is provided for the propellant-to-insulation interface bond. The propellant, consisting of 73% ammonium perchlorate, 15% aluminum and 12% carboxy-terminated polybutadiene binder, is the same used for both Intelsat II and III motors and is fully qualified. A contoured exit cone and a silver-infiltrated tungsten throat insert with a tape-wrapped carbon-phenolic entrance section and throat backup are provided for the nozzle assembly. The ignition system consists of a KR-80000 Minuteman standardized safe-and-arm device and an igniter chamber loaded with boron potassium nitrate pellets. A comparison of the inert motor weight with other proposed new motors indicates Aerojet's relatively conservative design approach. Later information received indicated that the inert motor weight could be reduced by approximately 7 lb if an unsubmerged nozzle is used and if the nozzle is fabricated from a lighter weight composite plastic material developed by Aerojet. The Aerojet estimated total program cost is the highest, but could possibly be reduced to less than $1,000,000 if fewer firings are required for development.

Table 9 - I CANDIDATE APOGEE MOTOR CHARACTERISTICS (I)

Motor Manufacturer	Aerojet	Hercules,	Inc.	UTC	Thiokol Chemical Corp.		
Motor Designation	--	258E6	--	FW-4S	Concept (a)	Concept (b)	Concept (c)
Status/Design Approach	New motor, based on Intelsatt II & III Technology	Existing motor, modified (3)	New motor similar to 258E6	Existing Motor, modified (3)	New motor, TE-M-442 Case, unsubmerged nozzle	New Motor, TE-M-442 Case, semi-submerged nozzle	New Motor, unsubmerged nozzle, 88% solids propellant
Total Impulse (lb-sec)	132720	132000	133600	132000	133710	133710	135245
Average Thrust (lb)	6140	6030	5130	4800	4693	4693	3711
Specific Impulse (sec)	290.3	281.7	296.3	287	292.39	292.39	296.85
Average Burn Time (sec)	21.6	22	26.1	27.5	33.0	33.0	42.0
Total Motor Weight (lb)	525.2	539	517.4	527.7	512.68	517.51	507.25
Propellant Weight (lb)	456.0	469	451	460	457.3	457.3	455.6
(2) Inert Weight (lb)	69.2	70	66.4	67.7	55.38	60.21	51.65
Mass Fraction	.868	.870	.871	.880	.891	.884	.898
Estimated Burn-out weight (lb)	62.8	65	61.4	62.7	53.6	58.26	50.00
Payload Weight (lb) (for 965 lb satellite)	439.8	426	447.6	437.3	452.32	447.49	457.75
Nozzle Expansion Ratio	40:1	25:1	40:1	48:1	53:1	53:1	48:1
Case Material	Fiberglass	Fiberglass	Fiberglass	Fiberglass	Titanium	Titanium	Titanium
Overall Length (in.)	40.74	59.25	56.6	58.5	55.68	52.00	51.80
Case Diameter (in.)	27.0	18.04	19.32	19.6	26.08	26.08	24.9
Throat Diameter (in.)	2.754	3.07	3.03	NA	2.66	2.66	2.47
Nozzle Exit Diameter (in.)	17.4	16.00	19.14	16.9	19.38	19.38	17.11

Notes: (1) Based on total weight of satellite in transfer orbit = 930 lb, V = 6350 ft/sec
(2) Inert weight arbitrarily increased by 5 lb. to allow for motor attachment and other hardware
(3) Modifications include propellant off - loading, addition of S and A device

Table 9.1 CANDIDATE APOGEE MOTOR CHARACTERISTICS (1)

9.3.2 Hercules, Inc.

Hercules, located in Magna, Utah, proposed either a modification of their Altair II 258E6 motor or the development of a new motor. The 258E6 motor, with a nominal total impulse capability of 142,000 lb-sec, is the only "Off-the-shelf" motor which nearly meets the total impulse requirements. Development of this motor for the Bureau of Naval Weapons and NASA was completed in 1963 and it has since been used for several upper stage launch vehicles and other applications. The motor consists of: (1) a Spiralloy (fiberglass) chamber with an integral glass fiber skirt; (2) a two-piece contoured insulator molded from EP-87 boric acid filled, Buna-S rubber; (3) a re-entrant type graphite throat nozzle, containing a composite exit cone, which is filament wrapped for reinforcement; (4) a high impulse, aluminized cast modified double base propellant case-bonded grain cast to a slotted tube design; and (5) a rocket type igniter containing a filament wound DGV propellant grain that is ignited by $BKNO_3$ pellets.

However, adaptation of the 258E6 motor to this application would require the following modifications:

. Removal of approximately 35 lb of propellant.
. A minor throat diameter reduction.
. Possible addition of a same and arm device.
. Replacement of internal insulation (presently qualified to a temperature range of +60 to +90°F) with insulation qualified to the required motor operational temperature range.

In addition, the thrust level is such that an acceleration load of approximately 12 g's would be imposed on the satellite during motor firing. Should this load impose an excessive penalty to the structure and equipment design, a different propellant may be required. The primary advantage of this motor is the relatively low total program cost. However, a modified 258E6 motor offers a serious disadvantage from the standpoint of payload weight capability.

The new motor proposed by Hercules would be similar to the 258E6 but would be an optimized configuration. This motor would use the same propellant (CYI-75) as the 258E6, and would have a contoured nozzle exit cone with an expansion ratio of 40:1, as opposed to the 25:1 expansion ratio for the 258E6. Payload capability of the new motor would thus be improved significantly, but estimated total program costs would also increase primarily because of the additional development and qualification firings required.

9.3.3 Thiokol Chemical Corp.

Thiokol, located in Elkton, Maryland, provided data for several motor design approaches as follows:

(a) Modification of the existing 26-inch spherical TE-M-442 motor to include an unsubmerged nozzle and the Surveyor Retro motor program igniter and Safe and Arm device.

(b) The same as (a), above, except that a semi-submerged nozzle would be provided.

(c) As optimized motor with a spherical, titanium case, and unsubmerged plastic nozzle, the Surveyor Retro pyrogen igniter and S & A, and TP-H-3135 (88% solids) propellant.

(d) The same as (c) above, except that the case material would be fiberglass, rather than titanium.

It was observed that the external configuration of the several motor designs presented was similar, and should be compaitble with satellite integration requirements. Therefore, the Thiokol motors were compared primarily on the basis of performance (payload weight capability), and the application of proven design concepts. Design concept (a) is essentially a new motor since the case material (titanium) replaces the TE-M-442 steel case, a different propellant formulation is used, and the ignition system and nozzle configurations vary from the existing TE-M-442 motor. Therefore, a comprehensive development and qualification program would be required. Design concept (b) would involve the same type of program as that for concept (a), and has a lower payload weight capability. Concept (c), which has been designated Mod 6 by Thiokol, involves the development of a new motor of optimum design. This motor has the highest payload weight capability, exclusive of concept (d). Theoretical data presented for concept (d) indicated that an inert weight of 47.3 lb could be provided, which is 40 to 48 percent less than the inert wieghts of motors proposed by other candidate suppliers of fiberglass motors. It was thus concluded that mass properties and payload capability of motor design concept (d) is questionable.

9.3.4 United Technology Center

UTC, located in Sunnyvale, California, suggested that their FW-4S motor be modified for the present application. This motor, like the Hercules 258E6 motor, was designed as an upper stage for the Thor and Scout boost vehicles. This motor is qualified for firing temperatures from +40 to +100°F at spin speeds up to 200 rpm. However, the nominal total impulse (174,000 lb/sec) of the motor is 32% greater than required and, therefore, would necessitate a propellant off-loading of 145 lb (compared with an off-loading requirement of 35 lb for the 258E6 motor). Modifications necessary to accomplish this relatively high propellant off-loading could intruduce a substantial overall program risk. Also, although the payload weight capability of this motor is greater than the Hercules 258E6 motor, the total program costs were also estimated to be higher.

9.4 MOTOR SELECTION

Final selection of the apogee for the program will be made after evaluation of firm cost proposals solicited by a formal RFP. However, satellite design, program planning, and other considerations emphasize the need for a tentative apogee motor selection. Factors which would tend to favor utilization of an existing motor include cost, delivery schedule, qualification status and reliability. However, since payload weight and other technical factors may be of critical importance, the development and qualification of a new motor may be justified.

9.4.1 Design Comparisons

As may be observed from Table 9-1, the primary design choice exists between motors with fiberglass or titanium cases. Although fiberglass case technology for space applications is well advanced in the United States, the use of titanium should permit less internal insulation provided that the higher allowable case temperature does not impose an excessive weight penalty for thermal control. However, it must be acknowledged that titanium forgings may require considerable lead time during the procurement phase of the program. Results of a preliminary investigation indicate that the external insulation required for postfire thermal control of the titanium motor should be within allowable weight limitations and the titanium case procurement schedule will not adversely affect program commitments.

From the standpoint of overall envelope, the satellite design can accommodate all motors proposed. Thus, the optimum expansion ratio to provide maximum performance consistent with minimum inert weight characteristics would tend to favor a new motor. Additional envelope considerations include case configuration, ease of installation and alignment. Motors of larger case diameter require a larger central support cylinder, with a potentially higher structural weight penalty, but spherical or semi-spherical cases are inherently more efficient pressure vessels and may offer an installation and alignment advantage over the lower diameter, longer case configurations. It should be noted that both Hercules and UTC suggested the possibility of a case length reduction (2.3 inches for the 258E6 motor and 8.3 inches for the FW-4S motor) for existing designs requiring a propellant off-loading. However, these structural changes would imply additional program risks and costs.

Since all candidate motor suppliers specified propellants with well formulized characteristics and production experience, the type of propellant is not considered to be an important factor for motor selection. One exception is the fact that the thrust level is affected by the propellant burning rate, which in turn affects the satellite acceleration during motor firing. Of the motors proposed, only the Aerojet new motor with a 3σ maximum acceleration of 11.0g's and the modified existing Hercules 258E6 motor with a maximum acceleration of 12g's exceed the preliminary specification requirement of 10g's. Similarly, the ignition system concepts proposed are all considered to meet the requirements for reliable motor ignition consistent with safety. Thiokol is the only motor manufacturer who has designed, developed and qualified a safe-arm unit and, therefore, should have an advantage over the other motor manufacturers by virtue of the fact that quality control surveillance and interface definition for integration of the S/A device will be simplified.

Thus, an examination of the various design features of the candidate motors does not reveal any significant characteristics which would preclude adaptation for this application and it was determined that the motor selection should be based on considerations of payload weight capability and total program cost.

9.4.2. Program Cost Versus Payload Weight

Figure 9-6 shows that the variation of total program cost increases at a rate of approximately $16,000 per pound of payload weight. It is recognized that the design and cost data submitted was based on estimates which would most probably vary at the time of contract negotiations, i.e., the curve should shift in the direction of increased cost and/or reduced payload weight. However, the consistency and trend of the data presented is considered significant, because of the fact that the originally submitted values were used with the exception that the UTC motor weight was increased (thus decreasing the payload weight) by the addition of a 4.65 lb KR80000 safe and arm device, and UTC program costs were increased by $100,000 to equalize the number of qualification firings (2) proposed by Hercules for the 258E6 motor. As shown, the only inconsistent value represented is that proposed by Aerojet, which may be as a result of a conservative cost approach.

Experience with satellite programs has indicated that the payload weight requirements tend to increase during program development, and, therefore, the highest payload weight contingency practicable should be provided to minimize the probability of redesign with attendant cost increases and/or failure to meet the total satellite weight limit imposed by launch vehicle constraints. Thus, consideration of the foregoing factors led to the selection of the Thiokol motor, designated Mod.6. This motor provides a total payload weight capability of 467 lb for a satellite initial weight of 965 lb.

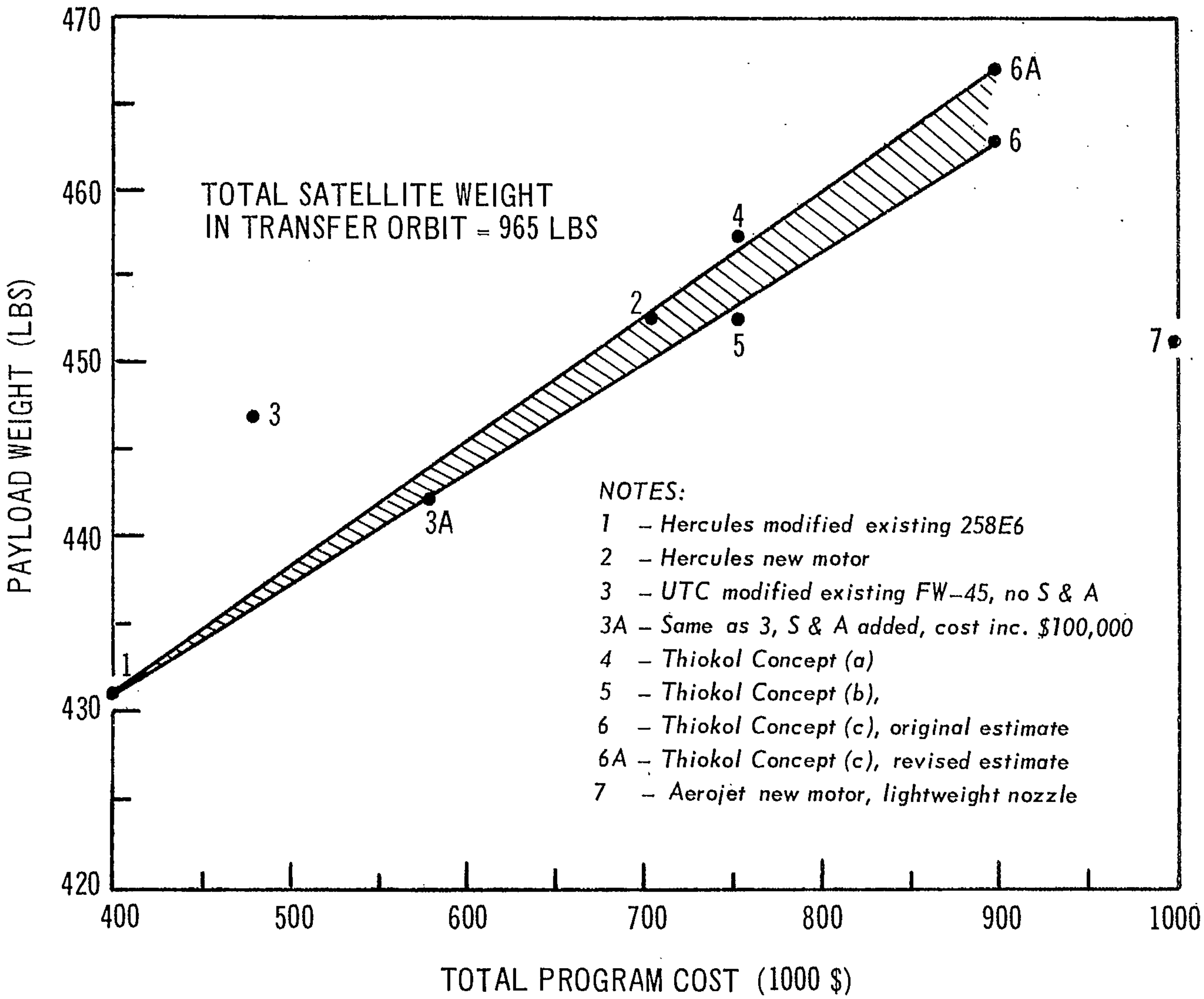

Figure 9–6 Apogee Motor Payload Weight – Estimated Program Cost Relationship

11 10
THERMAL DESIGN

10 THERMAL CONTROL SUBSYSTEM

10.1 SYSTEM DESCRIPTION

10.1.1 General

The thermal control subsystem for the spacecraft is designed to be completely passive. Fluctuations in the total internal heat load are minimized and a radiative heat balance is established between absorbed solar, internal dissipation, and emitted energy to maintain components within allowable temperature limits during steady state sunlit operation. The heat capacity of the spacecraft aids in maintaining allowable temperatures during transient eclpise conditions. Surface thermal radiation property requirements, insulation, structural coupling, and component grouping are the passive techniques utilized to obtain thermal control. The materials, finishes, and coatings specified, when critical, are the most stable materials now available for spacecraft use based on exposure to combined vacuum, ultraviolet, and charged particle environments.

The thermal control subsystem is designed to meet the following five conditions:

- o Synchronous Orbit - Sunlit and Eclipse
- o Transfer Orbit - Sunlit
- o Parking Orbit - Sunlit and Eclipse
- o Boost
- o Ground Hold

Thermal control concepts for the despun and spinning section of the spacecraft will be discussed separately in the following sections.

10.1.2 Despun Section

a Despun Mechanical Assembly

The despin mechanical assembly can be described thermally as an outer aluminum vertical spinning cylinder and inner steel vertical despun shaft having a spacecraft central cylinder adapter aft and antenna support adapter forward as shown in Figure 10-1. The outer cylinder internal surfaces and the external surface of the inner shaft will be coated with black Cat-a-lac paint ($\varepsilon = .86$) to thermally couple the two to minimize temperature differentials that might cause mechanical interference. The external surface of the cylinder will also be coated with black paint to thermally couple the

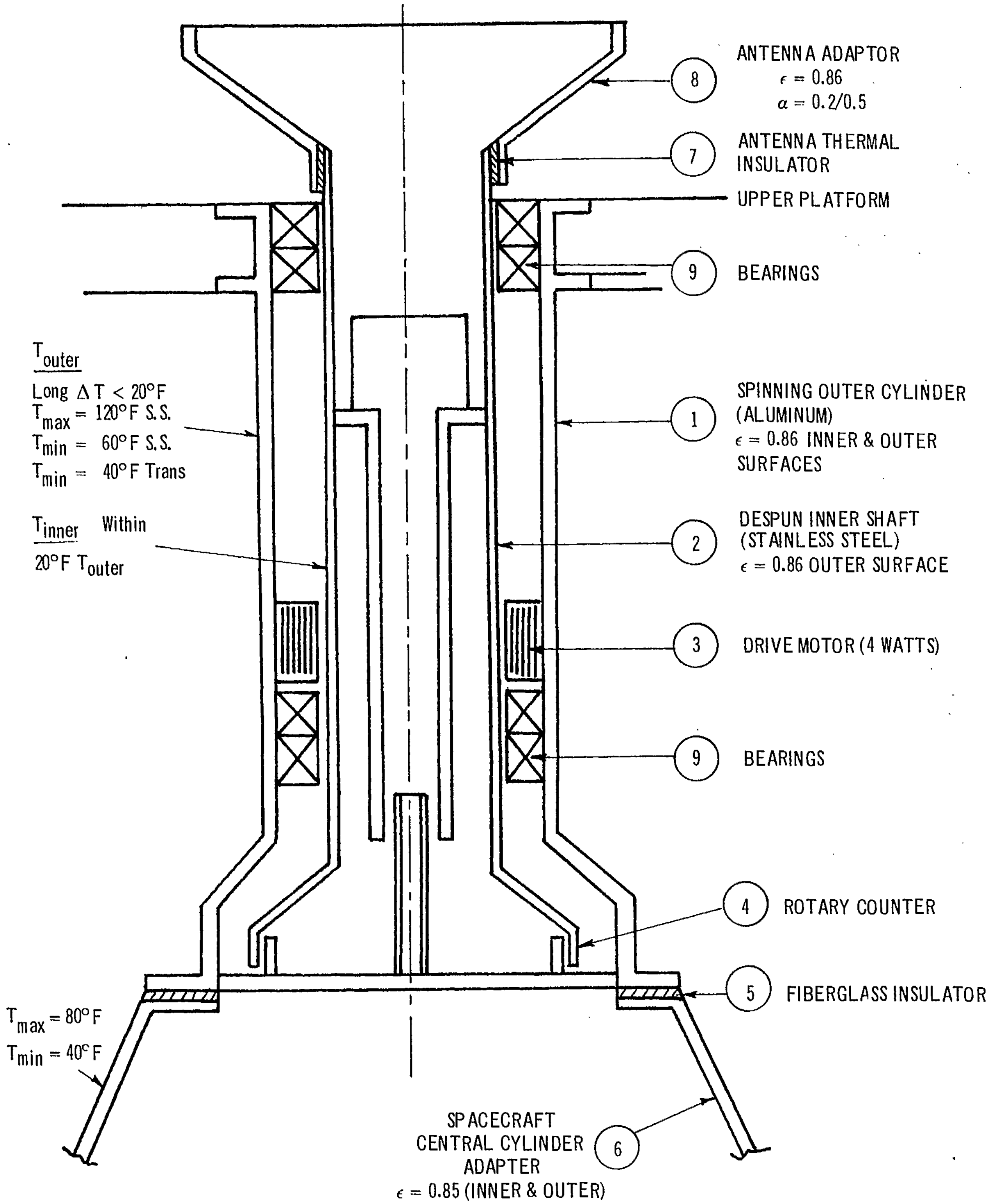

Figure 10-1 Despin Mechanical Assembly

despin assembly with the upper platform. The structural attachments of the outer cylinder to the upper platform will also provide good thermal coupling. The antenna support adaptor forward and central cylinder adaptor aft will be thermally decoupled from the despin mechanical assembly by means of fiber-glass insulators to minimize longitudinal temperature gradients in the assembly and heat leaks from the spacecraft.

The drive motors, slip rings, and cabling dissipate 4 watts under normal operating conditions. The aluminum spinning cylinder will tend to minimize longitudinal temperature gradients along the cylinder. The heat generated in the drive motors will be conducted along the spinning cylinder to be transmitted radiatively to the despun platform by good radiative coupling.

- Antennas

The despin mechanical assembly supports three despun antennas as shown in Figure 10-2. All the antennas are maintained within maximum and minimum allowable temperature limits by the selection of thermal coatings. The antennas will experience temperature gradients in the longitudinal and transverse directions as well as wide variations in the average temperature levels due to various sun angles and shadowing. The two telemetry and command antennas will be covered with white paint (Dow Corning 092-007 Zinc Oxide Pigment, Silicone base, $a_{initial} = .2$, $a_{degraded} = .5, \epsilon = .85$). The solar absorptivity degradation will not influence the performance of these antennas. Only the elliptical communications antenna has pointing accuracy requirements that require a detailed examination of thermally induced distortions.

The reflector portion of the elliptical antenna will be constructed of contoured aluminum honeycomb with aluminum face sheets. Different surface coatings will be applied to the reflector external surfaces to reduce longitudinal and transverse temperature gradients and thereby reduce thermally induced antenna pointing errors. White paint will be used on the concave surface to produce as low a solar absorptivity value as possible and still provide diffuse solar reflection to prevent specular focusing of solar energy on the antenna feed. Vacuum deposited aluminum (VDA, $a = .12$, $\epsilon = .04$) on the convex surface of the reflector will reduce transverse thermal gradients at the expense of somewhat higher average reflector temperatures for the various sun angles.

The elliptical antenna feed and reflector supports will be wrapped with multilayer aluminized Kapton insulation blankets (aluminized side facing inward) and painted with Cat-a-lac black paint ($\epsilon = .86$) internally to minimize circumferential thermal gradients in the supports that would cause antenna pointing errors. The multilayer aluminized Kapton insulation blanket will consist of 10 layers of 1/4 mil Kapton sandwiched between two layers of 2 mil Kapton.

FIGURE 10-2

THERMAL CONTROL SUBSYSTEM DESCRIPTION

I.D.	Description	Material	ε	α
	(Omni and Biconical Antennas)			
1	Antenna Coating	White Paint-Dow Corning 092-007	.85	.2/.5*
2	Support Coating	White Paint-Dow Corning 092-007	.85	.2/.5*
	(Elliptical Antenna Reflector)			
3	Reflector Concave Coating	White Paint-Dow Corning 092-007	.85	.2/.5*
4	Reflector Convex Coating	Vacuum Deposited Aluminum	.04	.12
	(Elliptical Antenna Feed and Reflector Supports)			
5	External Surface Insulation	Aluminized Kapton Insulation Blanket (10) 1/4 mil sheets (2) 2 mil cover sheets	.76	.43
6	Internal Surface Coating	Black Paint-Cat-a-lac	.86	--
7	Thermal Isolators	Fiberglass	--	--
	(Nutation Damper Assembly)			
8	Nutation Damper External Surface	Polished Aluminum	.04	--
9	Thermal Isolator	Fiberglass	--	--
10	Enclosure Insulation	Aluminized Kapton Insulation Blanket (10) 1/4 mil sheets (2) 2 mil cover sheets	.6	.3
11	Enclosure Solar Collector	Mosaic-VDA Tape second surface mirrors	.16	.12
	(Forward Equipment Platform)			
12	Forward Surface Radiating Surfaces	Second Surface Mirror	.8	.1
13	Forward Surface Insulation	Aluminized Kapton Insulation Blanket	.76	.43
14	Aft Surface and Component Coating	Black Paint-Cat-a-lac	.86	--
15	TWT Base Plate and Thermal Filler Material	.060" Aluminum Sheet RTV-11 Adhesive	-- --	-- --
16	TWT Insulation Enclosure	Aluminized Mylar Insulation Blanket (10) 1/4 mil sheets (2) 2 mil cover sheets	.8	--
17	Aft Surface Insulation	Aluminized Mylar Insulation Blanket (10) 1/4 mil sheets (2) 2 mil cover sheets	.8	--
	(Despin Mechanical Assembly)			
18	Internal and External Surface Coatings	Black Paint-Cat-a-lac	.86	--
19	Forward and Aft Thermal Isolators	Fiberglass	--	--
	(Central Spacecraft Cylinder)			
20	Internal and External Surface Coatings	White Paint-Cat-a-lac	.85	--
	(Solar Array and Substrate)			
21	Substrate Internal Surface Coating	White Paint-Cat-a-lac	.85	--
22	Solar Cell Thermal Properties	--	.82	.79
	(Lower Equipment Platform)			
23	Component and Platform Surface Coatings			
	High Heat	White Paint-Cat-a-lac	.86	--
	Low Heat	VDA Tape	.04	--
24	Component Attachment			
	High Heat	RTV-11 Adhesive	--	--
	Low Heat	Fiberglass Isolators	--	--
	(Positioning and Orientation System)			
25	Propellant Tank and Line Surface Coating			--
26	Propellant Tank and Line Insulation	Aluminized Mylar Insulation Blanket (10) 1/4 mil sheets (2) 2 mil cover sheets	.8	--
27	Propellant Tank and Line Thermal Isolators	Fiberglass	--	--
28	Axial Thruster Solar Collector	Incoloy	.11	.56
29	Axial Thruster Heat Sink	Beryllium	.08	--
30	Axial Thruster Insulator	Gold Coated Stainless Steel Foi.	.08	--
	(Apogee Motor)			
31	External Surface Insulation	Multilayer Aluminum Foil and Dexiglass	--	--
32	Thermal Isolators	Fiberglass	--	--
33	Nozzle Closure	Aluminized Mylar Insulation Blanket	.3	.8
	(Aft Closure)			
34	Forward Surface	Stainless Steel Bare	.15	--
35	Aft Surface	White Paint-Dow Corning 092-007	.85	.2/.5*

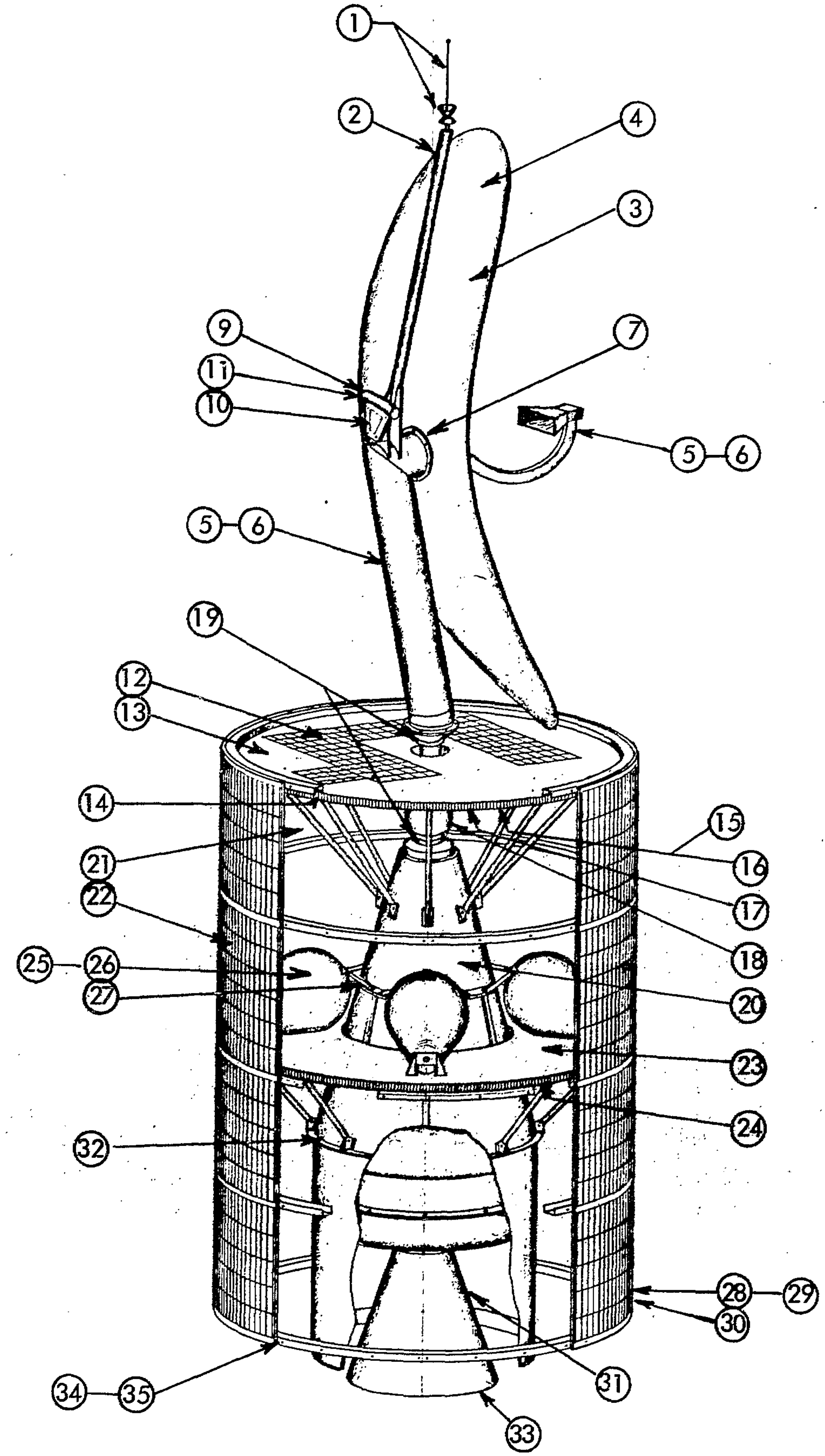

o Nutation Damper

The nutation damper will be attached to a bracket on the elliptical antenna reflector support near the center of the reflector (Figure 10-2). The damper will have a low emissivity surface finish (aluminum $\epsilon = .04$) and will be thermally decoupled from the bracket by fiberglass spacers. In addition the damper will be completely enclosed in a container having multilayer aluminized Kapton insulation and a mosaic solar collector surface of VDA tape and second surface mirrors. The interior surface of the enclosure will be coated with Cat-a-lac black paint ($\epsilon = .86$) to equalize temperature gradients in the enclosure. The a/ϵ ratio of the surface of the insulation ($a = .43, \epsilon = .76$) and 10 in ^{2} of mosaic solar collector ($a = .12, \epsilon = .16$) assures acceptable temperature of the damper during sunlit conditions. The low damper and solar collector surface emissivity, multilayer insulation, and fiberglass spacers minimize heat leak from the damper during eclipse and shadow conditions to maintain temperatures within allowable limits.

The cooling effect of the approximate 12 hour shadow period caused by the elliptical antenna reflector can be minimized by providing a pattern of holes through the reflector adjacent to the damper to allow solar radiation to be directly transmitted through the reflector to the damper.

10.1.3 Spinning Section

o Upper Equipment Platform and Components

The high power density and high allowable temperature components in the communication subsystem (TWT's) are grouped in three patterns and mounted on the inside of the upper platform as shown in Figure 10-3. Redundant TWT's are located between each pair of operating TWT's to maintain constant heat dissipation and resultant acceptable equipment temperatures on the platform during sunlit conditions with as many as three TWT's failed.

A local increase in the despun platform internal face sheet thickness is provided in the TWT area by means of a .060" aluminum mounting plate (4.8 ft^2 total). The TWTs will be thermally coupled to the mounting plate, and the mounting plate to the platform face sheet by RTV-11 interface material. The .060" mounting plate serves to distribute heat laterally to be conducted through the platform and radiated to space. The lateral conduction of heat in the 060" mounting plate lowers operating TWT baseplate temperatures and aids in maintaining non-operating TWT's within allowable temperature limits while the .010" platform face sheets limit conduction of heat to adjacent low temperature components. The

Figure 10-3

Forward Equipment Platform

I.D. No.	Number Required	Max Power Dissip (ea) (Watts)	Description
			Communication Subsystem
1	1	0	Bandpass Filter 6 GHZ
2	1	0	Command Reject Filter
3	2	0	Switch
4	1	0	Isolator
5	2	1.25	TDA 6 GHZ
6	2	0	Translator Mixer
7	2	0	L.O. RF Source
8	1	0	Comb Filter
9	2	0	Switch
10	2	1.25	TDA 4 GHZ
11	2	2.5	Driver TWT
12	2		Driver TWT Power Supply
13	1	0	Multiplexer-Input
14	9*	28.2	TWT
15	9*		TWT Power Supply
16	9	0	Isolator
17	1	0	Multiplexer-Output
18	1	0	LP Filter
19	1	0	HA Filter
20	1	0	TM Suppress Filter
21	6	0	Pin Diode Attenuator
22	6	0	Switch (Spot)
23	6	0	Switch (Transfer)
	Tot. Heat	179.2	
			Telemetry and Command
24	1	4.3	Command Receiver
25	1	2.0	Command Decoder
26	1	1.6+/.8	PCM Encoder 1
27	1	1.6+/.8	PCM Encoder 2
28	1	12.8+/6.4	Telemetry Transmitter
29	1	6.0+	Beacon Transmitter
	Tot. Heat	28.3+/14.3	

\+ Transfer orbit only
* Maximum 6 operating during sunlight
3 operating during eclipse

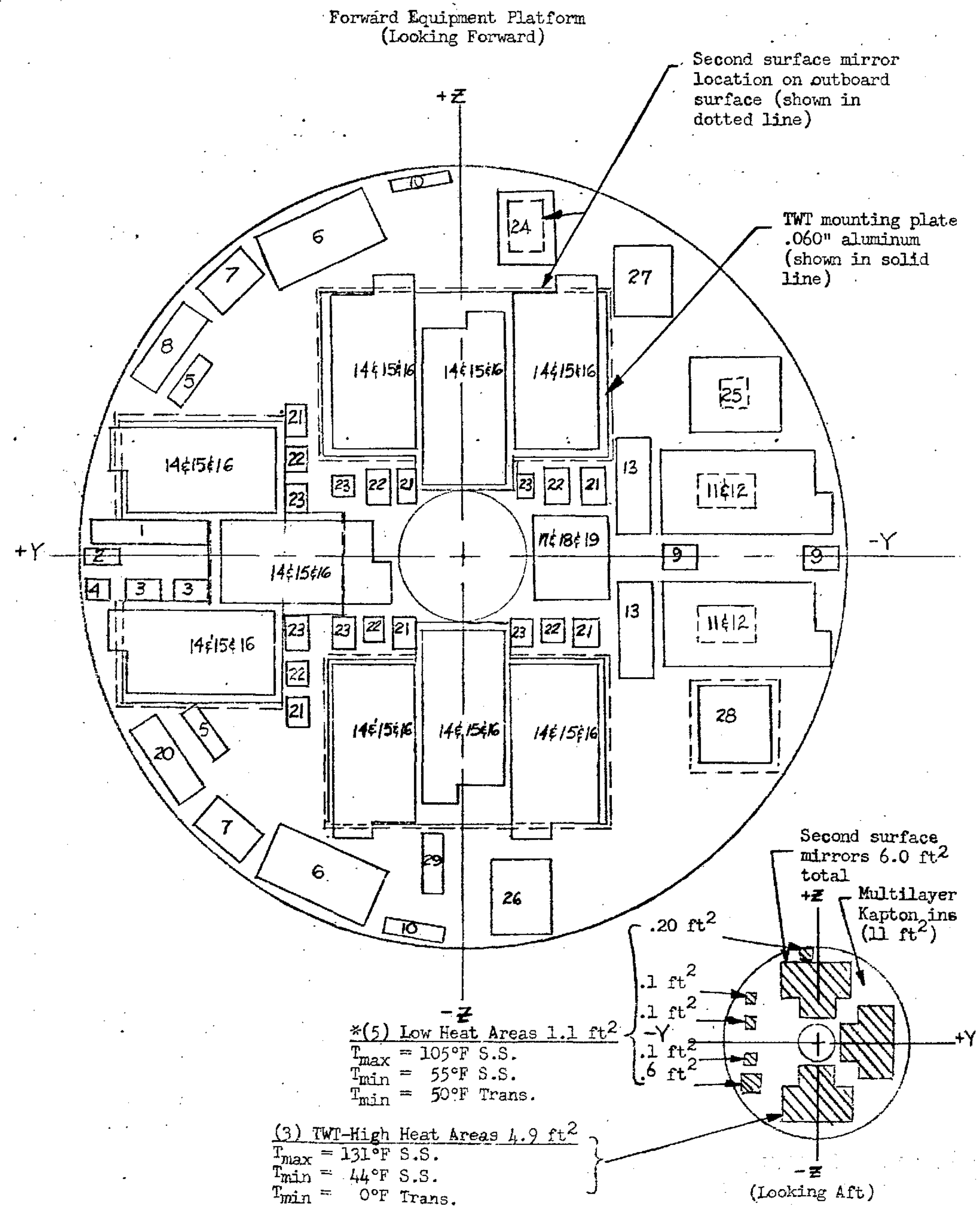

.060" mounting plate and TWT's will be covered with a multilayer Mylar insulation enclosure to radiatively isolate the high temperature TWT's from adjacent lower allowable temperature components. Second surface mirrors (α = .1, ε = .8) are mounted on the external face sheet of the platform in the high power density mounting plate area (4.8 ft^2 total) to minimize absorbed solar radiation while maximizing the radiating ability of the platform. Second surface mirrors consist of vapor deposited silver on fused silica with an inconel flash coating for protection. Second surface mirrors have been utilized on several TRW spacecraft with a maximum total radiating area of 7 ft^2 on one spacecraft.

The remaining low power density components in the communications, and telemetry and command systems are mounted directly to the inside face sheet of the platform as shown in Figure 10-3. The external face sheet of the platform in this area is covered with multilayer aluminized Kapton insulation except several small areas having second surface mirrors[TWT drivers (11 in^2 each) telemetry transmitter (56 in^2) and command receiver (19 in^2)]. The net effect of the mounting platform seeing space directly and grouping the higher and lower allowable temperature components together is a weight reduction of approximately 15 pounds compared to a lower platform installation concept with high and low allowable temperature components intermingled.

The entire inside surface of the platform, and the external surfaces of the components will be coated with black paint (ε = .86) to equalize temperature differentials on the platform. An aluminized Mylar insulation blanket consisting of ten layers of 1/4 mil Mylar sandwiched between 2 layers of 2 mil Mylar will enclose the entire inside portion of the platform as shown in Figure 10-2 to distribute heat around the despun platform. The insulation also thermally decouples the upper platform from the solar array heat sink which would tend to decrease upper platform component temperatures below allowable temperature limits during reduced power eclipse conditions. Lower cost aluminized Mylar insulation is utilized in this area since it will not be exposed to ultraviolet and charged particle environments

o Apogee Motor

The apogee motor will be enclosed in multilayer insulation to maintain allowable temperature during extended transfer orbit conditions prior to ignition and limit heat soak back to structure after ignition. In order to withstand apogee motor case temperatures at the end of firing an aluminum foil and dexiglass multilayer insulation similar to that on INTELSAT III will be used. The insulation will enclose the apogee motor shown in Figure 10-2. Multilayer aluminized Mylar insulation will be installed across the nozzle exit cone to limit heat losses from the throat and nozzle prior to the motor being fired.

The thermal coupling between the apogee motor and the central column supporting the motor is minimized by means of fibergalss insulators similar to INTELSAT III. The decoupling requirement is necessary to reduce heat soak back from the apogee motor after firing.

o Positioning and Orientation Subsystem Components

The propellant storage tanks will have multilayer aluminized Mylar insulation blankets, and fiberglass structural attachments insulators to thermally decouple the tanks from varying surrounding temperatures caused by internal power variations and eclipse conditions. The propellant feed lines to the thrusters will be wrapped with multilayer aluminized Mylar insulation and attached to surrounding structure with insulators similar to INTELSAT III. The axial thruster valve assembly will have a beryllium heat sink in contact with a high α/ϵ solar collector window in the solar array substrate (Figure 10-5) to maintain propellant temperatures within allowable limits during eclipse conditions. A low emissivity beryllium surface finish (ϵ = .08) will minimize radiation away during eclipse, while the high α/ϵ incoloy solar collector (α = .56, ϵ = .11) will maximize temperatures prior to eclipse and minimize radiation away during eclipse.

Two thrusters will extend through the solar array to control orientation (Figure 10-4) operating in a pulse mode. The plume will not impinge directly on the surrounding structure precluding local convective heating. Since the thrusters operate in a pulse mode only, local radiant heating from the thruster body will not be a problem. The axial thrusters extend through the end closures as shown in Figure 10-4 such that convective and radiant heating to the aft closure from the plume is insignificant. Insulation to limit radiant heating of the surrounding structure by the hot thruster body during extended axial mode firing and cool down will consist of alternating layers of stainless steel foil and microquartz separators with a gold coated stainless steel cover similar to the INTELSAT III design.

10.2 SYSTEM PERFORMANCE

10.2.1 Synchronous Orbit

The natural and induced thermal environments experienced during synchronous orbit are summarized in Table 10-1 for various mission sequences. Component maximum and minimum heat dissipations are summarized by subsystem and spacecraft section in Table 10-2 for various mission sequences and limit sun angles. Table 10-3 summarized component by component maximum allowable operating and non-operating temperature requirements. Synchronous orbit thermal capability predictions are also summarized in Table 10-3 and should be referred to for specific component operating temperatures.

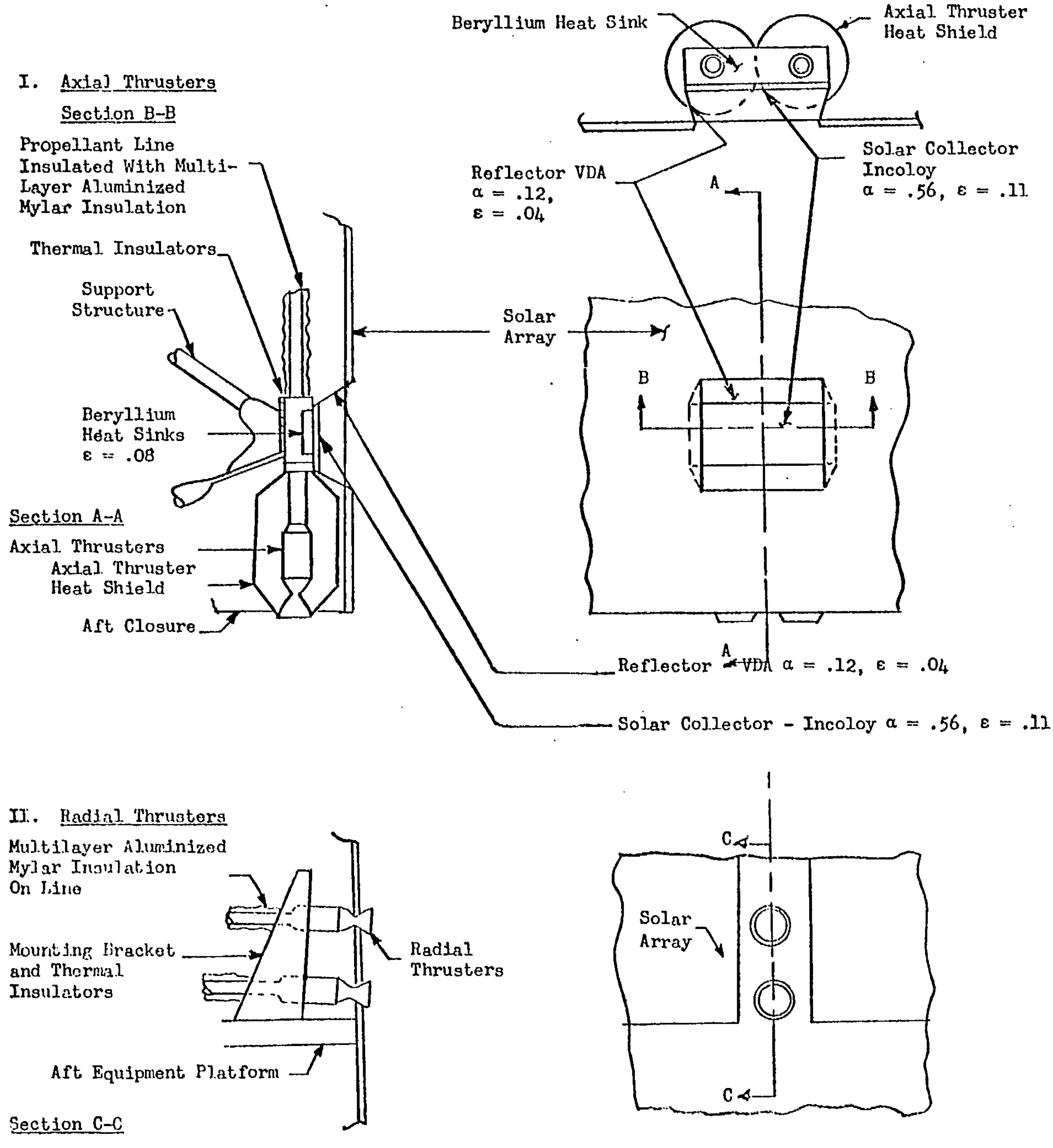

Figure 10-4 Positioning and Orientation System Thrusters

Table 10 - , 1A

SUMMARY NATURAL AND INDUCED THERMAL ENVIRONMENTS

Description of Environment	Mission Sequence: Ground Hold	Boost	Earth Orbit	Transfer Orbit	Synchronous Orbit		
I. Natural Environments							
A. Ambient Temperature							
Max (^{o}F)	110	110	-	-	-	-	-
Min (^{o}F)	40	-60	-	-	-	-	-
B. Winds							
Max (M.P.H.)	50	50	-	-	-	-	-
Min (M.P.H.)	0	0	-	-	-	-	-
C. Solar Constant							
Max (Btu/Hr-ft^2)	300	300	480	480	440	460	480
Min (Btu/Hr-ft^2)	0	0	400	400	400	420	440
D. Earth Emission							
Max (Btu/Hr-ft^2)	-	-	68	1.5	1.5	1.5	1.5
Min (Btu/Hr-ft^2)	-	-	37	0.5	0.5	0.5	0.5
E. Albedo Heat Load							
Max (Btu/Hr-ft^2)	-	-	168	3.0	3.0	3.0	3.0
Min (Btu/Hr-ft^2)	-	-	68	1.0	1.0	1.0	1.0
F. Eclipse Times							
Max - (Hr)	-	-	.6	0*	1.2	1.2	1.2
Min - (Hr)	-	-	0	0	0	0	0
G. Sun Angle Off Normal to Spin Axis							
Max - (Deg)	+90	+90	90	+23 1/2*	+23 1/2	0	
Min - (Deg)	-90	-90	-90	-23 1/2*			-23 1/2

* Limit Launch Window

Table 10-1B

SUMMARY NATURAL AND INDUCED THERMAL ENVIRONMENTS

Description of Environment	Mission Sequence: Ground Hold	Boost	Earth Orbit	Transfer Orbit	Synchronous Orbit		
II. Induced Environment							
A. Equipment Heat (see Tables 2 & 3)							
Max - (Watts)							
Min - (Watts)							
B. Shroud Temperature (Estimated) (See Figure 12)							
Max - (°F)	-	300	-	-	-	-	-
Min - (°F)	-	0	-	-	-	-	-
C. Aerodynamic Heating							
Max - (Btu/ft^2-sec)	-	.35	-	-	-	-	-
Min - (Btu/ft^2-sec)	-	0	-	-	-	-	-
(Shroud Separated 400,000 ft) I - IV							
D. Apogee Motor Plume Heating (See Figure 9)							
Max - (Btu/ft^2-sec)	-	-	-	-	5.0	5.0	5.0
Min - (Btu/ft^2-sec)	-	-	-	-	2.0	2.0	2.0
(Interpolate I - IV, & I - 3							
E. Axial Thruster Plume Heating							
Max - (Btu/ft^2-sec)	-	-	-	-	.09	.09	.09
Min - (Btu/ft^2-sec)	-	-	-	-	.02	.02	.02

Mission Phase	Array	Sun Angle (Degree)	Heat Load	Solar Constant (Btu/hr-ft²) Max	Solar Constant (Btu/hr-ft²) Min	Diode Losses	Solar Array Capability	Shunted In Array	1 Shunt Assembly	2 Power Control Unit	Total Bus Power Available	Spacecraft Platform	3 Communications Heat	Subsystem Mode	4 Telemetry and Command	5 Attitude Determination and Control	6 Electrical Integration	7 Converter Losses	8 Battery Heat	9 Auxiliary Heaters	Total H at Load 1 - 9	Comments	
Ground	New	0	Max	300	0	-	0	0	0	0	0	Upper	179	N.T.(6)	28.3/14.3	0	0	0	0	0	207.3/193.3		
Hold	New	0	Max	300	0	-	0	0	0	4	0	Lower	0	N.T.(6)	0	14.5	5.0	4.6	6.6	0	34.7		
	New	0	Max	300	0	-	0	0	0	4	0	Total	179	N.T.(6)	28.3/14.3	14.5	5.0	4.6	6.6	0	242/228		
Ascent	New	0	Min	480	400	-	0	0	0	0	0	Upper	0	N.T.(0)	0	0	0	0	0	0			
	New	0	Min	480	400	-	0	0	0	0	0	Lower	0	N.T.(0)	0	0	0	0	0	0			
	New	0	Min	480	400	8	0	0	0	0	0	Total	0	N.T.(0)	0	0	0	0	0	0			
Parking	New	0-360°	Min	480	400	-	0			0	0	Upper	0	N.T.(0)	0	0	0	0	0	0			
Orbit	New	36'	Min	480	400	-	TBD	TBD	TBD	0	0	Lower	0	N.T.(0)	0	0	0	0	0	0			
	New	Eclipse	Min	480	400	8	TBD	TBD	TBD	0	0	Total	0	N.T.(0)	0	0	0	0	0	0			
Transfer	New																						
Orbit	New	SAME AS SYNCHRONOUS ORBIT - NO ECLIPSE BY SELECTING LAUNCH TIME																					
	New																						
Synchronous	New	0	Max	460		-	-	0	0	0	193.3	Upper	179	N.T.(6)	14.3	0	0	0	0	0	193.3	Max. S.S.	
Orbit	New	0		460		-	-	38	51	4	30.7	Lower	0	N.T.(6)	0	14.5	5.0	4.6	6.6	0	85.7	Max. S.S.	
1	New	0		460		11	317	38	51	4	224.0	Total	179	N.T.(6)	14.3	14.5	5.0	4.6	6.6	0	279.0	Max. S.S.	Not Transmitting 6 TWT Available
1E	New	0		0		-	-	0	0	0	114.3	Upper	95	N.T.(3)	14.3	0	0	0	0	5	114.3		
(Eclipse)	New	0		0		-	-	0	0	4	47.1	Lower	0	N.T.(3)	0	14.5	5.0	4.6	23	0	51.1		
	New	0		0		0	0	0	0	4	161.4	Total	71	N.T.(3)	14.3	14.5	5.0	4.6	23	5	165.4		
2	New	+23 1/2		440		-	-	0	0	0	193.3	Upper	179	N.T.(6)	14.3	0	0	0	0	0	193.3		
	New	+23 1/2		440		-	-	22	32	4	30.7	Lower	0	N.T.(6)	0	14.5	5.0	4.6	6.6	0	66.7		
	New	+23 1/2		440		8	282	22	32	4	224.0	Total	179	N.T.(6)	14.3	14.5	5.0	4.6	6.6	0	260.0		
3	New	-23 1/2		480		-	-	0	0	0	193.3	Upper	179	N.T.(6)	14.3	0	0	0	0	0	193.3		
	New	-23 1/2		480		-	-	31	42	4	30.7	Lower	0	N.T.(6)	0	14.5	5.0	4.6	6.6	0	76.7		
	New	-23 1/2	Max	480		8	301	31	42	4	224.0	Total	179	N.T.(6)	14.3	14.5	5.0	4.6	6.6	0	270.0		
4	Old	0	Min		420	-	-	0	0	0	193.3	Upper	131	T.(6)	14.3	0	0	0	0	0	145.3		
	Old	0			420	-	-	10	13	4	30.7	Lower	0	T.(6)	0	14.5	5.0	4.6	6.6	0	47.7		
	Old	0			420	11	251	10	13	4	224.0	Total	131	T.(6)	14.3	14.5	5.0	4.6	6.6	0	193.0		
4E	Old	0			0	-	-	0	13	0	114.3	Upper	71	T.(3)	14.3	0	0	0	0	5	90.3	Min. Trans	
	Old	0			0	-	-	0	0	4	47.1	Lower	0	T.(3)	0	14.5	5.0	4.6	23	0	51.1		
	Old	0			0	0	0	0	0	4	161.4	Total	71	T.(3)	14.3	14.5	5.0	4.6	23	5	141.4	Min. Trans	Transmitting 6 TWT Available
5	Old	+23 1/2			400	-	-	0	0	0	193.3	Upper	131	T.(6)	14.3	0	0	0	0	0	145.3	Min. S.S.	
	Old	+23 1/2			400	-	-	0	0	4	30.7	Lower	0	T.(6)	0	14.5	5.0	4.6	6.6	0	34.7	Min. S.S.	
	Old	+23 1/2			400	8	228	0	0	4	224.0	Total	131	T.(6)	14.3	14.5	5.0	4.6	6.6	0	180.0	Min. S.S.	
6	Old	-23 1/2			440	-	-	0	0	0	193.3	Upper	131	T.(6)	14.3	0	0	0	0	0	145.3		
	Old	-23 1/2			440	-	-	5	7	4	30.7	Lower	0	T.(6)	0	14	5.0	4.6	6.6	0	41.7		
	Old	-23 1/2	Min		440	8	240	5	7	4	224.0	Total	131	T.(6)	14.3	14	5.0	4.6	6.6	0	187.0		

N.T. = Not Transmitting (TWT)
TBD = To Be Determined

Table 10-2
SPACECRAFT POWER PROFILE AND HEAT

Table 10-3 Equipment List

Sub-System	Description	Location U. Platform L. Platform	No. Req'd	Unit Wt. Total (lb)	Dimensions L (In)	W (In)	H (In)	Unit Ht. Dissip. Total (Watts)	Baseplate Allowable Operating Temp. Limit (°F) Min	Max	Baseplate Allowable Non-Operating Temp Limit (°F) Min	Max	Baseplate Predicted Synchronous Orbit Temperature (°F) Min	Max
Communications	Preamplifier													
	Bandpass Filter-6GHZ	U. Plat	1	1.2	8.0	2.0	0.5	0	20	120	-20	120	35	118
	Command Rej. Filter		1	0.5	3.0	2.0	1.5	0						
	Switch		2	0.6	2.0	2.5	1.5	0						
	Isolator		1	0.3	1.5	1.5	1.5	0						
	TDA-6 GHZ		2	1.8	4.0	1.0	1.0	2.5						
	Translator Mix.		2	2.5	8.0	4.0	2.0	0						
	L.O. R.F. Source		2	2.7	3.5	2.0	1.5	0						
	Comb Filters		1	0.5	6.0	2.0	1.5	0	20	120	-20	120	35	118
	Driver Stage													
	Switch		2	.6	2.0	2.5	1.5	0	20	120	-20	120	35	118
	TDA-4 GHZ		2	1.8	4.0	1.0	1.0	2.5	20	120	-20	120	35	118
	Driver TWT		2	1.6	11.5	2.5	2.0	3.5	20	120	-20	120	90	118
	TWT Power Supply		2	4.5	10.5	3.5	2.0	1.5	20	120	-20	120	90	118
	Amplifier Stage													
	Multiplexer-Input		2	4.0	7.0	2.5	2.0	0	20	120	-20	120	35	118
	TWT		9	11.3	11.5	2.5	2.0	130*	20	160	-50	160	-40	151
	TWT Power Supply		9	22.1	10.5	3.5	2.0	40*	20	160	-50	160	-40	151
	Isolator		9	2.3	1.5	1.5	1.5	0	20	160	-50	160	-40	151
	Multiplexer-Output		1	4.0	5.0	5.0	5.0	0	20	120	-20	120	35	118
	L.P. Filter		1	.2	-	-	-	0	20	120	-20	120	35	118
	H.A. Filter	U. Plat.	1	.3	-	-	-	0	20	120	-20	120	35	118
	Antenna													
	Antenna Feed/Wave G	Despun	1	2.4	-	-	-	0	-350	250	-350	300	-350	150
	Antenna Support	Despun	1	4.7	-	-	-	0	-350	250	-350	300	-350	150
	Antenna Reflector	Despun	1	3.7	-	-	-		-350	250	-350	300	-350	150
	TOTAL			60.5				180						
Telemetry & Command	Command Rec.	U. Plat	1	3.5	4.0	5.0	5.0	4.3	20	120	-20	120	35	118
	Command Dec.		1	2.0	6.0	5.0	3.0	2.0						
	PCM Encoder		2	7.0	5.0	4.0	8.0	3.2/1.6						
	Tel. Transm.		1	3.5	5.0	5.0	4.0	12.8/6.4						
	Beacon Transm.	U. Plat.	1	2.0	4.0	1.5	1.5	6.0/0	20	120	-20	120	35	118
	Antenna	Despun	2	.7	-	-	-	-	-250	250	-300	300	-350	150
	Antenna Support	Despun	1	1.2	-	-	-	-	-250	250	-300	300	-350	150
	Coax	Despun U. Plat	1	1.0	-	-	-	-	-250	250	-300	300	-350	150
	TOTAL			20.9				28.3/14.3						
Power	Solar Array	-	1	52.4	-	-	-	-	-175	80	-175	200	-165	70
	Battery	L. Plat.	1	30.5	12.0	8.0	15.0	6.5/23.0	50	90	40	100	50	90
	PCU	L. Plat.	1	7.3	7.0	10.0	5.0	4.0	20	120	-20	120	40	100
	Converter	L. Plat.	1	7.0	7.0	12.0	6.0	4.6	20	120	-20	120	40	100
	Shunts	Cylinder	4	2.6	14.0	6.0	1.0	32/0	-20	150	-50	250	0	200
	TOTAL			99.8				47.1/31.6						
Elect. Int.	EIA	L. Plat	1	3.0	7	6	7	.4	20	120	-20	120	20	90
	Harness & Conn.	L. Plat	1	16.0	-	-	-	-	20	120	-20	120	20	90
	TOTAL			19.0				.4						
Attitude Determination	Earth Sensors	L. Plat	2	2.4	-	-	-	1.4	50	110	40	120	55	100
	Sun Sensor	L. Plat	1	0.3	-	-	-	0	40	110	30	120	55	100
	Valve Driver	L. Plat	1	1.5	7	5	1	.3	20	120	-20	120	40	100
	Despin Mech.	U. Plat.	1	13.4	4	4	8	4	20	130	10	140	40	120
	Despin Elect.	L. Plat.	1	9.0	8	8	8	8	20	120	-20	120	40	100
	Damper	Despun	1	1.5	4	2	4	-	0	200	-10	200	30	180
	TOTAL			28.1				13.7						
Positioning and Orientation	Ordnance Valve	L. Plat	1	0.4	-	-	-	-	40	100	40	120	40	70
	Pressure Transducer	L. Plat	2	0.4	-	-	-	-	40	100	40	120	40	70
	F & D Valve	L. Plat	2	0.6	-	-	-	-	40	100	40	120	40	70
	Filter	L. Plat	2	.7	-	-	-	-	40	100	40	120	40	70
	Heat Sink	Thruster	2	0.1	0.5	1	3	-	40	700	40	120	40	700
	Plumbing	L. Plat	1	2.3	-	-	-	-	40	700	40	120	40	80
	Radial Thruster	L. Plat	2	1.1	0.5	0.5	2.	-	40	1750	40	120	40	1750
	Axial Thruster	End Closure	2	1.6	0.5	0.5	2.	-	40	1750	40	120	40	1750
	Propellant Tank	L. Plat	4	9.5	12	12	12	-	40	100	40	120	40	70
	Propellant	L. Plat	-	76.4	-	-	-	-	40	100	40	120	40	70
	Pressurant	L. Plat	-	1.8	-	-	-	-	40	100	40	120	40	70
	TOTAL			94.9				0						
Apogee Motor	Apogee Motor	Cent.	1	45.7	14	14	21	-	30	90	20	120	35	90
	Propellant	Cylinder	1	452.3				-	30	90	20	120	35	90
	TOTAL			498.0				0						

* Only 6 operating at one time 3 are redundant

The spacecraft will be oriented toward the sun as shown in Figure 10-5 during synchronous orbit. The spacecraft will experience a maximum eclipse time of 72 minutes every 24 hours when the sun angle is normal to the spin axis. As the sun angle with the normal to the spin axis increasesin a positive or negative direction, the eclipse time will decrease reaching zero at a $\pm 8^{\circ}$ angle. The spacecraft will encounter the following four synchronous orbit limit sun conditions. The maximum and minimum solar constants used for the limit cases are also given taking into account 3σ and seasonal variations.

	Solar Constant	
	Maximum ($Btu/hr\text{-}ft^2$)	Minimum ($Btu/hr\text{-}ft^2$)
Case 1 sun 0° off normal to spin axis - steady state	460	420
Case 1E eclipse transient - 72' using Case 1 as initial conditions	---	---
Case 2 sun $+23\text{-}1/2^{\circ}$ off normal to spin axis - steady state	440	400
Case 3 sun $-23\text{-}1/2^{\circ}$ off normal to spin axis - steady state	480	440

Two major spacecraft internal heating conditions will affect temperatures in addition to the solar heating and sun angles. The extent of solar array degradation will influence the amount of excess solar array power that is dissipated as heat in the shunts, while the number of TWT's operating will determine the amount of heat that is dissipated on the upper component mounting platform. Six TWT's not transmitting but operating will present minimum steady state heat conditions while three TWT's transmitting during eclipse will present minimum transient heat conditions. Redundant TWT's for the three TWT failure case will prevent the upper equipment platform heat dissipation from falling below the minimum steady state conditions. Table 10-2 summarizes the sun angles solar constant, solar array and TWT operating condition combinations that will produce maximum and minimum steady state spacecraft temperatures as well as minimum transient sclipse temperatures. The predicted temperatures are discussed in detail for the despun and spinning section of the spacecraft in the following sections.

10.2.1.1 Despun Section

- Despin Mechanical Assembly

Figure 10-1 presents despin assembly temperature for a worst summer solstice sun angle case. The radiant thermal coupling between the spinning outer cylinder and despun inner shaft minimizes the maximum temperature differences between the two to less than 20°F. The good thermal conduction in the aluminum cylinder minimizes longitudinal temperature gradients to less than 20°F. The fiberglass thermal insulators between the aluminum spinning cylinder and the main central spacecraft cylinder also minimize longitudinal temperature gradients in the outer spinning aluminum cylinder. The despin assembly will experience average temperatures from 120°F to 40°F during synchronous orbit conditions.

o Antennas

During synchronous orbit the three antennas (1 omni, 1 horn, 1 elliptical) will receive daily variations in incident solar heating due to varying sun angle and shading caused by antenna geometry and placement (Figure 10-5) as well as complete shading during dclipse seasons. The daily variations will produce temperature gradients in the longitudinal and traverse direction for the elliptical antenna, and in the transverse direction for the omni and horn antennas. The omni and horn antennas will receive direct solar radiation on one side except for eclipse and shadowing conditions. White paint on these antennas will produce a maximum temperature of 150°F during sunlit conditions and a minimum of -250°F during eclipse conditions. This range of temperatures will not affect antenna performance appreciably.

Due to pointing accuracy requirements for the elliptical antenna the prediction of thermal gradients and mean temperature variations are important so that thermally induced deflections can be determined. The antenna feed and reflector were designed to be supported by single supports insulated with multilayer aluminized Kapton. The supports will vary in temperature during a typical 24 hour sunlit day as shown in Figure 10-6. The 100°F mean temperature variation in support temperatures as shown in Figure 10-7 would produce significant antenna pointing error in a conventional unequal length 3 strut support even if each strut experienced an equal temperature change. The single support design will not produce antenna pointing errors since the mean temperature variation in the support will only cause the reflector to move vertically, and the feed in a line along the central axis of the reflector. The single support insulation reduces circumferential temperature gradients to less than 15°F to minimize antenna pointing errors caused by support differential expansion. Uninsulated single supports would experience temperature differentials up to 40°F which would produce significant antenna pointing errors. The 40°F gradient across a single uninsulated support is caused by the sun being incident on only one side and the small minimum temperature equalizing effect offered by lateral conduction in the thin wall sections. Thus, the single insulated support design eliminates any need for system penalizing techniques such

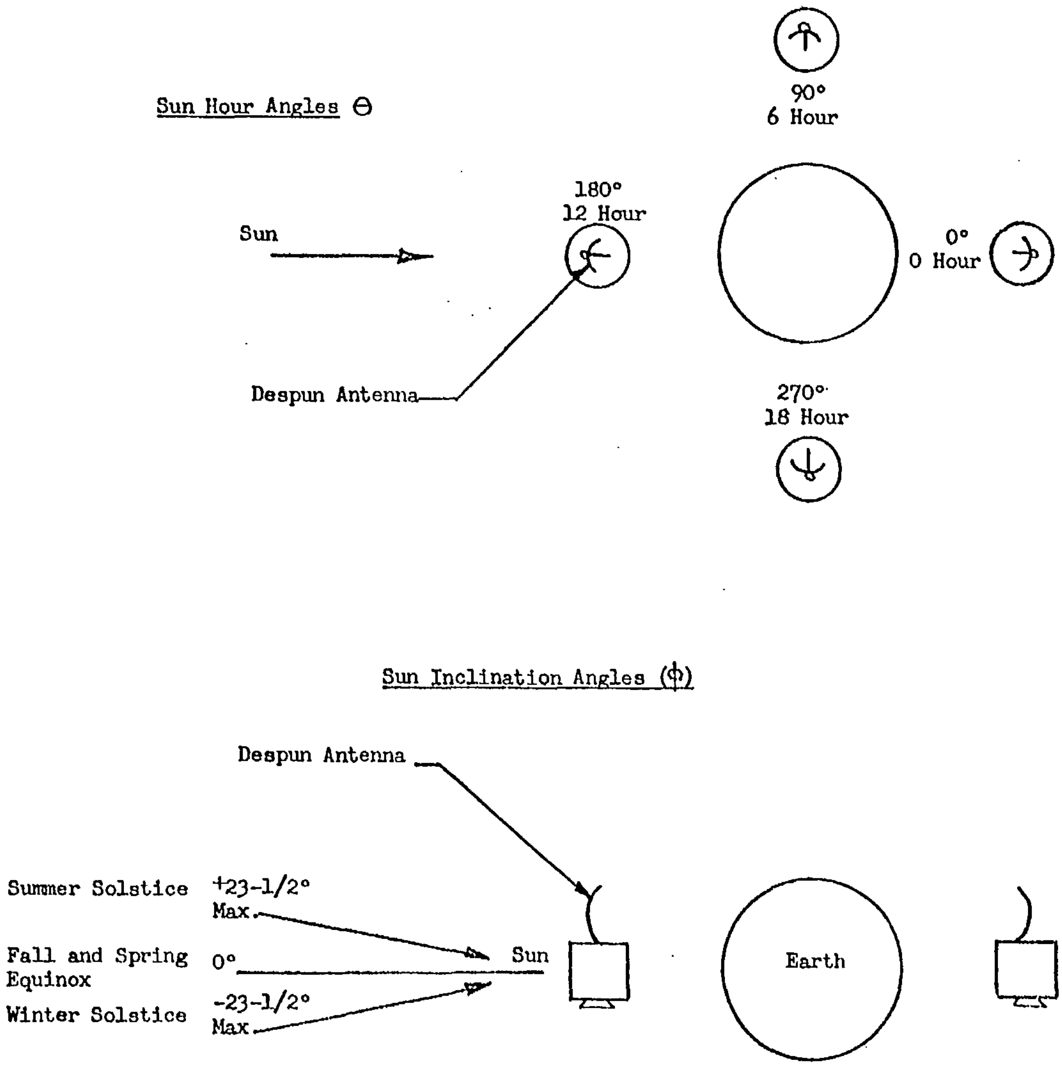

Figure 10-5 Spacecraft Sun-Hour and Inclination Angles

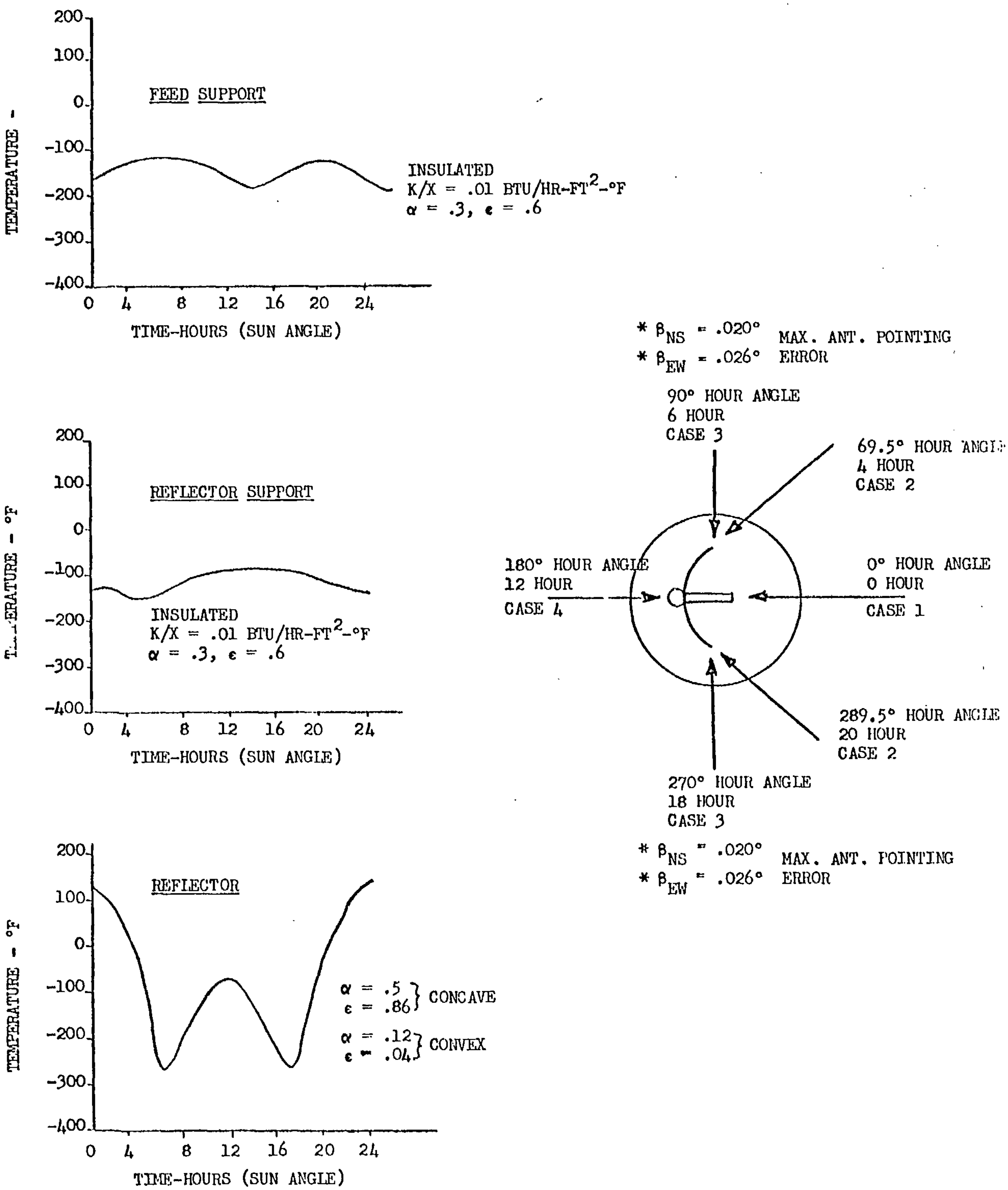

Figure 10-6 Antenna Feed Support, Reflector Support and Reflector Mean Temperature versus Spacecraft Hour Angle

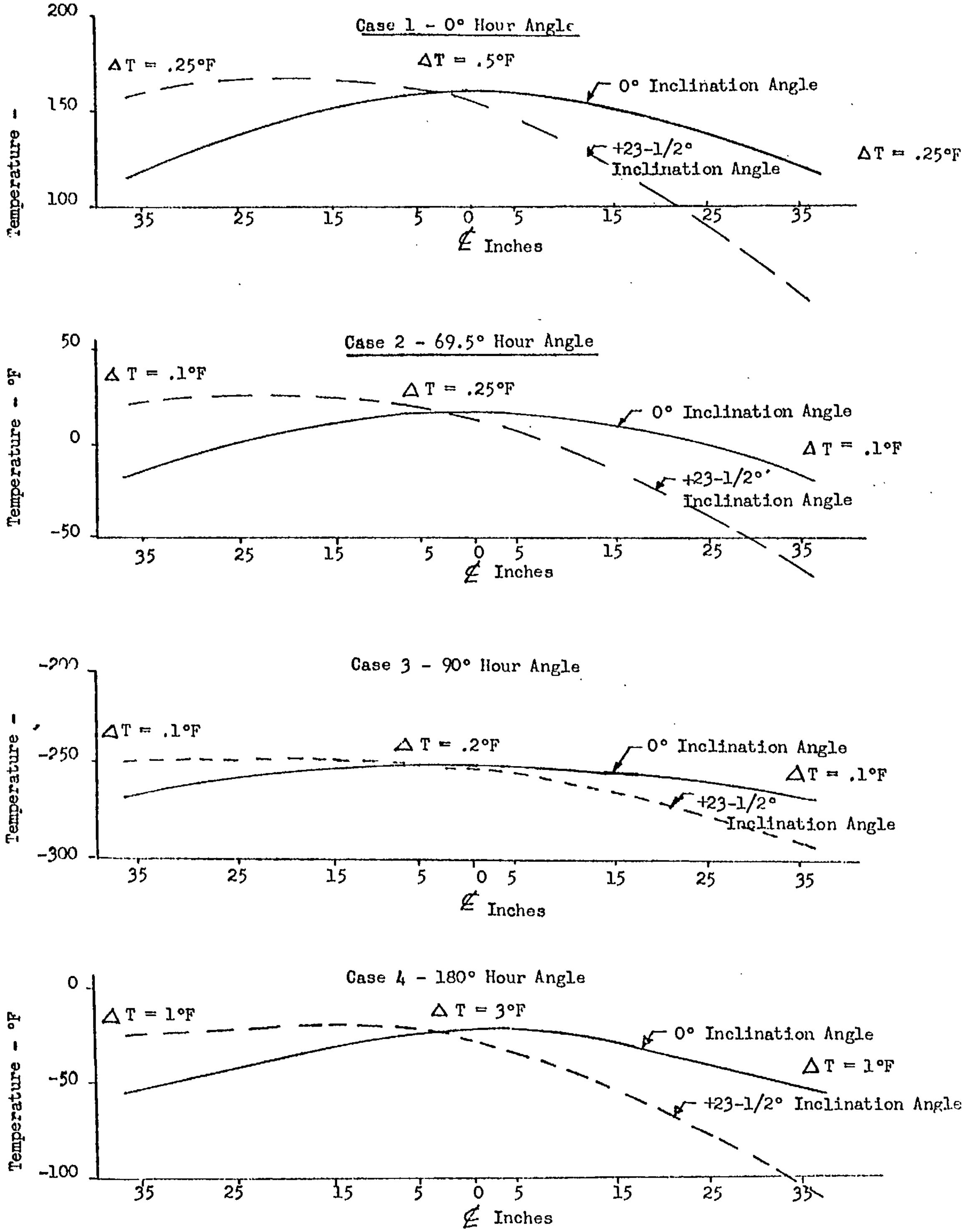

Note: ΔT = Transverse temperature gradient face sheet to face sheet

Figure 10-7 Antenna Reflector Vertical Axis Temperature versus Distance as heavy low thermal expansion materials (Invar) or thermal coupling to the structure (heat leaks) in an effort to maintain ground alignment strut temperatures.

The elliptical antenna reflector will experience lateral and transverse temperature gradients as shown in Figure 10-8 due to daily variations in sun angles. Seasonal variation in sun angle will also cause lateral temperature gradients as shown in Figure 10-8.

The worst combination of reflector support, feed support and reflector induced antenna pointing errors occurs at a sun hour angle of 90° (Case 3) and a solstice sun angle of 23-1/2°. A maximum north-south antenna pointing error of .02° is caused by a reflector longitudinal temperature gradient of 100°F (.007°) and a feed support longitudinal temperature gradient of 20°F (.010°) and transverse temperature gradient of 5°F (.003°). A maximum east-west antenna pointing error of .026° is caused by a reflector longitudinal temperature gradient of 300°F (.022°), and feed support transverse temperature gradient of 15°F (.004°).

. Nutation Damper

The nutation damper mosaic solar collector will be sized such that a maximum temperature of 180°F will be obtained during sunlit conditions. During the 12 hour shadow period caused by the elliptical antenna reflector the enclosure insulation and low solar collector emissivity will limit the nutation damper minimum temperature to 30°F.

. Lower Equipment Platform, Central Column

The component mounting platform will experience average steady state temperature between 100°F and 30°F during sunlit conditions. The minimum eclipse temperature will be limited to 10°F since the mounting platform is conductively decoupled from the solar arrays similar to INTELSAT III. Temperatures from 100°F to 0°F will be obtained on the central thrust cylinder.

The component mounting arrangement on the spinning section platform and expected maximum and minimum temperatures are given in Figure 10-9. Selection of component thermal surface properties and structural thermal coupling to the platform will maintain all component temperatures within allowable limits. The following specific component temperatures were obtained from Intelsat III tests which are representative. The batteries experience temperatures from 90°F to 50°F steady state sunlit and eclipse conditions when they have a surface of white Cat-a-lac paint (ε = .85)

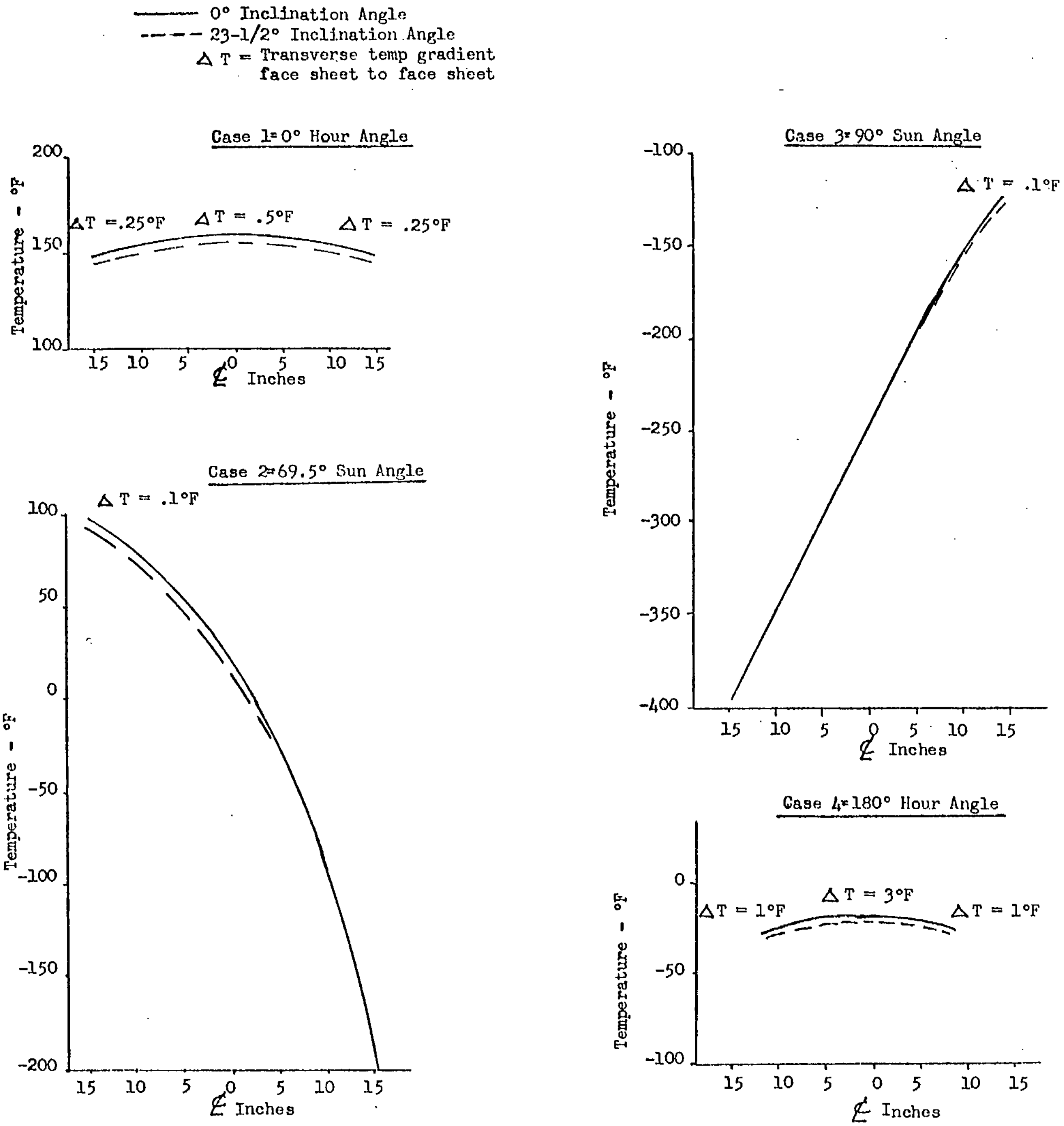

Figure 10-8 Antenna Reflector Horizontal Axis Temperature versus Distance

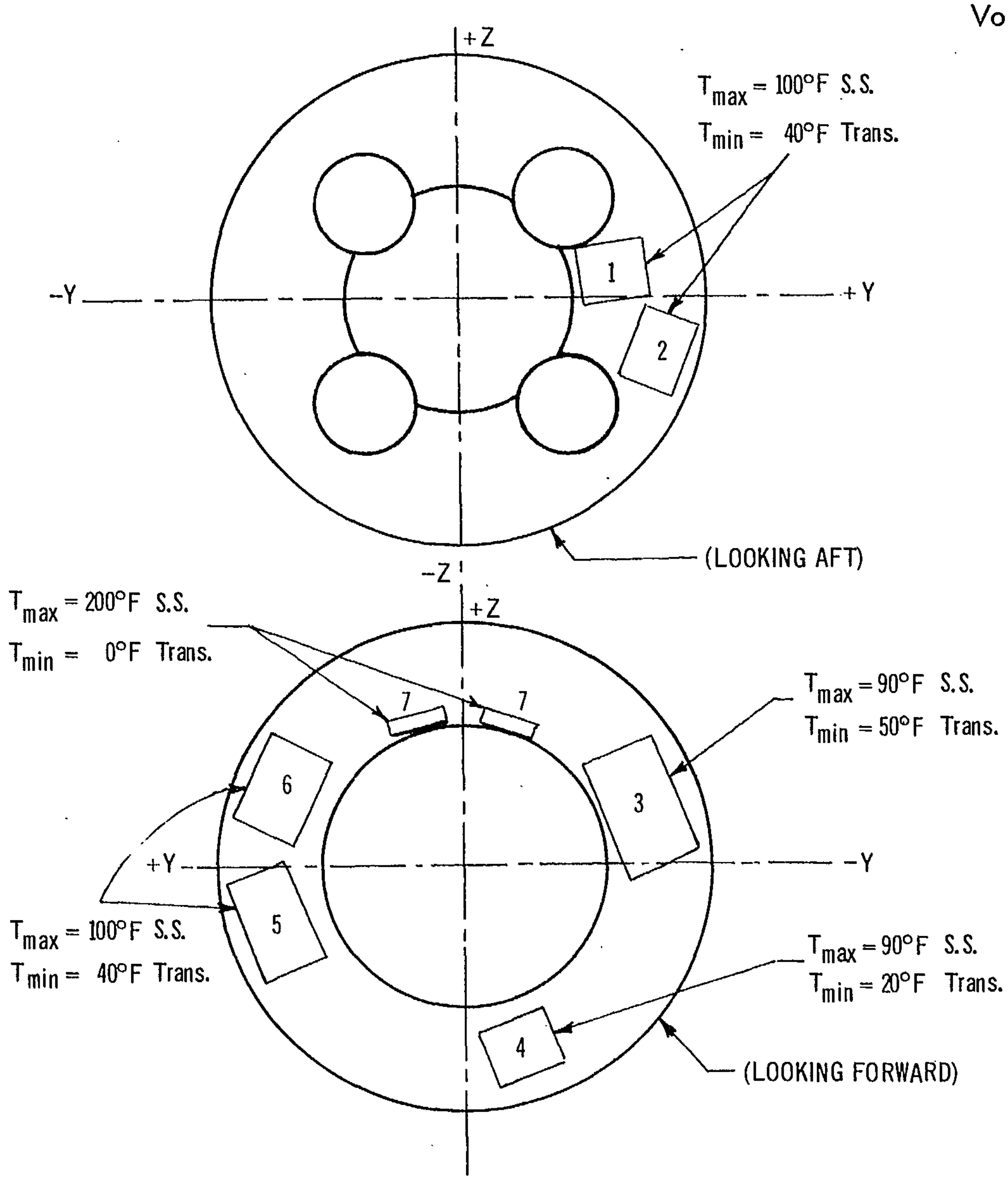

I.D. No.	No. REQ.	MAX POWER DISSIP (ea) (WATTS)	DESCRIPTION	SUBSYSTEM
1	1	0.3	Valve Driver Assy.	Attitude Determination
2	2	8.8▲	Despin Electronics Assy.	Attitude Determination
3	1	6.6●/23*	Battery	Power
4	1	0.4	Electrical Integration Assy.	EIA
5	1	5.6	Equipment Converter	Power
6	1	4.0	Power Control Unit	Power
7	2	16.0	Shunts	Power
TOTAL HEAT Σ		41.7/42.1		

* Eclipse Only
● Tickle Charge Heating
▲ Total of Two
Excess Solar Array Capacity

Figure 10-9 Aft Equipment Platform

and are thermally decoupled from the platform with honeycomb standoffs. The despin bias assembly, despin electronic assembly, converters and power control unit maximum and minimum temperatures will be from 100°F to 40°F.

. Solar Arrays and Aft Closure

The solar arrays will experience temperatures from 70°F to 35°F during steady state sunlit conditions. During eclipse transient conditions the solar arrays will drop to a minimum temperature of -165°F. These temperatures are based on solar cell thermal properties of a - .79, = .82 on the external surface and solar array substrate weight greater than .65 lb/ft^2.

The axial positioning and orientation thruster will not produce appreciable convective plume impingement heating on the solar arrays or aft end closure. The radiation shield around the axial thruster (Figure 10-4) will minimize radiant heat transfer to the end closure as accomplished in INTELSAT III. During the approximate 30 second apogee motor firing, the aft end closure will experience maximum temperatures of 1100°F when exposed to the radiant plume heating rates given in Figure 10- 10. These temperatures are within 200°F of those predicted for the same type aft closure material used on INTELSAT III. Tests performed on INTELSAT III aft closure material indicate that it will withstand these higher temperatures.

. Apogee Motor

The high temperature aluminum foil and dexiglass insulation around the apogee motor and the fiberglass structural thermal isolators will maintain the motor within allowable temperature limits prior to firing and prevent excessive spacecraft temperatures due to heat soak back after firing. The apogee motor insulation and thermal isolators are designed to withstand temperatures up to 800°F. The apogee motor will be maintained between 30°F and 90°F prior to engine firing by the thermal capacity of the motor and the surrounding insulation and thermal isolators as on INTELSAT III.

. Positioning and Orientation Subsystem Components

The hydrazine propellant tanks will experience temperatures from 70°F to 40°F during steady state sunlit conditions. During eclipse conditions multilayer Mylar insulation is required to limit the hydrazine tank temperature decrease to 10°F when they are nearly empty. The hydrazine tank temperatures will decrease less than 2°F when they are full. The lines to the thrusters and the valves will experience temperatures similar to the hydrazine tanks during steady state conditions. The low heat capacity of the supply line filled with hydrazine makes multilayer insulation necessary to limit temperature decreases during eclipse conditions to less than 10°F. The valves near the thruster

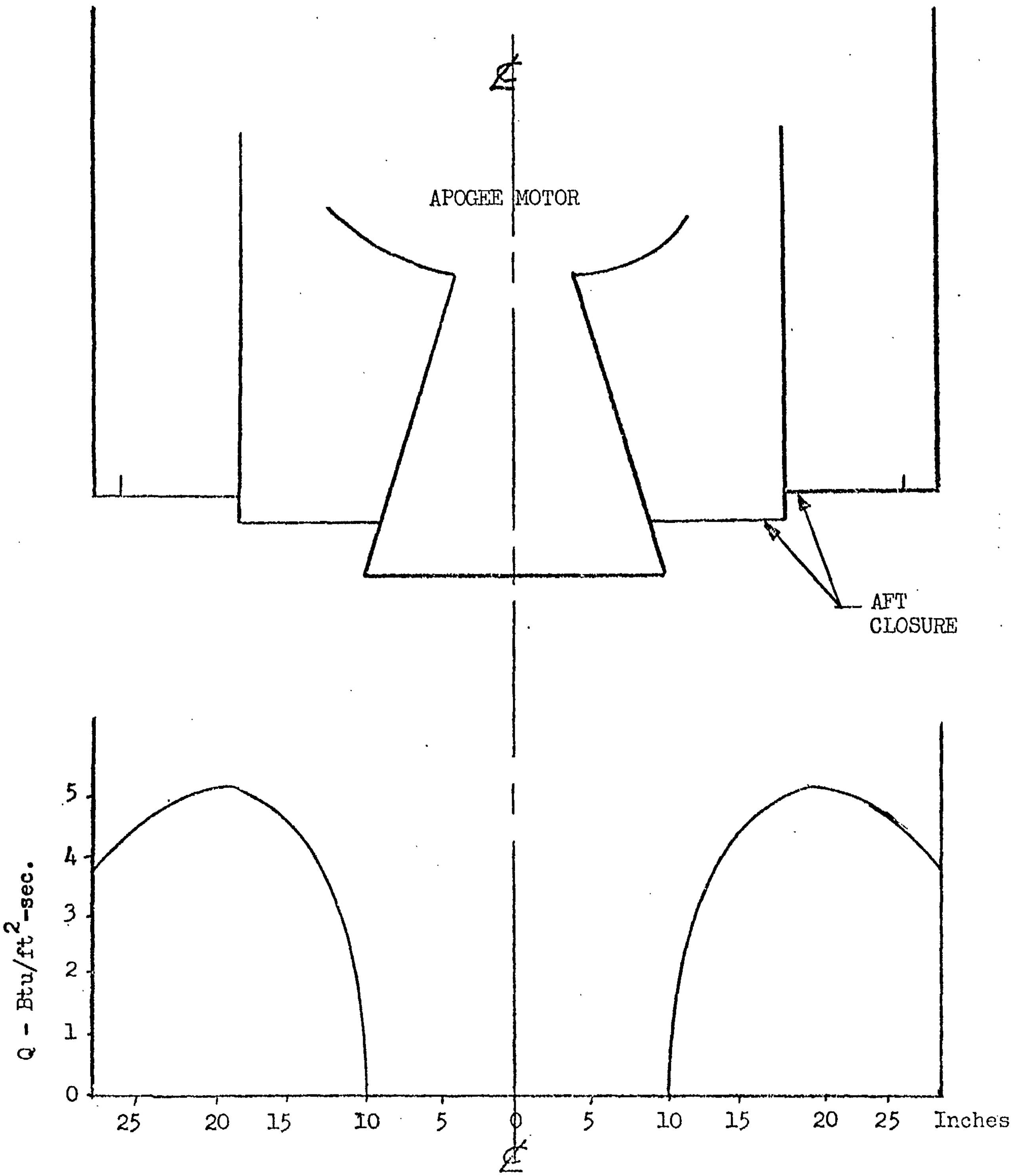

Figure 10-10 Estimated Apogee Motor Radiant Heating on Aft Closure versus Distance

incorporate INTELSAT III type low emissivity high thermal capacity heat sinks and solar collector high α/ϵ windows to maintain valve temperatures within allowable limits. The axial thruster may operate for minutes reaching temperatures of 1750°F and are therefore enclosed in previously described insulation to limit local heating of structure.

10.2.2 Transfer Orbit

The spacecraft will be injected into a transfer orbit from parking orbit. Several transfer orbits may be required before the apogee motor places the spacecraft into synchronous orbit. The synchronous orbit natural environments given in Table I are used for analysis, except specific transfer orbit charged particle effects. To maintain spacecraft temperatures within allowable limits with a passive design during extended transfer orbit times, equipment will have to operate at near full power levels. Figure 10-11 presents a plot of spacecraft/sun angles experienced during transfer orbit for three seasonal sun/earth angle condition (summer solstice, spring and fall equinox, and winter solstice). The horizontal hour scale indicates the relative time at which the spacecraft is injected into the transfer orbit. The horizontal dotted lines represent spacecraft/sun angles of $\pm$ 23-1/2° off the normal to the spin axis similar to the sun angles experienced during synchronous orbit. It can be seen that by limiting the launch and parking orbit times, the spacecraft will see transfer orbit sun angles within the range seen during synchronous orbit.

Spacecraft sun angles up to $\pm$ 45°, which would still allow sufficient power output due to the excess array capacity at this time, are acceptable. Due to the low solar absorptivity thermal design features incorporated for optimum synchronous orbit performance, the increased solar load on the end closure and upper platform with even greater sun angles would not compensate for the loss of array power and internal component heating.

The $\pm$ 23-1/2° sun angle can be achieved by limiting launch times to approximately 4 hours out of every 24 while the $\pm$ 45° angle limits launch times to 12 hours out of every 24. Equinox eclipse at apogee in the transfer orbit could exceed 2 hours which would be excessively long to maintain temperature control. Figure 10-11 indicates this possibility by a dark line on the 0° sun/earth angles line. Proper selection of launch times during eclipse seasons can prevent such an eclipse from occurring. This consideration only applies four months of the year for near equinox launches with no restriction during the rest of the year.

Since the transfer orbit spacecraft/sun angles, eclipse times, and internal power levels can be maintained within synchronous orbit limits, the synchronous orbit performance will apply and be quite similar up to

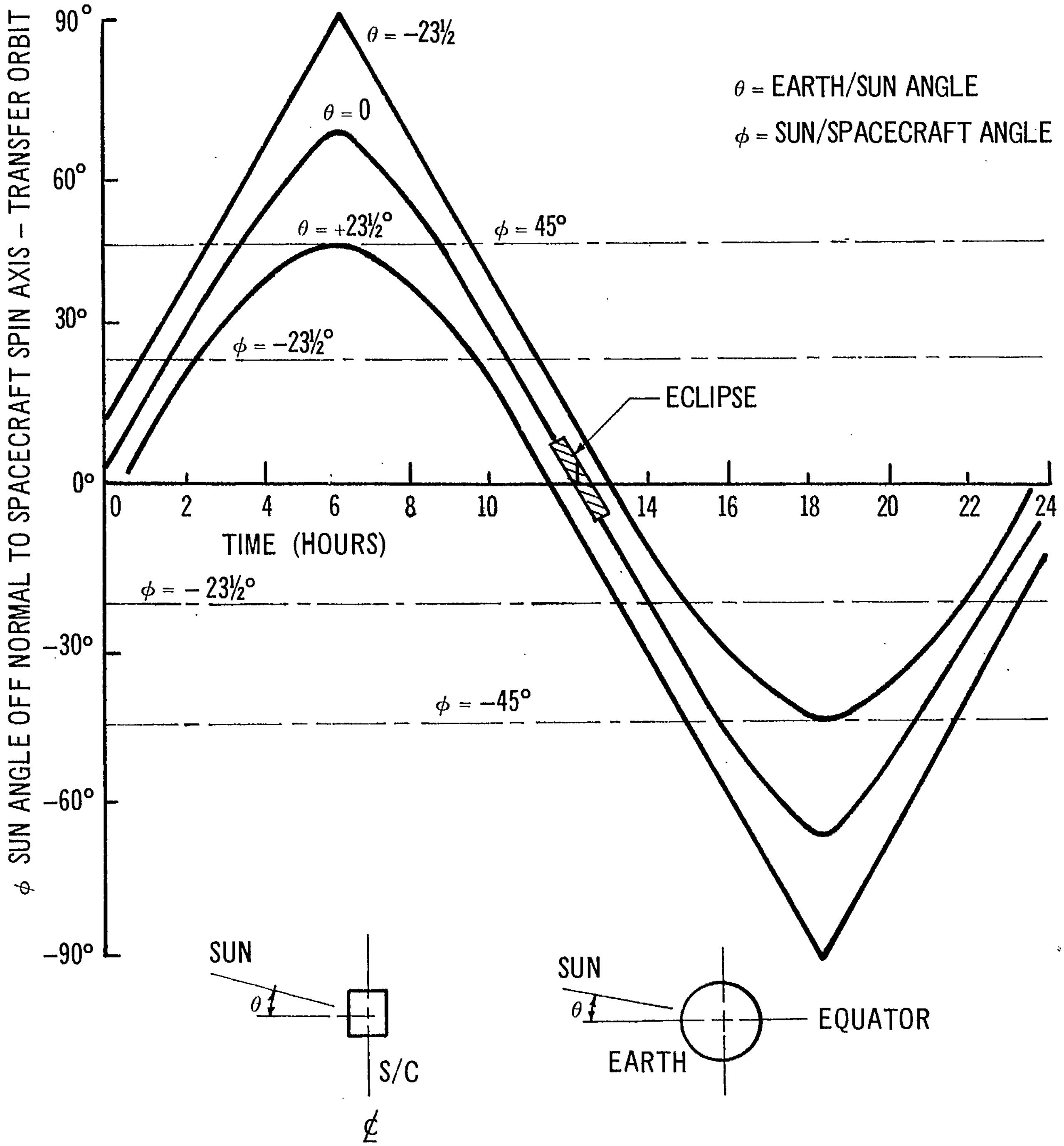

Figure 10–11 Launch times to obtain given spacecraft/sun angles during transfer orbit

$\pm 45^{\circ}$ spacecraft/sun angles. The apogee motor minimum temperature limit prior to firing, apogee motor radiant plume heating and soak back, associated specifically with transfer orbit conditions, have been discussed in the synchronous orbit section.

10.2.3 Parking Orbit

The spacecraft will be injected into parking orbit and remain attached to the booster. The spacecraft and booster will not be spinning, and the aerodynamic shroud will be removed. Natural environments given in Table I will apply. Due to the limited battery power, electrical components will not be operating and dissipating heat during earth orbit.

Spacecraft component temperatures might cool or warm slightly depending on whether injection is followed by earth eclipse or sun conditions. In either case temperatures will not change appreciably due to the heat capacity of the spacecraft and the limited parking orbit time. The parking orbit time will be limited to the first or second crossing of the equator (15 to 45 minutes).

10.2.4 Boost

The spacecraft will be protected by shroud during boost that will not exceed $300^{\circ}F$ based on past experience. The maximum radiant heat rate (.1 Btu/ft^2) from the shroud will be insignificant. The shroud is normally separated when the external aerodynamic stagnation heating rate is below a level determined by spacecraft external material temperature limits and response times. A temperature limit of the order of $500^{\circ}F$ for thin film low heat capacity Kapton insulation, would require an aerodynamic free molecular stagnation heating rate of .35 Btu/ft-sec or less to exist before the shroud is separated. The spacecraft will not be dissipating appreciable heat internally in order to conserve battery power. The heat capacity of the spacecraft will limit significant temperature excursions during boost.

10.2.5 Ground Hold

When the spacecraft is enclosed in the shroud during ground hold, internal component heating must be limited or cooling air must be supplied to maintain components within allowable temperature limits. For example, 50 cfm of 70° air directed over the external surface of the upper platform, would allow operation of the upper platform components. Natural convection cooling internal to the spinning section of the spacecraft, in conjunction with the air being circulated in the shroud, would allow operation of lower platform components.

II 11
STRUCTURE

11. STRUCTURE

11.1 VEHICLE LOADS AND ENVIRONMENTS

Design of the proposed satellite structure is based on the vibration environments described in Section 11.1.1 and on the "quasi-static" loads described in Section 11.1.2. These quasi-static loads represent loads induced by in-flight dynamic events such as engine ignition and burnout, stage separation, and orbit injection.

Preliminary design included formulation of dynamic models -- a lateral beam model, and a lumped-mass longitudinal model - to determine vibration induced loads in the antenna support structure and in the despin controller, and to ascertain frequencies and mode shapes for the spacecraft.

11.1.1 Vibration Environments

For the two launch vehicles presently under consideration -- Thor Delta and Atlas Burner II -- applicable sinusoidal and random vibration environments are presented in the following. Loads quoted are to be applied through a suitable fixture to the spacecraft separation ring.

11.1.1.1 Thor Delta

Levels shown are acceptance levels. Sinusoidal levels are scaled-up by a factor of 1.5, and sweep rate is reduced by a factor of 2 for qualification.

Table 11-1 Thor Delta Sine Acceptance Levels

	Sinusoidal Vibration (2 Octaves/Min)	
	Frequency (Hz)	Level (G's, 0 to p)
Thrust Axis	10-17	2.0
	17-23	4.0
	23-100	1.5
	100-250	2.0
	250-400	3.0
	400-2000	5.0
Lateral Axis	5-250	1.5
	250-400	2.0
	400-2000	5.0

Lateral vibration levels may be notched in the vicinity of fundamental lateral bending modes such that loads in the primary structure do not exceed quasi-static boost loads.

Radom levels are to be scaled-up by a factor of 2.25 for qualification. Test duration is to be increased by a factor of two for qualification.

Table 11-2 Thor Delta Random Acceptance Levels

	Random Vibration (Duration:) (1 Minute)	
	Frequency (Hz)	Level (G^2/Hz)
Thrust Axis and Lateral Axis	20-150 150-300 300-2000	0.01 +3 DB/Octave 0.02

Component Qualification for Thor Delta

Assemblies which mount onto the spacecraft equipment platform or central cylinder except for the propellant tanks and battery may be tested to levels shown in Table 11-3. The battery and propellant tanks may be tested to the levels shown in Table 11-4. A qualification test may be derived for the despun antenna assembly by analytically modeling the spacecraft and determining the response fo the analytic model at the MDA/spacecraft interface due to an input of 1.5 times Table 11-1 at the separation plane. A random test level may be similarly derived using 2.25 times Table 11-2.

Table 11-3 Qualification Levels for Components
Other Than Battery and Propellant Tanks

Test	Axis	Frequency (Hz)	Level
Sinusoidal 2 Octaves/ Minute	Longitudinal and Lateral	10-35	0.4 d.a.
		35-120	18.0 G rms (6.0 G rms for shunt)
		120-2000	3.5 rms
Random (4 minutes)	Longitudinal and Lateral	20-150	0.03 G^2/Hz
		150-300	Increase to 0.06 G^2/Hz at +3 db/octave
		300-1500	0.06 G^2/Hz
		1500-2000	Decrease from 0.06 G^2/Hz at -12 db/octave

Table 11-4 Qualification Levels for
Battery and Propellant Tanks

Test	Axis	Frequency (Hz)	Level
Sinusoidal 2 Octaves/ Minute	Longitudinal	10-38	0.4 inch d.a.
		38-100	21.2 G rms
		120-400	10.6 G rms
		400-2000	5.3 G rms
	Lateral	10-24	0.4 inch d.a.
		24-400	8.5 G rms
		400-2000	5.3 G rms
Random (4 minutes)	Longitudinal and Lateral	20-400	0.23 G^2/Hz
		400-1500	0.02 G^2/Hz
		1500-2000	Decrease from 0.02 at - 12 db/octave

Levels tabulated have been derived from INTELSAT III specifications and should be verified for the present configuration using analytic modeling and data from the structural dynamic model.

Each assembly designated for qualification vibration should be attached to the vibration exciter by means of a rigid fixture simulating normal service mounting. Vibration should be applied consecutively along each of three mutually perpendicular axes at points of attachment of the assembly to the test fixture.

11.1.1.2 Atlas Burner II

The sinusoidal acceptance levels for the longitudinal axis only are suggested as a preliminary sinusoidal environment. These levels are considered to be conservative since they were derived from Atlas-Agena flight data which include a significant contribution from the Agena ignition and shutdown events. Should this conservatism cause a significant weight penalty, the environment should be further evaluated.

Table 11-5 Atlas Burner II Since Acceptance Level

	Sinusoidal Vibration (2 Octaves/Min)	
	Frequency (Hz)	Level (G's, 0 to p)
Thrust Axis	10-50	1
	50-90	1.4
	90-100	linear rise from 1.4 to 2.1
	110-280	2.1
	280-320	linear rise from 2.1 to 3.4
	320-2000	3.4

For items weighing over 50 pounds the random flight levels quoted in Table 11-6 apply.

Table 11-6 Atlas Burner II Random Flight Levels for Items Over 50 lbs.

	Frequency (Hz)	Level (G^2/Hz)
Items Over 50 #	22-300 300-650 650-1000	+6 DB/Octave .014 -4.5 DB/Octave .0075

For items weighing less than 50 pounds the random flight levels quoted in Table 11-7 apply.

Table 11-7 Atlas Burner II Random Flight Levels for Items Under 50#

	Frequency (Hz)	Level (G^2/Hz)
Items Under 50#	17-37 37-160 160-600 600-1000 1000-2000	.006 +6 DB/Octave .12 -4.5 DB/Octave .06

11.1.2 Load Factors

Limit design load factors are presented in the following for both Thor Delta and Atlas Burner II. Loads aft are taken as positive. The longitudinal direction defines the thrust axis; the lateral axis referred to is any axis normal to the thrust axis.

Table 11-8 Thor Delta Load Factors

	Load Factors (G's)	
	Longitudinal	Lateral
THOR:		
Max. Longitudinal	8.0	± 2.0
Min. Longitudinal	-3.0	± 2.0
Max. Lateral	8.0	± 2.0
TE-364-3 B.O.	9.6*	0
Apogee Motor B.O.	7.3*	0

Table 11-9 Atlas Burner II Load Factors

	Load Factors (G's)	
	Longitudinal	Lateral
SLV-3		
Max. Longitudinal	8.1	± 0.5
Min. Longitudinal	-2.0	± 0.5
Max. Lateral	3.0	± 2.5
Burner II B.O.	8.0*	0
Apogee Motor B.O.	7.3*	0

*A steady-state spin-rate of 110 rpm will act in conjunction with this load factor.

11.1.3 Acoustic Environment

For small payloads normally flown on a Thor-Delta, acoustic tests are not normally specified. The vibration testing specified in the previous sections is usually deemed adequate to cover the launch environments. However, because of the improved payload capabilities of the Thor-Delta, the payload weights and sizes are reaching such a magnitude that vibration testing of the complete vehicle may not be realistic. The vibration levels reaching the upper portions of the spacecraft may be substantially attenuated during conventional testing. Therefore, it is recommended that qualification testing of the assembled spacecraft include an acoustic test instead of a vibration test. Acceptance testing of the complete spacecraft would still include a low level vibration test.

Moreover, certain external components, e.g., solar arrays and antenna, may be particularly sensitive to flight acoustics. Components such as these should be subjected to acoustic testing during the component qualification phase.

The acoustic levels for these tests are shown in Tables 11-10 and 11-11. In the test chamber, the spacecraft should be suspended with a system whose natural frequency for all modes is less than 25 Hz.

Table 11-10 Acoustic Levels
for Spacecraft Flown on Thor-Delta

Frequency (Hz)	Sound Pressure Level - db (ref. .0002 dynes/cm^2) Qualification	Acceptance
37.5-75	128	124
75-150	133	129
150-300	136	132
300-600	138	134
600-1200	139	135
1200-2400	136	132
2400-4800	132	128
4800-9600	127	123
OVERALL	144	140
TIME	60 Sec.	30 Sec.

Table 11-11 Acoustic Levels
for Spacecraft Flown on Atlas

Frequency (Hz)	Sound Pressure Level - db (ref. .0002 dynes/cm^2)	
	Qualification	Acceptance
37.5-75	128	124
75-150	136	132
150-300	138	134
300-600	139	135
600-1200	137	133
1200-2400	135	131
2400-4800	132	128
4800-9600	128	124
OVERALL	145	141
TIME	60 Sec.	30 Sec.

11.1.4 Shock Environment

The shock transients which occur during the launch phase have been considered in the derivation of the vibration test levels listed in 3.1.1., and the damaging effects of the launch shocks and normal handling and transportation are adequately covered by the vibration tests.

To simulate pyrotechnic separation shock a sinusoidal sweep test (Table 11-12) may be applied to the spacecraft/attach fitting assembly for qualification. No system acceptance test is recommended. In addition, sensitive components -- those small, high density components mounted adjacent to the separation plane -- may be reviewed, and shock tests on individual components may be performed as required.

Table 11-12 Qualification Shock Test Levels for Spacecraft Flown on Thor-Delta
(Applied along thrust and 2 lateral axes)

Frequency (Hz)	Acceleration G's 0-P
150-200	1.5 lateral 2.3 thrust
250-400	4.5
400-2000	7.5

11.2 VEHICLE STRUCTURE

11.2.1 Design Criteria

The spacecraft structural subsystem has been designed using the vibration and quasi-static loads described in Section 11.1. The load factors in Tables 11.1.8 and 11.1.9 are limit loads in g's, and for structural design, are multiplied by an ultimate factor of safety of 1.5. All structural components are designed to have a positive margin of safety above ultimate design load.*

Three of the load conditions described in Section 11.1 govern the structural design; max "q", first stage burnout, and apogee motor burnout. The latter two conditions design all of the primary structure. For those components which are critically loaded by vibration during max "q" (e.g. the solar array substrates), ultimate "g" factors were determined by calculating the dynamic response of the component at its natural frequency.

11.2.2 Design Configuration

The chosen design corresponds closely to INTELSAT III and the proposal for INTELSAT IV, which would enable the utilization of analysis and fabrication techniques that are already developed. The central support structure is the "core" of the spacecraft structural subsystem: all component loads feeding directly into it, and then transferring to the booster (see figure 11.1). The antennas and their support structure are despun relative to the spin stabilized spacecraft and all loads from the antennas go directly into the central support structure through the despin mechanism. The two equipment platforms are supported by struts attached directly to the central support structure and the solar array substrates are attached to the aft equipment platform. The motor is internal to the central support structure and is attached to it by a support ring. The system thus has extremely simple load

---

* Limit load is defined as the maximum load the structure will be subjected to while in normal service.

Ultimate design load is defined as that load at which no failure will occure; wherein, failure is described as either excessive stress, deformation or buckling such that the structural member can no longer function.

$$\text{Margin of Safety} = \frac{\text{Stress which would cause failure}}{\text{Stress at ultimate design load}} - 1.0$$

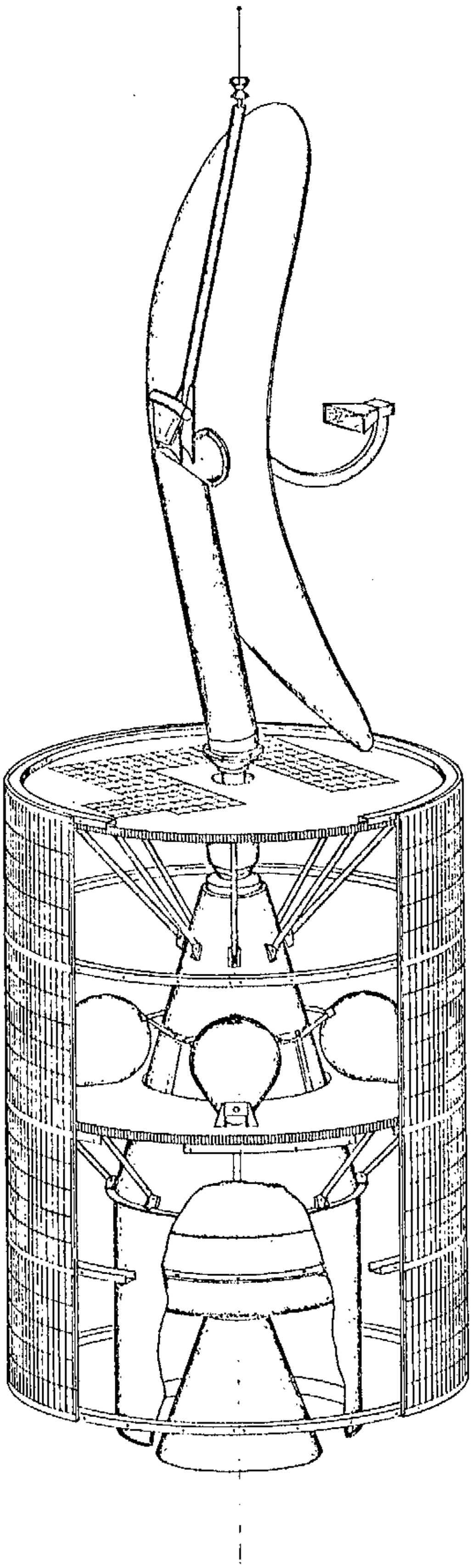

Figure 11-1 Vehicle Structure

paths, yet still contains enough redundancy to insure a high degree of reliability at minimum weight. All metallic components are made from aluminum alloys. The substrates are made with fiberglass face sheet, curved honeycomb panels.

11.2.2.1 Antenna Support Structure

The large contoured parabolic antenna (Figure 11 -1) is a 3/8" thick honeycomb panel with .006" aluminum face sheets supported by a 5" dia. x .050" aluminum tube, which is bolted directly to the despin mechanism. The assembly has been designed for stiffness, having a lateral fundamental frequency of 36.5 Hz, which will assure decoupling from any vehicle modes. The maximum equivalent static deflection of the CG of the antenna system at ultimate loading will be 0.50". The small omni antenna is supported on a 1-1/2" dia. x .050" aluminum boom, and it also has a lateral natural frequency greater than 30 cps. Thermal distortions of the antenna support structure are reduced by using a single insulated support for each antenna to minimize thermal gradients.

11.2.2.2 Forward Equipment Platform

The forward equipment platform is a 0.75" thick aluminum honeycomb shelf with .012"-2034-T3 aluminum facesheets bonded to 2.4 - lb/ft^3 core. The outer diameter is approximately 52" and the inner diameter is approximately 8". It is supported outboard by eight - 9/16" dia. x .035", equally spaced; aluminum struts and by the despin mechanism housing at the center. The primary criteria in designing the platform is stiffness, so that the first natural frequency is decoupled from any body modes and vibration amplitudes are minimized. Based on a preliminary dynamic analysis, using a Rayleigh approximation, the first mode (the "umbrella mode") of the platform is between 30 and 40 Hz.

11.2.2.3 Aft Equipment Platform

The aft equipment platform supports more mass than the forward platform, and its geometry is slightly different, having a 22" diameter cut-out in the center. Based on the loading, it was determined that the aft equipment platform could be the same size as the forward platform, i.e., 0.75" thick with .012" aluminum facesheets at top and bottom. The aluminum honeycomb core is more dense (3.1 lb/ft^3), however, to account for the increased shear at each of the eight support struts, due to the greater loading. Because of its smaller area the aft platform is an inherently stiffer structure than its counterpart, using the same materials. By use of empirical similarity factors for vibration of circular plates, the first mode of this platform is calculated to be between 40 and 50 Hz.

11.2.2.4 Central Support Structure

The Central Structure transfers all loads from the antenna, the solar array substrates, the platforms, and the motor to the booster adapter. It is basically a semimonocoque structure with eight equally spaced longerons and intermediate circumferential rings. The forward portion is a conical frustrum which mates with the aft portion, a cylinder.

Treating the Central Support Structure as a cantilever beam, and using a Rayleigh approximation with variable moment of inertia, it is found that the lateral natural frequency of the structure is between 50 and 60 Hz. The lateral deflection at the forward equipment platform is found to be less than .20" under ultimate dynamic load conditions.

11.2.2.4.1 Conical Section

The conical portion is covered with .020" x 2024-T3 aluminum sheeting, riveted to 1.00" x 0.50" x .030" - 2024-T3 aluminum channel section longerons. These line up with the attach points of the struts of both the forward and aft equipment platforms, and can react the longitudinal loads in direct tension or compression. There is a circumferential ring at both the top and bottom of the concial portion to react the kick loads.

11.2.2.4.2 Cylindrical Section

This portion mates with the conical section, but is of heavier materials due to the increased loading. Skin thickness is .028" and the eight longerons are 1.75 x .75 x .040" channel section. The flange at its aft end forms the interface with the booster adapter. The motor support ring is located at the forward end of the central support structure and is designed assuming that the motor is continuously attached to the ring, while the ring is supported at eight equal hardpoints by the longerons. A 2.00" x 0.75" x .050" - 2024-T3 aluminum channel is found to be adequate.

11.2.2.5 Solar Array Structure

The solar array substrates are similar to those used on INTELSAT III; eight curved sandwich panels, made from .010" thick fiberglass faces with an aluminum core, 3/8" thick. Each substrate panel is supported at its 1/4 points by circumferential aluminum rings, approximately 55" in diameter. Stiffness is the governing factor of this design to prevent "popping" of the solar cells. Each panel is calculated to have a natural frequency of 50-60 Hz. The panels are not structurally connected to each other along their longitudinal edges.

The circumferential rings tie the substrate assembly together and distribute shear loads. The total longitudinal load of the assembly is transferred by the center ring to the aft equipment platform.

11.2.3 Performance

Using the design criteria and safety factors discussed in Section 11.2.1 internal load distributions were determined for the various flight and test conditions. All major structural members and assemblies were analyzed for their critical loads to verify positive margins of safety and to provide data for a realistic weight estimate. Table 11.2.1 lists critical design conditions, most probable failure modes and margins of safety for major items of the spacecraft structural subsystem. Details of the stress analysis can be found in Appendix A for this volume.

TABLE 12-13

Structural Performance Survey

Item	Description	Critical Condition	Failure Mode	Margin of Safety
Antenna *	Honeycomb Sandwich	Max q	Bending	Large
Antenna Support Structure *	5.0" x .050" Tube	Max q	Bending	Large
Fwd. Equip. Platform *	Honeycomb Sandwich	Apogee Motor Burnout	Core Shear Failure	+0.08
			Facesheet Bending	+2.61
Support Struts	9/16 - 0.35" Tube	Apogee Motor Burnout	Column Buckling	+0.14
Aft Equip. Platform *	Honeycomb Sandwich	Apogee Motor Burnout	Core Shear Failure	Positive
			Facesheet Bending	+0.58
Support Struts	9/16 - .035" Tube	Apogee Motor Burnout	Column Buckling	+0.56
Central Support Structure:				
Conical Portion Skin	.020" Skin	First Stage Burnout	Panel Shear Buckling	+0.53
Conical Portion Longerons	Section	First Stage Burnout	Column Buckling	+0.60
Cyl. Portion Skin	.028" Skin	First Stage Burnout	Panel Shear Buckling	+0.18
Cyl. Portion Longerons	Section	First Stage Burnout	Flange Buckling	+0.19
Motor Support Ring	Section	Apogee Motor Burnout	Flange Buckling	+0.85
Array Substrate *	Honeycomb Sandwich	Max q	Core Shear Failure	Large
			Facesheet Bending	+5.0
Array Support Ring	Section	Max q	Buckling	+0.61

*These items designed primarily for stiffness.

MASS PROP

12. MASS PROPERTIES

During the spacecraft study a complete analysis of the mass property characteristics of the vehicle was accomplished. The objectives of the analysis were as follows:

Insure that the spacecraft weight does not exceed the capability of the boost vehicle, and that an adequate weight margin exists to allow for possible growth.

Position subsystem components within the vehicle to insure that:

a) The center of gravity lies on the spin axis.
b) Lateral moments of inertia are nearly equal.
c) Center of gravity travel due to expulsion of hydrazine is minimized.
d) Products of inertia are held to a minimum to lessen the amount of balance weight required to dynamically balance the spinning portion of the spacecraft.

Spacecraft mass property characteristics are shown on Tables 12-1, 12-2, and 12-3. Table 12-1 is a payload weight summary and Table 12-2 gives detailed spacecraft subsystem weights. Presented in Table 12-3 are spacecraft weights, centers of gravity, and moments of inertia at launch, apogee motor burn out, and end of mission.

12.1 WEIGHT

As shown in Table 12-1 the spacecraft weight without contingency has been estimated to 927 pounds. The Thor/Delta allowable payload weight is 1005 pounds and 40 pounds has been allocated for the booster adapter; therefore the spacecraft contingency is 38 pounds. This weight is 9.6% of the spacecraft hardware weight and provides an adequate margin for growth. The apogee motor has been sized for the maximum spacecraft weight, 965 pounds, and similarly the hydrazine system has been sized for a 965 pound spacecraft, less apogee motor expendables. Therefore, the contingency weight may be used entirely for added hardware or increases in existing hardware weights.

12.2 CENTER OF GRAVITY

The centers of gravity of the spinning and despun portions of the spacecraft have been computed to be on the spin axis and the center of gravity of the composite spacecraft remains on the spin axis throughout the life of the spacecraft. A longitudinal shift of approximately 0.3 inches does, however, occur after apogee motor firing but this is not considered to be excessive.

12.3 MOMENTS OF INERTIA

As can be seen on Table 12-3 the ratio of the roll moment of inertia to the maximum transverse moment of inertia is for all conditions less than unity. The wobble damper, as a result, was placed on the despun portion of the spacecraft to maintain stability.

Table 12.1

PAYLOAD WEIGHT SUMMARY

Item	Weight (lbs)
Communications	71.0
Telemetry & Command	19.0
Antennas	13.7
Electrical Power	99.8
Electrical Integration	19.0
Attitude Determination	29.0
Structure	64.7
Thermal Control	14.9
Positioning & Orientation	94.9
Apogee Motor	498.0
Balance Weight	3.0
SPACECRAFT -- LESS CONTINGENCY	927.0
Contingency Allowance	38.0
TOTAL SPACECRAFT	965.0
Booster Adapter	40.0
TOTAL PAYLOAD	1005.0

Table 12-2

ESTIMATED SPACECRAFT WEIGHT

Subsystem	Weight (lbs)
Communications	71.0
Preamplifier	10.1
6 gHz Bandpass Filter	1.2
Command Reject Filter	0.5
Switch (2)	0.6
Isolator	0.3
6 gHz TDA (2)	1.8
Translator Mixer (2)	2.5
L. O. RF Source (2)	2.7
Comb Filter	0.5
Driver Stage	8.5
Switch (2)	0.6
4 gHz TDA (2)	1.8
Driver TWT (2)	1.6
TWT Power Supply (2)	4.5
Power Amplifier Stage	50.4
Multiplexer - Input	4.0
TWT (9)	11.3
TWT Power Supply (9)	22.1
Isolator (9)	2.3
Multiplexer - Output	4.0
LP Filter	0.2
HA Filter	0.3
Telemetry Suppress Filter	0.5
Pin Diode Attenuator (6)	1.5
Switch - SPDT (6)	1.9
Switch - Transfer (6)	2.3
Coax	2.0
Telemetry & Command	19.0
Command Receiver	3.5
Command Decoder	2.0
PCM Encoder 1	3.5
PCM Encoder 2	3.5
Telemetry Transmitter	3.5
Beacon Transmitter	2.0
Coax	1.0

Table 12-2 (Cont'd)

ESTIMATED SPACECRAFT WEIGHT

Subsystem	Weight (lbs)
Antennas	13.7
Communications Antenna	3.7
Communications Antenna Feed & Waveguide	2.4
Communications Antenna Support Structure	4.7
TT&C Antenna (2)	0.7
TT&C Antenna Coax	1.0
TT&C Antenna Support Structure	1.2
Electrical Power	99.8
Solar Array	52.4
Battery	30.5
Power Control Unit	7.3
Converter	7.0
Shunts	2.6
Electrical Integration	19.0
Electrical Integration Assembly	3.0
Harness and Connectors	16.0
Attitude Determination	29.0
Earth Sensor (2)	2.4
Sun Sensor	0.3
Valve Driver	1.5
Sensor Interface Electronics	0.8
Despin Mechanism	13.0
Despin Electronics	9.0
Damper Assy	2.0
Structure	64.7
Upper Frustum	6.8
Cylinder	10.5
Despin Support Ring	0.2
Inner Platform Ring	0.9
Lower Frustum Ring	1.0
Motor Support Ring	2.3
Separation Ring	3.9
Upper Platform	8.6
Upper Platform Struts	1.8
Lower Platform	8.5

ESTIMATED SPACECRAFT WEIGHT

Subsystem	Weight (lbs)
Structure (cont'd)	
Lower Platform Struts	1.4
Solar Array Ring (4)	6.4
Solar Array Supports	1.6
Tank Supports	3.4
Thruster Supports	0.5
Sensor Supports	0.5
S & A View Tube	0.5
Attaching Hardware	5.9
Thermal Control	14.9
Central Cylinder Blanket	3.0
Tank and Line Insulation	0.9
Second Surface Mirrors	0.6
Platform Heat Sinks	4.3
Upper Platform Insulation - Exterior	0.6
Upper Platform Insulation - Interior	0.9
Aft Closure	1.7
Nozzle Cover	0.1
Thermal Paint	2.8
Positioning & Orientation	94.9
Ordnance Valve	0.4
Pressure Transducer (2)	0.4
Fill & Drain Valve (2)	0.6
Filter (2)	0.7
Heat Sink (2)	0.1
Plumbing	2.3
Radial Thruster (2)	1.1
Axial Thruster (2)	1.6
Propellant Tank (4)	9.5
Pressurant	1.8
Usable Propellant	74.2
Residual Propellant	2.2
Apogee Motor	498.0
Inert Motor	45.7
Propellant	452.3
Balance Weights	3.0
Contingency	38.0
TOTAL SPACECRAFT	965.0

Table 12-3

MASS PROPERTIES MISSION HISTORY

Spacecraft Flight Condition	Weight (lb)	XCG* (in)	Moment of Inertia (slug-ft^2) Ix**	Iy	Iz	Ix/Iy	Ix/Iz
Booster Separation	965.0	42.64	40.87	114.20	113.13	0.36	0.36
Apogee Motor Burnout	511.1	52.97	34.51	83.45	82.39	0.41	0.42
End of Mission	436.9	53.31	30.15	81.19	80.14	0.37	0.38

*Measured from Station O (Spacecraft Separation Plane)

**Ix moment of inertia values do not include the inertia of the despun portion of the spacecraft.

XCG and ZCG values are nominally zero.

Figure 12-1

Coordinate Axes System

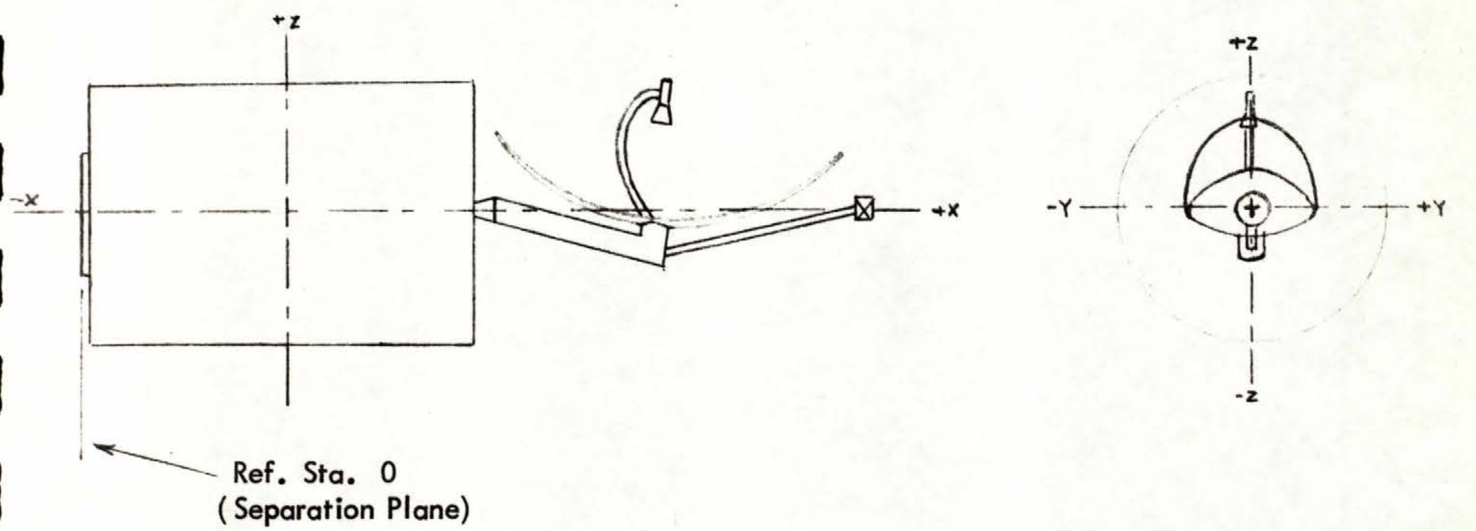

13

YNAMICS

13. DYNAMICS

In the following sections the results of the spacecraft rigid body analysis are presented along with supporting equations and actual numbers used for computation.

In Section 13.1 spin rate and spin rate variation are discussed. Injection errors are treated in Section 13.2. In Section 13.3 long term attitude drift is analyzed. Balance requirements are enumerated in Section 13.4, and in Section 13.5 nutation damper design information is presented and damper performance is evaluated over the anticipated range of parameter variations.

In summary, the dynamic analysis of the proposed configuration revealed no significant problem areas. Acceptable dynamic performance may be obtained using present technology.

13.1 SPIN RATE AND SPIN RATE VARIATION

A nominal spin rate of 100 rpm has been selected for the spacecraft. This value is compatible with Douglas third-stage stability requirements; it provides small injection errors, and permits the minimum number of attitude corrections during the life of the spacecraft.

Tolerances on the nominal rate will depend on such factors as spin-up tolerance, misalignments of axial and radial thrusters, momentum transfer, and apogee motor misalignment. Spin rate tolerances due to these factors are shown in Table 13-1.

Table 13-1 3σ Spin Rate Tolerances

	Thor Delta	Atlas Burner II
Start of Life	100 ± 10	100 ± 1
End of Life	100 ± 21.8	100 ± 19.4

13.1.1 Factors Contributing To Spin Rate Tolerances

Spin rate tolerances presented above were computed using the following spacecraft properties:

$\bar{m}$ - Time average mass = 14.6 slugs

$\bar{C}$ - Time average spinner spin axis inertia = 32.2 slug-ft^2

l_t - Radial distance to fuel centroid in the P&O tanks = 1.33 ft

For the axial thrusters:

l_a - Radial distance to nozzle = 2.13 ft

α - 3σ angular misalignment = .00283 radian

ΔV_a complement (each of 2 thrusters) = 515 ft/sec

For the radial thrusters:

l_r - Radial distance to nozzle = 2.23 ft

ε - rss of 3σ misalignments = .012 ft

ΔV_r complement (each of 2 thrusters) = 57.2 ft/sec

13.1.1.1 Spinup

The tolerance provided for the Thor Delta spin table is $\pm$ 10% or $\pm$ 10 rpm for a nominal rate of 100 rpm. The proposed Boeing spin table for Burner II uses closed-loop control and is expected to provide $\pm$ 1% or $\pm$ 1 rpm for a nominal rate of 100 rpm.

13.1.1.2 Axial Thrusters

Misalignment of axial thrusters will produce a spin variation over the life of the spacecraft which may be approximated by

$$\Delta\Omega_A = \pm \frac{\bar{m}\,\Delta V_a\, l_a \sin\alpha}{\bar{C}} = \pm\, 13.4 \text{ rpm}$$

for each thruster.

13.1.1.3 Radial Thrusters

Misalignment of radial thrusters will produce a spin variation over the life of the spacecraft which may be approximated by

$$\Delta\Omega_R = \pm \frac{\bar{m}\,\Delta V_r\,\varepsilon}{\bar{C}} = \pm\ 2.97 \text{ rpm}$$

for each thruster.

13.1.1.4 Momentum Transfer

Transfer of propellant from the tanks to axial and radial thrusters will cause a reduction in spin rate over the life of the spacecraft. This effect may be compensated for by canting the thrusters slightly to provide a small roll axis torque in the direction of spacecraft spin. The cant may be determined from the equations:

$$\text{axial thruster angle} = \phi_a = \sin^{-1}\left[\frac{\Omega(l_a^2 - l_t^2)}{\bar{I}_{sp}\,g\,l_a}\right]$$

$$\text{radial thruster angle} = \phi_r = \sin^{-1}\left[\frac{\Omega(l_r^2 - l_t^2)}{\bar{I}_{sp}\,g\,l_r}\right]$$

where $\bar{I}_{sp}$ is the time average specific impulse over the life of the spacecraft = 225 seconds.

The angular cant for axial thrusters is thus .107°, and the angular cant for radial thrusters is .119°.

13.1.1.5 Apogee Motor Burn

Linear and angular misalignments of the apogee motor will produce an initial spin rate change. This effect has been analyzed and found to be insignificant.

13.1.1.6 Summary of Effects

The effect of the individual factors described above are combined in Table 13-2 to produce an end of life spin rate tolerance. The total 3σ tolerance represents an rss combination of individual effects.

Table 13-2 Summary of 3σ Spin Rate Tolerance Contribution For End Of Life

Source	Thor Delta	Atlas Burner II
Spinup	$\pm$ 10	$\pm$ 1
Axial Thruster*	$\pm$ 13.4	$\pm$ 13.4
Radial Thruster*	$\pm$ 2.97	$\pm$ 2.97
Momentum Transfer	Negligible	Negligible
Apogee Motor Burn	Negligible	Negligible
Final Spin Rate	100 $\pm$ 21.8	100 $\pm$ 19.4

Experience obtained during the fabrication and test of INTELSAT III indicates that the figure chosen for the angular misalignment of the axial thrusters -- .00283 radians may be somewhat conservative. It appears possible using state-of-the-art alignment techniques to maintain the throat of the axial thrusters perpendicular to the spacecraft centerline to within .001 radian. A current estimate for the uncertainty of actual thrust vector direction with respect to thruster geometrical center line is .001 radian. The worst case sum of effects may then be approximately .002 radians. Use of this figure would produce final spin rate figures of 100 $\pm$ 17.2 for Thor Delta and 100 $\pm$ 14.1 for Atlas Burner II.

13.2 INJECTION ERRORS

Prior to apogee motor burn, spacecraft motion is simple spin about the roll axis, that is, the roll axis and the angular momentum vector are aligned. This is the case since transverse rates acquired prior to and during separation are damped-out during the coast phase by the nutation damper.

---

* Spin rate tolerance given for each of two thrusters

The apogee motor thrust vector will generally be offset from the spacecraft center of mass. Firing the apogee motor will thus cause a reorientation of the angular momentum vector, wobble of the roll axis about the momentum vector, and a degradation in the accuracy of the velocity increment imparted by the apogee motor.

The angle between the roll axis and the angular momentum vector describes wobble. The angle between the momentum vector after apogee motor burn and the momentum vector prior to burn is the attitude error. It describes the spacecraft orientation for times after the wobble damper has removed transverse rates. The angle between the roll axis after apogee motor burn and the momentum vector prior to burn is the angle of attack. The velocity dispersion angle is the angle between the spacecraft velocity vector and the initial angular momentum vector orientation. Limiting values for these angles are given in Table 13-3 in addition to the velocity increment degradation.

Table 13-3 Summary of Injection Errors

Error	Limiting Value	
	Thor Delta	Atlas Burner II
Attitude Error	.723°	.617°
Angle of Attack	.474°	.404°
Wobble Angle	1.20°	.99°
Velocity Dispersion Angle	.367°	.313°
Velocity Degradation	1.0 ft/sec	1.0 ft/sec

13.2.1 Factors Contributing to Injection Error

Injection errors presented above were computed using the following spacecraft properties:

$\bar{m}$ - Time average mass = 22.8 slugs

$\bar{C}$ - Time average spinner spin axis inertia = 37.6 slug-ft^2

$\bar{A}$ - Time average of total transverse moments of inertia = 95.0 slug-ft^2

s - 3σ lower bound spin rate = 90 rpm (Thor Delta)
= 99 rpm (Atlas Burner II)

t - Duration of apogee motor burn = 42 seconds

T - Time average apogee motor = 3710 lbs

ε - Thrust vector offset measured at spacecraft c.g.* = .00568 ft

ζ - Angular misalignment of thrust vector with respect to the body-fixed longitudinal center line = .0026 radian

λ - Inertia parameter, $\left|\frac{\bar{C} - \bar{A}}{\bar{A}}\right| = .6042$

13.2.1.1 Attitude Error

The attitude error, δ , is the angle between the angular momentum vector at any given time and its orientation prior to firing the apogee motor. Since the nutation damper acts to remove residual transverse rates, the attitude error represents the final orientation of the spacecraft roll axis after sufficient time has elapsed. This angle is less than or equal to:

$$\delta \leq \frac{2T\varepsilon}{\bar{C}s^2}$$

$$\delta \leq .723^\circ \text{ for Thor Delta,}$$

$$\delta \leq .617^\circ \text{ for Atlas Burner II.}$$

13.2.1.2 Angle of Attack

The angle of attack, α , is the angle between the spacecraft roll axis at any specified time and its orientation prior to firing the apogee motor. This angle is less than or equal to:

---

* Thrust vector offset used represents the rss total of 3σ offsets due to all causes, i.e., angular and linear misalignments, spacecraft static imbalance, etc.

$$\alpha \leq \frac{2T\varepsilon}{\overline{A}\, s^2\, \lambda}$$

$$\alpha \leq .474^\circ \text{ for Thor Delta,}$$

$$\alpha \leq .404^\circ \text{ for Atlas Burner II.}$$

13.2.1.3. Wobble Angle

The wobble angle, θ , is the angle between the angular momentum vector and the spacecraft roll axis. After apogee motor burn, its value is approximated by:

$$\theta \doteq \frac{2T\varepsilon}{\overline{C}\, s^2\, \lambda}$$

$$\theta \doteq 1.20^\circ \text{ for Thor Delta,}$$

$$\theta \doteq .99^\circ \text{ for Atlas Burner II.}$$

13.2.1.4 Velocity Dispersion Angle

The velocity dispersion angle, α_v , is the angle between the spacecraft velocity vector and the initial spin axis angular momentum vector orientation. This angle is less than or equal to:

$$\alpha_v \leq \frac{F\varepsilon}{\overline{C}\ s^2} + \frac{2}{t}\left\{\frac{\zeta}{s} + \frac{F\varepsilon}{\overline{A}\lambda\ s^3}\left[1 + \frac{1}{(\lambda + 1)^2}\right]\right\}$$

$$\alpha_v \leq .367^\circ \text{ for Thor Delta}$$

$$\alpha_v \leq .313^\circ \text{ for Atlas Burner II}$$

13.2.1.5 Velocity Degradation

The velocity degradation, ΔV , is the amount by which the magnitude of the velocity increment is less than its intended value. Its value is approximately:

$$\Delta V = \frac{T\ t}{\overline{m}}\left[1 - \cos\ (0.66\ \alpha)\right] = 1.0 \text{ ft/sec}$$

for both Thor Delta and Atlas Burner II.

13.3 A TTITUDE DRIFT

During the life of the spacecraft transverse torques cause the antenna beam to drift from its earth target. The three factors contributing most strongly to drift are solar-induced torque, latitude stationkeeping, and longitude stationkeeping. Other factors -- nodal regression, gravity gradient, and magnetic torque -- are small by comparison for this design.

Solar torque is a relatively strong effect as a consequence of a center of mass to center of pressure distance of approximately 10 inches. Table 13-4 illustrates average 3σ daily attitude drift for the first and last years of spacecraft life due to solar torque.

Table 13-4 3σ Daily Attitude Drift Due To Solar Torque

	First Year Of Life Daily Attitude Drift (deg/day)	Fifth Year Of Life Daily Attitude Drift (deg/day)
Thor Delta	$.0544^{\circ}$	$.0686^{\circ}$
Atlas Burner II	$.0497^{\circ}$	$.0661^{\circ}$

The above data indicates that an attitude correction may be required every one to three days depending upon limit cycle dead band.

An attitude correction is carried-out by pulsing one of the axial thrusters over a 48° arc for a nominal 100 rpm with the timing of the arc choosen to make the average thrust vector lie in a plane defined by the spin axis and a line normal to the plane of desired motion. The spin axis will then precess in the plane defined by the initial position of the spin axis and the normal to the orbit plane.

Each stationkeeping maneuver will produce an attitude shi ft due to thruster offsets and misalignments. Three sigma values for an average stationkeeping maneuver during the first and last year of life are illustrated in Table 13-5.

Table 13-5 3σ Attitude Error Due to Stationkeeping

	Thor Delta		Atlas Burner II	
	Attitude Error 1st Year	Attitude Error 5th Year	Attitude Error 1st Year	Attitude Error 5th Year
Each Latitude Stationkeeping Maneuver	.284°	.163°	.237°	.151°
Each Longitude Stationkeeping Maneuver	.0070°	.0078°	.0064°	.0075°

13.3.1 Solar Torque

The results presented above for solar torque induced drift are computed using the following approach. The net torque exerted on the spacecraft by absorbed and specularly reflected solar radiation is given by the integral

$$T = -p \int_S [(1-R)(\bar{e}_n \cdot \bar{e}_p)(\bar{r} \times \bar{e}_p) + 2R\,(\bar{e}_n \cdot \bar{e}_p)^2(\bar{r} \times \bar{e}_n)]\, ds$$

where the integral is taken over that portion of the surfact illuminated by the sun, and

P - Solar Radiation

R - Surface Reflectivity

$\bar{e}_n$ - Outward Normal From The Surface

$\bar{e}_p$ - Unit Vector Directed From Sun to Spacecraft

$\bar{r}$ - Vector Directed From Spacecraft c.g. To Elemental Area ds.

Once obtained, the torque, T, may be used to obtain the daily drift by using

$$\delta = \frac{\int T\, dt}{Cs}$$

Where the integral is taken over the applicable 24-hour period and where

C - Spin Axis Inertia Of Rotor

s - Spin Rate Of Rotor

For the purpose of analysis the spacecraft was modeled by the configuration shown in Figure 13-1.

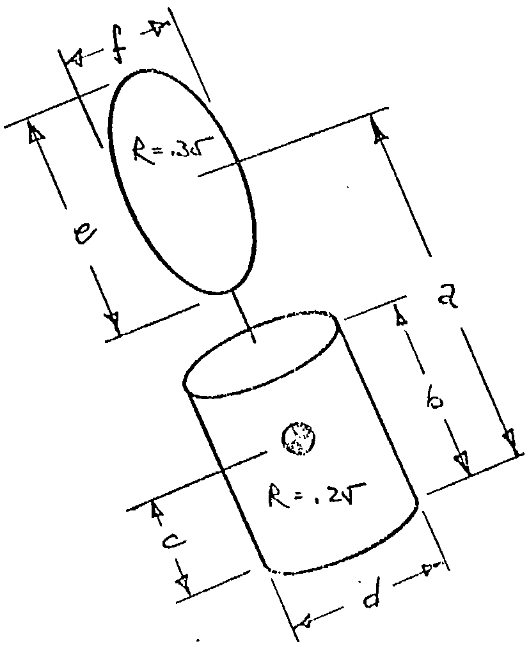

a = 125.5
b = 81.
c = 52.97 (start of life)
c = 53.31 (end of life)
d = 55.4
e = 81.
f = 33.

Figure 13-1

For the configuration shown, daily drift was evaluated for the vernal equinox -- considered a limiting case. Evaluation of the integral is somewhat complicated so that details are not presented here.

13.3.2 Latitude Station Keeping

Each latitude station keeping maneuver will induce an attitude shift less than or equal to

$$\delta \leqslant \frac{2\pi r}{C s^2}^{*}$$

* Attitude drift due to latitude stationkeeping may be substantially reduced by firing the axial thruster(s) for an integral number of spacecraft revolutions. The equation given assumes that no such control of thrust duration is included.

where

T - Thrust

r - Radial offset of the axial thruster

An average latitude station keeping maneuver may be evaluated by using average properties for the year in question.

	First Year	Fifth Year
$\bar{T}$	3.26 lb	1.34 lb
$\bar{C}$	33.96 slug-ft^2	30.44 slug-ft^2
$\bar{s}$ (3σ lower) for Thor Delta	88.82 RPM	79.38 RPM
$\bar{s}$ (3σ lower) for Atlas Burner II	97.16 RPM	82.44 RPM

with r = 2.23 ft.

Using these values first year attitude shifts are:

$$\delta \leq .284^{\circ} \text{ for Thor Delta}$$

$$\delta \leq .237^{\circ} \text{ for Atlas Burner II}$$

13.3.3 Longitude Station Keeping

Each longitude station keeping maneuver will induce an attitude shift of

$$\delta \doteq \frac{m \, \Delta V \, \varepsilon}{Cs}$$

where

m - Spacecraft mass

ΔV - Velocity increment

ε - Radial thruster offset measured at the spacecraft c.g.

An average longitude station keeping may be evaluated by using average properties for the year in question:

	First Year	Fifth Year
$\bar{m}$	15.54 slugs	13.70 slugs

with

$$\Delta V = .2 \text{ ft/sec}$$
$$\varepsilon = .0125 \text{ ft}$$

Using these values first year attitude shifts are:

$$\delta \doteq .0070^{\circ} \text{ for Thor Delta}$$

$$\delta \doteq .0064^{\circ} \text{ for Atlas Burner II}$$

13.4 SPACECRAFT BALANCE

Constraints on spacecraft balance are established by launch vehicle requirements and by antenna pointing accuracy requirements over the life of the spacecraft.

For the at-launch configuration, the spacecraft center of gravity shall not be displaced from its centerline by a distance greater than 0.015 inches. The spacecraft principal axes of inertia shall be perpendicular (pitch and yaw) and parallel (roll) to the centerline within an angle of 0.002 radians.

For the component tolerances given in Section 13.4.1, and for the balancing procedures given in Section 13.4.2, the 3σ balance appearing in Table 13-6 are obtained.

Table 13-6 3σ Static and Dynamic Unbalance for Spacecraft

Configuration	Static Imbalance (inches)	Dynamic Imbalance (radians)
At Launch	.0153	.00107
Post Apogee Motor Burn	.0282	.001
End of Life	.0280	.001

13.4.1. Summary of Component Balance Requirements

The balance requirements for the individual spacecraft components are summarized below.

- Spacecraft with apogee motor case in place, hydrazine tanks empty, compensating weights used to simulate full hydrazine lines:

  Static imbalance = I lb - in.
  Dynamic imbalance = 10 lb - in.^{2}

- Apogee motor case:

  Static imbalance - .5 lb - in.
  Dynamic imbalance = 5 lb - in.^{2}

- Loaded apogee motor:

  Static imbalance = 3 lb - in.
  Dynamic imbalance = 20 lb - in.^{2}

- Antenna (despun components):

  Static imbalance - .5 lb - in.
  Dynamic imbalance = 20 lb - in.^{2}

The above figures assume the following alignments:

- o Apogee motor to spacecraft:

  Linear offset (3σ composite due to all factors) = .0164 inches
  Angular offset = .001 radian

- o Antenna to spacecraft:

  Linear offset = .01 inches
  Angular offset = .001 radian

13.4.2. Balance Procedure

The following procedure has been developed on the basis of experience gained with INTELSAT III.

- o The despun portion of the antenna assembly is statically balanced with respect to the despunaxis to within .5 lb-in. The antenna is dynamically balanced to within 20 lb-in^2. Balance weights may be added to the antenna, if necessary, to keep the overall spacecraft dynamic imbalance sufficiently small when the antenna spins with the rest of the spacecraft.

- o The despun antenna and a balanced, empty apogee motor are installed in the spacecraft. The motor case acts as a fixture to hold connecting equipment. Weights are attached to simulate hydrazine in the plumbing. The hydrazine tanks are left empty. The spacecraft is balanced with respect to its centerline to within l lb-in. static and 10 lb-in.^{2} dynamic with the antenna despun. (The despun antenna is attached to an external support with a light weight fixture.)

- o The antenna assembly is allowed to spin with the rest of the spacecraft and the static and dynamic imbalance are measured.

- o The flight apogee motor case is statically and dynamically balanced to withon .5 lb-in. and 5 lb-in.^{2}, respectively. After loading the motor, propellant is trimmed to balance the motor assembly to within 3 lb-in. static and 20 lb-in.^{2} dynamic.

- o The empty apogee motor is replaced by the loaded flight motor; the hydrazine simulation weights are removed. Hydrazine is loaded. There is no further balancing.

13.5 NUTATION DAMPER

Nutational stability is maintained by providing a positive damping source on the despun antenna. The selected blade-mass nutation damper which was developed and tested at TRW, satisfies this requirement while exhibiting the following desirable features:

- o Simplicity, reliability
- o Rugged enough to withstand the boost-phase vibration environment without a caging mechanism.
- o Good performance over the expected wide range of parameter variations.
- o The damper is passively "locked out" when the antenna spin rate gets high enough to result in an unstable configuration.
- o Performance is easily verified in a gravity field.

13.5.1 General Description of Selected Design

The blade-mass nutation damper consists of a tuned, single-axis, cantilevered beam (blade) with a tip mass (bob), immersed in a viscous fluid. (An engineering model of the damper is shown in Figure 13-2.) Damping is provided by viscous effects as the tip mass oscillates in the fluid for small nutation angles and by impact of the mass on the damper case at large angles. The damper is mounted on the despun antenna support assembly with the bob end upward and nominally located 76.5 inches above the spacecraft's center of mass and offset 10 inches from the spin axis.

The spacecraft's transverse moment of inertia is higher than the spinning moment of inertia. Therefore, a nutation damper on the despun portion of the antenna provides a very simple means of maintaining stability. The damper is located as far from the spacecraft's center of mass as possible so that even small wobbling motion of the spacecraft acts to produce relatively large linear motion of the damper. The motion of the mass is amplified further by mounting it on a cantilevered beam and tuning it to the exciting frequency. The damper then dissipates energy as the translational motion forces the tip mass to move through a viscous fluid for small nutation angles, and to impact on the end of the case for large angles. The viscosity of the fluid has been selected so that amplification occurs over a broad range of exciting (precession) frequencies. Thus, as the spin rate and inertia properties of the spacecraft vary, the precession frequency varies correspondingly, and the nutation damper continues to provide good performance.

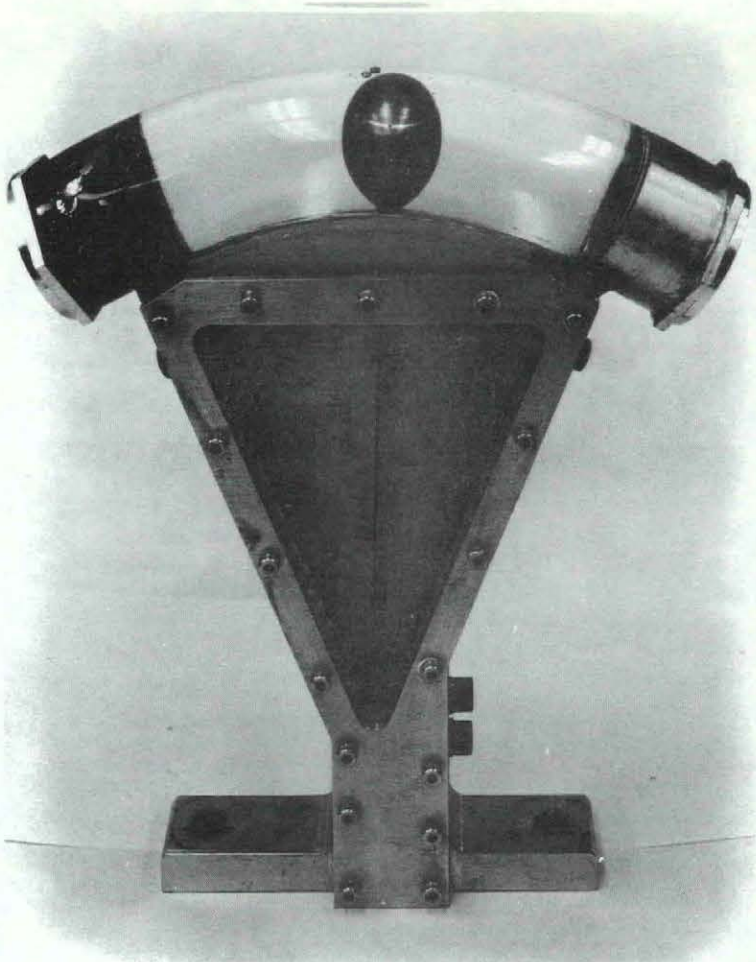

Figure 13-2 Engineering Model Blade-Mass Nutation Damper

Performance of the blade-mass nutation damper has been verified by a model built and tested at TRW Systems as part of its independent research and development program.

The undamped natural frequency of the 0.3 pound mass on the cantilevered beam in a zero-gravity field is 0.66 Hz. The viscous fluid is Dow Corning 200 silicone fluid, which provides a viscosity of 100 centistokes at the nominal operating temperature of 175°F. The damper's temperature is kept to between 0 and 175° F by use of thermal insulation. Compensation for fluid volume changes over this range is provided by a bellows system. The viscosity change in Dow Corning 200 silicone fluid with temperature is shown in Figure 13-3.

A summary of the critical size and performance paraneters is presented in Table 13-7.

Table 13-7 Summary of Damper Characteristics

Size/Performance Parameter	Value
Time Constant	1 to 9 minutes
Total Weight	1.8 lbs.
Natural Undamped Frequency	0.66 Hz
Damping Fluid	Dow Corning 200 Silicone Fluid; Nominal viscosity 100 centistokes
Temperature	0 to 175° F
Location	Attached to despun antenna; 76.5 in. above c.m. and offset 10 in. from centerline

13.5.2 Approaches Considered and Evaluation

13.5.2.1 Selection of Damper Type

Several alternate types of dampers were considered for use on this design. The criteria for evaluating the possible designs were; (1) ability to provide good performance despite a wide variation in parameters, (2) ease of verifying operation in a 1-g environment, (3) ability to withstand boost-phase vibration loads, (4) reliability and simplicity of design, and (5) capability of being passively locked-out if the antenna rotates fast enough to cause the system to be unstable. Each of the designs considered is listed below and compared to the selected nutation damper.

Viscous Ring Damper

This design consists of a toroidal ring filled with a viscous fluid. Such dampers have been built by TRW Systems for the Advanced VELA, LES IV, and INTELSAT III spacecraft. Motion of the fluid relative to the ring is induced by angular motion associated with spacecraft precession, and energy is dissipated through viscous fluid friction. This damper works over a broad range of values, but does not dissipate energy as fast as the proposed design. The viscous ring damper does not perform as well as the proposed design because

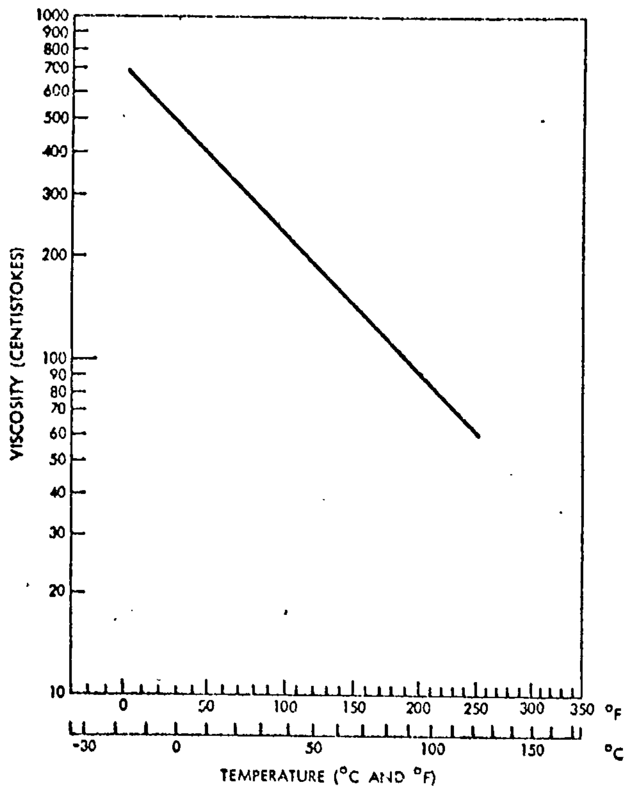

Figure 13-3 Silicone Fluid Viscosity

it does not take advantage of the large offset of the damper from the center of mass-motion of the fluid being induced by angular rather than translational motion of the damper - and it is not tuned. The viscous ring damper scores well on the other evaluation criteria but cannot be locked-out if the despin control system fails.

Two-Axis Cantilevered Mass

This design is similar to the proposed design except that the mass is free to move in two directions. This is a good design and was successfully employed on OSO. However, it requires a caging mechanism to hold the mass during boost. The mass is released once the spacecraft is in orbit. Because the proposed design can withstand the boost-phase environment without a caging mechanism, it is much more reliable. Also, the two-axis damper is difficult to test in a l-g field.

Impact Damper

This is a simple, reliable design which was used on Pioneer 6, 7, and 8 by TRW Systems. It employs a ball in a tube which dissipates energy by impacting the end of the tube. The main drawback of this design is that it does not perform well for small nutation angles and input motion is not amplified by tuning.

Spring-Mass Damper

This design is very similar to the selected design except that the mass is supported by a helical spring instead of a cantilevered beam. The main problem associated with this type of damper is that it is difficult to verify its performance characteristics in a 1-g field.

13.5.2.2 Damper Sizing

The damper is designed to (1) have a resonant frequency of 0.66 Hz (the precession frequency at mid-life), (2) have a total weight of approximately 1.8 pounds, (3) perform well over the expected range of parameters, (4) withstand the boost-phase vibration environment, and (5) not leak due to vacuum or temperature extremes. The blade size is based on the frequency requirement and vibration loading considerations, while the bob weight is dictated by the amount of energy to be dissipated and the damper location. The particular viscous fluid was chosen since it will yield good performance over the expected temperature variation. The preliminary gap size between the bob and the damper was chosen to be the same as that used in the damper tested at TRW. This was done so that the test performance data could be used to predict the time constant of the proposed design over the expected range of parameter variations.

13.5.2.3 Damper Tests

The engineering model nutation damper (Figure 13-2) was tested to determine its ability to dissipate energy over a wide variation of forcing frequencies and amplitudes, and damping fluid viscosities. The test results were normalized so that they could be applied to a damper with an arbitrary natural frequency and to a spacecraft with arbitrary inertia properties.

The energy dissipation rate of the damper was determined from measuring the decay rate of a torsional pendulum with the damper attached. (See Figure 13-4.) For the linear range, the pendulum was displaced 5 degrees from its rest position and then allowed to oscillate freely. The time history of the pendulum's angular position was recorded on an oscillograph. For the nonlinear range, this was repeated but with a 9 degree initial input displacement. Various runs were made at pendulum frequencies from 0.75 to 1.4 times the damper's natural frequency and for viscosities of 50, 100, 200, and 700 centistokes.

The normalized test data was used to predict the damper performance for this spacecraft which is summarized in Figure 13-5. The performance curves present the time constant as a function of spin rate. The time constant, τ, defines the exponential decay rate of the nutation angle, θ, from an initial value, θ_o:

$$\theta = \theta_o e^{-t/\tau}$$

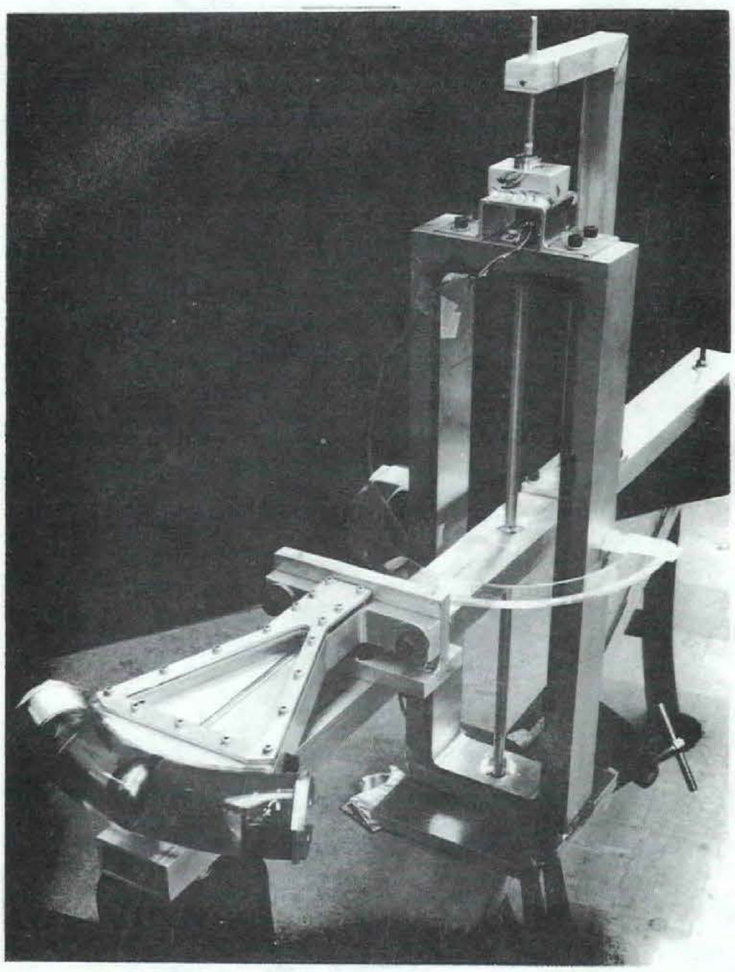

Figure 13-4 Nutation Damper Test Setup

13.5.2.4. Temperature Effects

With the nutation damper located behind the antenna and wrapped with thermal insulation, the nominal temperature will be kept at 175° F. During an eclipse, the temperature will drop as low as 0° F. The effect of temperature change on damper performance is brought about primarily because the viscosity of the silicone fluid changes with temperature. From Figure 13-3 it can be seen that the fluid viscosity varies from a nominal value of 100 centistokes to a maximum value of 700 centistokes at the lowest expected temperature. Temperature effects were accounted for in the performance tests conducted at TRW by using fluids with varying viscosities.

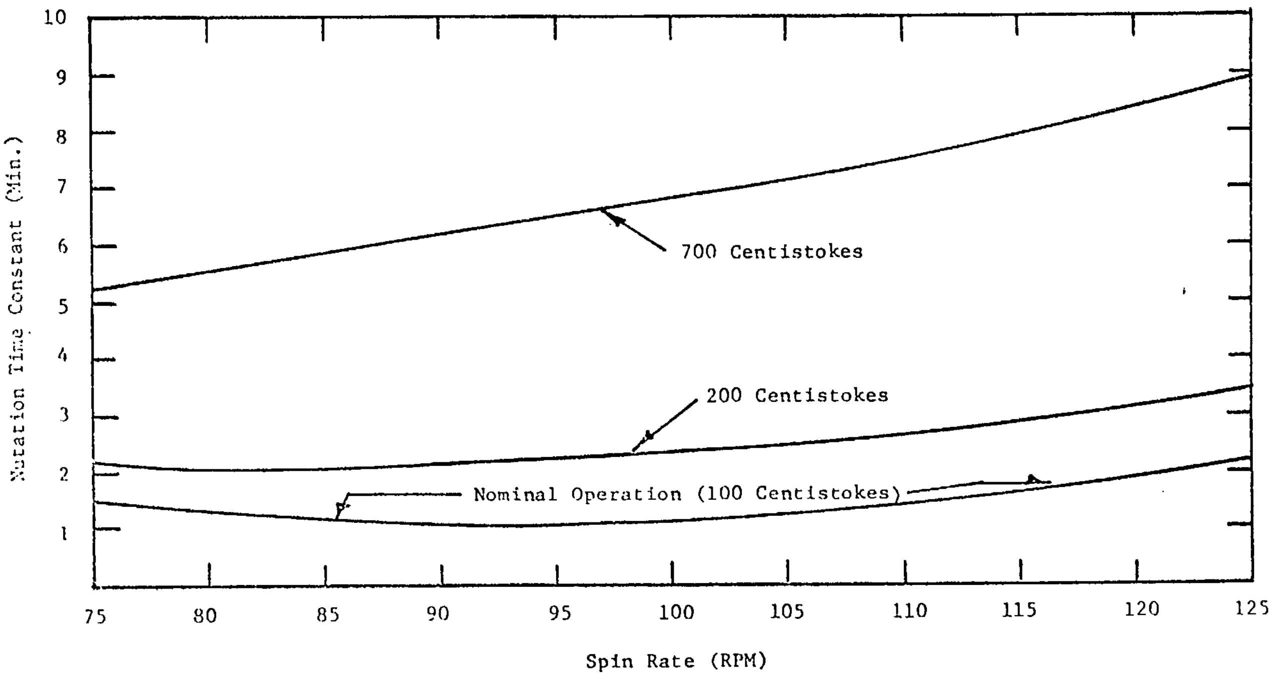

Figure 13-5 Nutation Damper Performance

13.5.2.5 Radiation Effects

The radiation environment tends to increase the fluid's viscosity. For nominal radiation dosage, there will be no appreciable change in viscosity. For a worst-case radiation dosage, the viscosity might double at the end of five years. This would have a small effect on performance of the damper. The greatest effect that doubling the viscosity will have is to increase the worst-case time constant expected during an eclipse at the end of life. For this situation, the time constant is increased from 70 seconds to about 3 minutes. (See Figure 13-4.)

13.5.2.6 Effects of Spin Rate Variation

The damper mass responds as a highly damped, single degree-of-freedom, spring-mass system to the spacecraft wobble motion. As such, transmissibility from the damper input motion to the response of the bob, and hence, damper performance, is dependent upon the forcing frequency. With the damper mounted on the despun antenna, the forcing frequency associated with wobble is equal to the inertial precession frequency, which is, in turn, equal to the spin rate times the spacecraft inertia ratio (spin moment of inertia of the rotating body divided by the total spacecraft transverse moment of inertia).

The variation in performance with spin rate was accounted for in the nutation damper tests which provided the damper design data. The damper was mounted on an arm which was supported by a torsion spring and the damper was then attached to the arm for different runs. The exciting frequency was varied, and the damping time-constant was found as a function of frequency.

13.5.3. Detailed Design

13.5.3.1. Mechanical Configuration

A conceptual drawing of the nutation damper's mechanical configuration is presented in Figure 13-6. Both the cantilevered blade and the bob are made of steel. The maximum deflection of the bob is chosen so that the blade will not experience a fatigue failure over its lifetime in orbit. The gap between the bob and the case is chosen to give a damping factor about 35 percent of critical at the nominal viscosity of the silicone fluid, 100 centistokes. The gap size is the same as was used on the damper which was tested. Not shown in Figure 13-6 are the fill port and an expansion bellows. The bellows allows the fluid volume to change without causing voids in the fluid as the temperature varies.

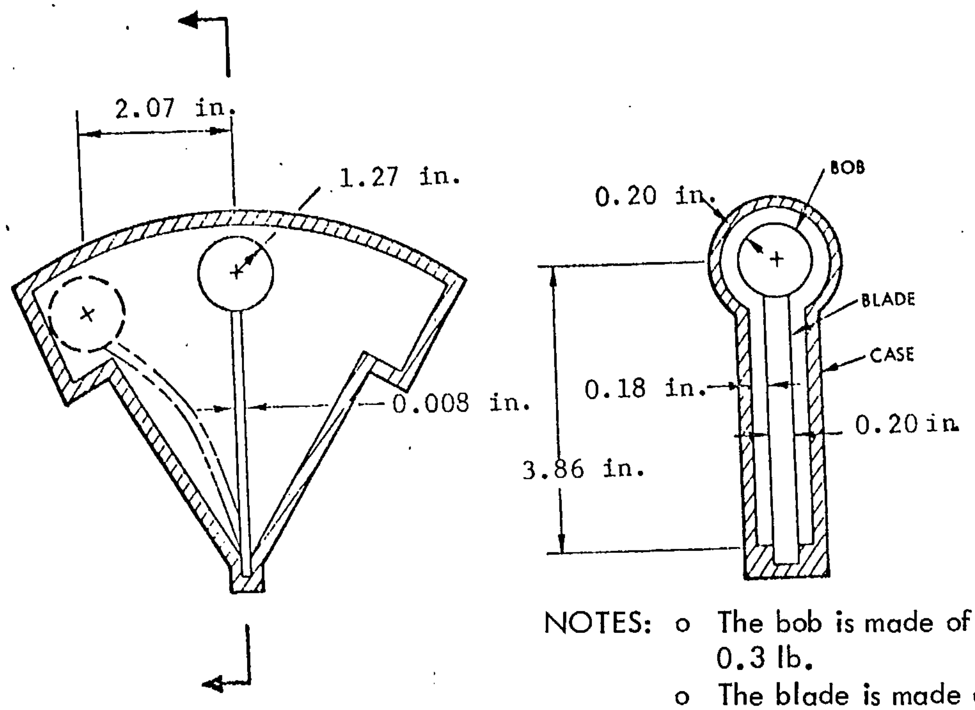

NOTES:
- o The bob is made of steel and weighs 0.3 lb.
- o The blade is made of steel.
- o The case is filled with silicone fluid which has a viscosity of 100 centistokes at 175° F.

Figure 13-6 Conceptual Drawing of the Nutation Damper

13.5.3.2. Thermal Control

The temperature variation of the silicone fluid has to be kept within a controlled, minimal band to preserve good damper performance. Thermal control is provided by covering the nutation damper with thermal insulation. With this arrangement, the nominal operating temperature of the silicone fluid is 175° F when the damper is in the sunlight, and drops to 0° F during an eclipse.

13.5.3.3 Performance

The experimentally determined curves for nutation damper time constant in Figure 13-5 are valid for wobble angle amplitudes which do not cause impacting of the bob against the case (nominally, the bob will not impact for wobble angles less than 1.1 degrees). For large wobble angles, the effects of impacting become an important factor on performance. From the engineering model test data, the time constant is found to increase somewhat for nutation angles slightly larger than the threshold of impacting.

13.5.3.4. Damper Location

Selection of the nutation damper's location is dictated by several criteria:

(a) The damper must be attached to the despun antenna to provide nutational stability.

(b) It should be located as far as practical from the spacecraft's center of mass (c.m.) with the line of action of the mass oriented perpendicular to the radius vector from the c.m. to bob. This will maximize the energy dissipation rate.

(c) The c.m. to damper distance should not be so great that damper mass motion will cause instability.

(d) When the antenna spins at a high enough rate so that energy dissipated by the damper will be destabilizing, the damper should become ineffective. This is accomplished by offsetting the damper from the centerline so that the spin inertial force holds the bob against its case.

The first two criteria are met by attaching the damper to the forward most part of the antenna support tube.

Likins* has shown that the non-trivial nutational stability criteria which must be met by the damper is

$$1 - \frac{m}{M} - \frac{mr^2}{A} > 0$$

where

m - Damper mass
M - Spacecraft mass
r - Center of mass to bob distance
A - Spacecraft's transverse moment of inertia

This criteria is easily met by this configuration. Thus, the third criteria is met.

By offsetting the damper 10 inches from the spacecraft's centerline with its line of action passing through the spacecraft's centerline, the

* Likins, Peter W., "Attitude Stability Criteria for Dual Spin Spacecraft", J. Spacecraft and Rockets, Vol. 4, No. 12, December 1967

final criteria is met. Equating the spring force and the inertial force, the spin rate that will just cause the bob to touch the case is found to be

$$\omega_a = \frac{60}{2\pi} \sqrt{\frac{\delta k}{mR}} = 16 \text{ rpm}$$

where

- ω_a - Antenna spin rate
- δ - Bob deflection, 2.07 in.
- k - Blade spring rate, 0.01338 lb/in.
- m - Mass of the bob, $0.3/386$ lb-sec^2/in.
- R - Radial offset of the bob from the spin axis, $10 + 2.07 = 12.07$ in.

Thus, the bob will be free to oscillate for antenna spin rates below 16 rpm. If the antenna is spinning faster than 16 rpm, a small wobble angle will develop before the bob is free to dissipate energy.

There are two events during which it is desirable for the damper to be inoperative. The first event occurs just after separation of the third stage and spacecraft from the Delta. At this time, the spacecraft is in an unstable configuration until the antenna is despun to below 38* rpm.

Immediately after separation, the antenna will be spinning at the same rate as the rotor. For the short time required by the despin control motor to decrease the antenna's spin rate to less than 29 rpm, the spacecraft will be in an unstable configuration. During this time, energy dissipation

---

* Simple energy sink analysis of the spacecraft indicates that energy dissipation on the antenna will stabilize the configuration when

$$\omega_a < \frac{C_r}{A - C_a} \omega_r$$

where ω_a and ω_r are the antenna and rotor spin rates, respectively, C_a and C_r are the antenna and rotor spin moments of inertia, and A is the spacecraft's transverse moment of inertia. At launch ω_r is between 90 and 110 rpm. Using the lower bound value of ω_r, it is found that $\omega_a < 38$ rpm insures stability.

due to fuel motion and structural oscillations will cause the nutation angle to grow slightly. Once the antenna spin rate is below 16 rpm the nutation damper will provide stabilizing energy dissipation which will rapidly reduce the nutation angle.

The other event which requires the bob to "bottom out" is a failure mode. If the spacecraft goes into an eclipse with a failed battery, the despin control motor will lose power until the solar cells are illuminated again. Therefore, bearing friction will be able to spinup the antenna to the speed of the rotor. During the eclipse, the main sources of energy dissipation is provided by propellant motion in the hydrazine tanks. The time constant associated with the exponential increase of the nutation angle is conservatively estimated to be 20 hours. Thus, referring to Figure 13-7, the wobble angle, θ , is described as a function of time as

$$\theta = \frac{\pi}{2} (1 - e^{-t/\tau})$$

The damper must be offset from the spacecraft's centerline so that as the nutation angle increases and the spin vector to bob distance decreases the bob will not be pulled free from its case for the duration of the longest eclipse.

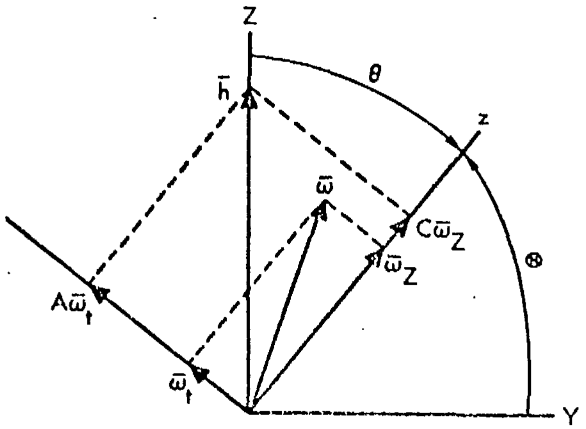

NOTES:

1. Z, Y ARE INERTIAL COORDINATES
2. z IS A BODY-FIXED COORDINATE
3. $= \frac{\pi}{2} e^{-t/\tau}$
4. ω, IS THE TRANSVERSE ANGULAR RATE

Figure 13-7 Arrangement of Vectors

As shown in Figure 13-7, the minimum displacement of the angular velocity vector from the spin axis, ξ , increases as θ increases. The relationship between ξ and θ is

$$\tan \xi = \frac{(A\ \omega_t/A}{(Cs/C)} = \frac{C}{A} \tan \theta$$

and for small angles

$$\xi = \frac{C}{A}\,\theta$$

Thus, ξ may be written as a function of time as

$$\xi = \frac{C}{A}\,\frac{\pi}{2}\,(1 - e^{-t/\tau})$$

As $\bar{\omega}$ cones in body fixed-coordinates, the minimum distance from $\bar{\omega}$ to the bob, ρ, is as shown in Figure 13-7. For small angles of ξ, ρ is given by

$$\rho = 12.07 - 76.5\,\xi$$

$$= 12.07 - 76.5\,\frac{C}{A}\,\frac{\pi}{2}\,(1 - e^{-t/\tau})$$

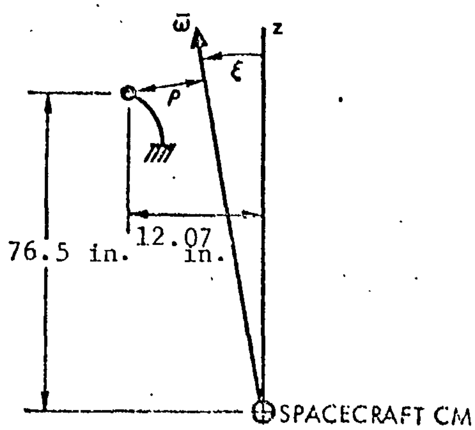

Figure 13-8 Location of $\bar{\omega}$ with Respect to Bob

At the end of a 72 minute eclipse (maximum duration)

$$\rho = 9.03 \text{ in. at the beginning of life } \left(\frac{C}{A} = 0.379\right)$$

$$\rho = 9.40 \text{ in. at the end of life } \left(\frac{C}{A} = 0.375\right)$$

The maximum net force acting on the bob when it is against the case is then

$$F = m \rho \omega_z^2 - 2.07\,k$$

where outward is positive. Using the 3σ lower bound spin rates at the beginning of life (90 rpm) and end of life (78.2 rpm) and the minimum values of ρ (9.03 and 9.40 in.), the net force is always found to be positive. Thus the bob remains against the case for the duration of the eclipse.

The only destabilizing effect comes from propellant motion, so that at the end of a 72 minute eclipse the wobble angle is

$$\theta = 90^\circ \left(1 - e^{-t/\tau}\right) = 5.2 \text{ deg}$$

II 14
RELIABILITY

14. RELIABILITY

14.1 Introduction

The first paragraph of this section deals with the reliability of the respective spacecraft subsystems. The failure rates for the various specialized components are quoted for each subsystem, with rates for general parts summarized in Table 14-14. Except as specified, the active component failure rates are for 50% confidence at stress levels of 25% rating at 30° Centigrade. These data are basically those used in reliability analysis of COMSAT programs.

The second part of this section presents information regarding the overall system reliability, mission time, and duty cycle assumptions. Also presented are data regarding reliability vs weight tradeoffs, showing that not only has the reliability target of 0.7 for five years been achieved but the design is optimized for the weight available.

14.1.1 Structures and Thermal Subsystem

Structural and passive thermal reliability is largely a matter of design philosophy with respect to stresses, design strength and safety factors. Since the design of this spacecraft will incorporate philosophies similar to Intelsat III, reasonable reliability estimates for these subsystems are

R(STRUCT, THERMAL) = .9995

14.1.2 Positioning and Orientation Subsystem (POS)

The Positioning and Orientation Subsystem incorporates two independent assemblies. Each assembly provides half of the total impulse required. In the event of a failure of one solenoid valve in the axial or radial thrusters, the subsystem has the capability of completing the mission. This capability is provided by a normally-closed ordnance valve which manifolds the propellant tanks of each assembly together. The current subsystem design provides no protection against an open propellant valve (except the normal valve design features of dual seats and springs to reduce the probability of an open valve).

The reliability block diagram of the POS is given in Figure 14-1. Failure rates, operating times, and reliabilities of time - and - cycle - dependent hardware used in the POS are given in Table 14-1. For the serial - reliability elements depicted on the top two lines of Figure 14-1 the mathematical model

$$R = (e^{-\lambda t})^n$$

Number (n)	Hardware	Mode	Failure Rate (λ)	Mission Definition	Probability of Success Each Unit	Symbol
1	Pressure Vessel	Leakage	34 x 10 - 9 / hour	43830 hours	.9985	R_P
2	Fill and Drain Valves	Leakage	20×10^{-9} / hours	43830 hours	.9991	R_D
4	Propellant Valves	Closed	420×10^{-9} / cycle	21100 cycles	.9912	
		Open	30×10^{-9} / cycle	21100 cycles	.9941	R_O
2	Filter		30×10^{-9} / hour	43830 hours	.9987	
4	Thruster		166×10^{-9} / cycle	21100 cycles (total)	.9965	R_T
1	Ordnance Valve		.9997 / operation	1 operation	.9997	

Table 14-1. Failure Rate, Mission Definition and Reliability of POS Hardware

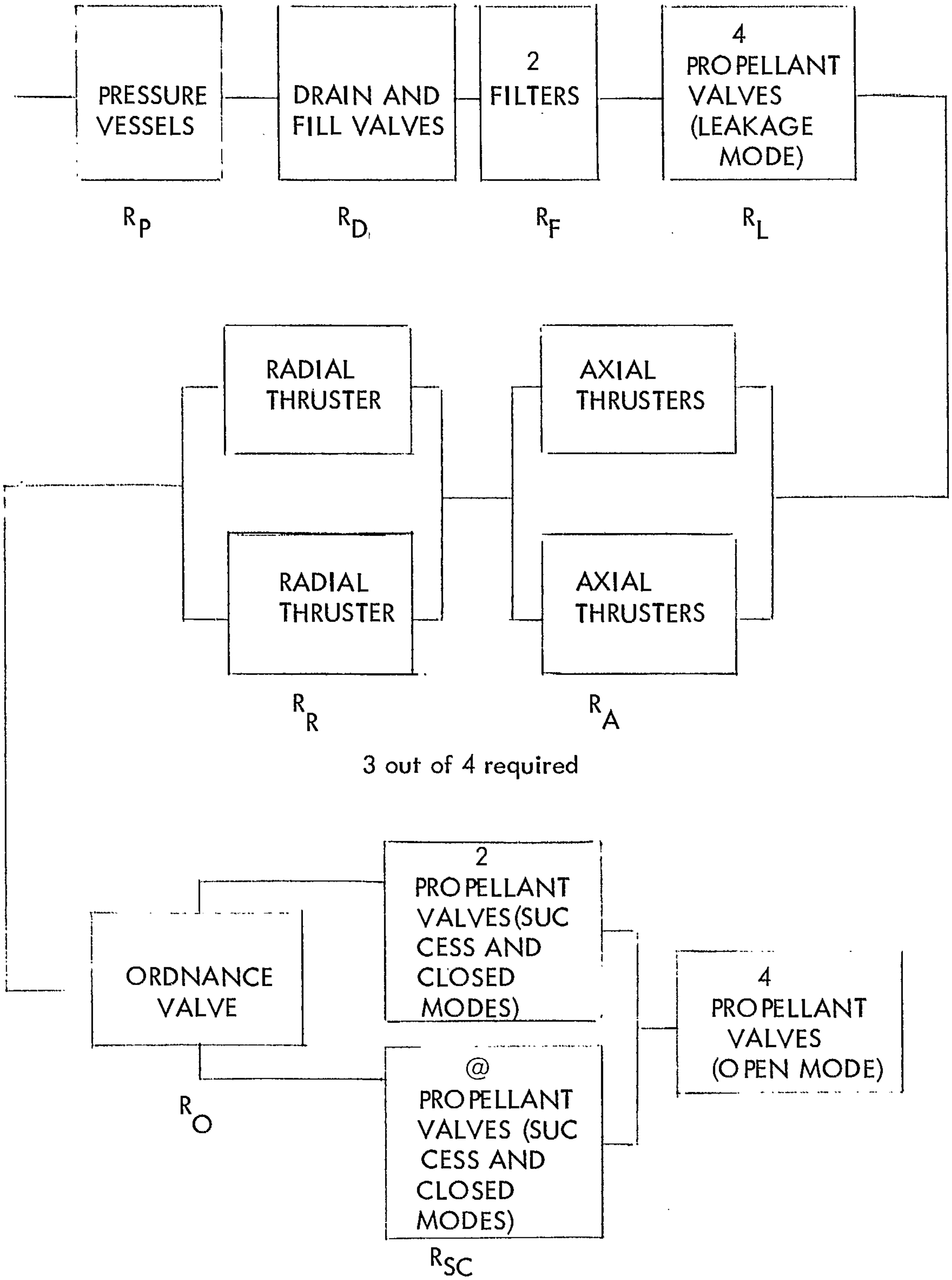

Figure 14-1. Reliability Block Diagram of Positioning and Orientation Subsystem

is used, where R, λ, t and n are defined in Table 14-1. To model the lower line of the reliability block diagram (propellant valves) the reliability success matrix of Table 14-2 is derived to illustrate the nine acceptable operating modes of the valves.

The following mathematical model results:

$$R(\text{Valves}) = R_S^2(\text{axial})\, R_S^2(\text{radial}) + R_S\,(\text{ordnance}) \Big\{ 2R_S^2(\text{axial}) R_S(\text{radial}) R_C(\text{radial})$$

$$+ 2R_S(\text{axial})\, R_C(\text{axial}) R_S^2(\text{radial}) + 4R_S(\text{axial}) R_C(\text{axial})\, R_S(\text{radial})\, R_C(\text{radial}) \Big\}$$

where R_S = Probability of having no failures $= e^{-(\lambda C + \lambda O) T}$

R_C = Probability of having a valve fail in the closed mode

$= 1 - e^{-\lambda_C T}$ = .0014 axials, .0076 radials

T = 3165 cycles for axial valves, 17935 cycles for radial valves.

The resulting mathematical model for the POS subsystem is

$$R(POS) = R_P R_D^2 R_F^2 R_L^4 [4R_T + 3R_T(1-R_T)]\ (2R_A - R_A^2)\ (2R_R - R_R^2)\quad R(\text{valves}) = .9686$$

	-Primary Valves-		-Backup Valves-		Ordnance Valves
Mode	Axial	Radial	Axial	Radial	
1	S	S	S	S	-
2	S	S	S	C	S
3	S	S	C	S	S
4	S	S	C	C	S
5	S	C	S	S	S
6	S	C	C	S	S
7	C	S	S	S	S
8	C	S	S	C	S
9	C	C	S	S	S

S=No failure
C=Fails Closed

Table 14-2. Reliability Success Matrix illustrating success operating modes of propellant valves. One or two valves failing closed is acceptable as long as both axial or both radial valves are not failed. No open-valve failures are acceptable.

14.1.3 Injection Motor Subsystem

This subsystem consists of a single apogee motor and its safe/arm and control circuitries. Current indications are that the motor will be supplied in its entirety from Thiokol. That supplier quotes five-year reliability at 0.9931, based on engineering evaluations and comparisons to similar apogee motors being produced, and on supplier's in-house tests.

14.1.4 Electrical Power Subsystem (EPS)

The EPS Subsystem is considered in four separate entities:

- Battery and Auxiliary Electrode Control Circuit
- Power Control Unit
- Power Converter
- Solar Arrays

14.1.4.1 Battery and Auxiliary Electrode Control Circuit

A single battery of sufficient reliability is provided. The battery is composed of twenty cells, three of which are designated "Auxiliary Electrodes". Nineteen of the twenty cells are required for successful operation.

Each auxiliary electrode temperature and current is measured, amplified and issued to a "two of three voting" circuit. Depending on the majority reading from the voting circuit, alternate operating modes of charging the battery is provided. The reliability block diagram depicts the binomial nature of control circuits, auxiliary electrodes and battery cells. Parts counts and failure rates are given in Table 14-3 and Table 14-4. The reliability math model* is

$$R(BATT) = R_V\,[R_C^3 + 3R_C^2\,(1-R)_C]\,\Big\{R_A^3[R_B^{17} + 17R_B^{16}\,(1-R_B)] + 3R_A^2\,(1-R_A)\,[R_B^{17}]\Big\}.$$

$$= .9813\ [\,.9980]\ \Big\{.9930\ [\,.9937] + .0024\ [\,.8874]\Big\}$$

$$= .9684$$

*A model simplifying assumption made here is that, if a failure occurs in one of the auxiliary sensing circuits, any one of the three auxiliary electrodes may still fail.

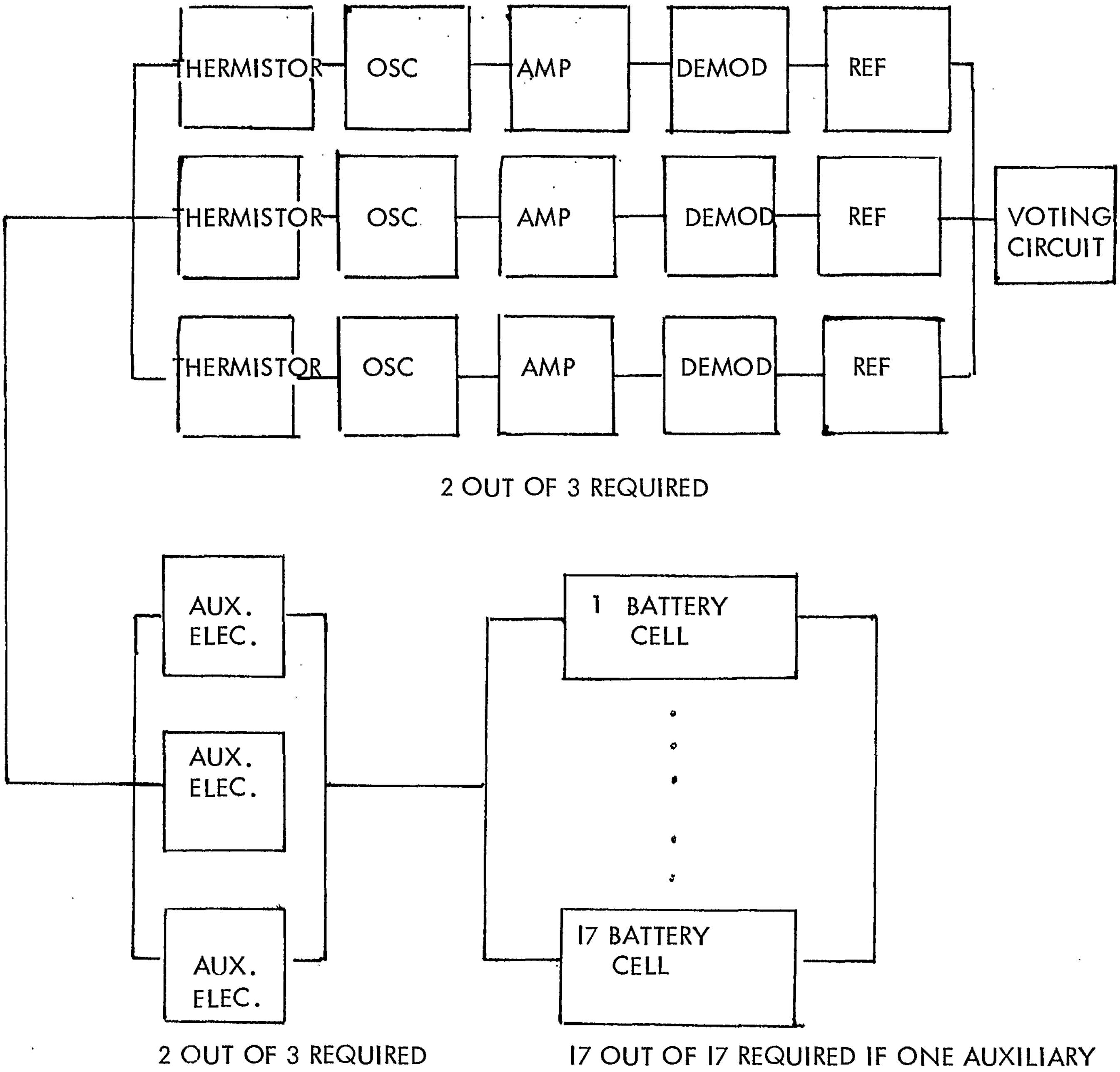

FIGURE 14-2. RELIABILITY BLOCK DIAGRAM OF EPS BATTERY AND AUXILIARY ELECTRODE CONTROL CIRCUIT

	F.R.	THERM/OSC/AMP Demod/	Ref.	Voting	Circuit
G.P. Diode	10	5	50	3	30
Transistor	50	7	350	6	300
Carbon Resistors	5	20	100	20	100
Ceramic Capacitor	3	5	15		
Thermistor	10	2	20		
Zener or V.R.	50	1	50		
Transformer	10	1	10		
Total			595		430
Reliability		$R_C = .9742$		$R_V = .9813$	

Table 14-3. Parts Count, Failure Rate, Reliability of Auxiliary Electronic Control Circuit

Estimated Battery Cell Failure Rate (Time-Varying)

Failure Rate (Failures / 10^9 Hours), Each Cell, By Year

Cell	Year 1	Year 2	Year 3	Year 4	Year 5	Total
Auxiliary Electrode	10	10	10	20	40	90
Other Cells	73	86	112	187	338	796

$R_A = e^{-90 \times 10^{-9}} \times 8766 = 0.9992$

$R_B = e^{-796 \times 10^{-9}} \times 8766 = 0.9930$

Table 14-4. Time - dependent Failure Rate of Battery Cells utilizing auxiliary electrode charging.

14.1.4.2 Power Control Unit

The reliability block diagram of the PCU subassembly of the Electrical Power Subsystem is given in Figure 14-3 (exclusive of that circuitry directly monitoring battery cell currents, which is included with the battery reliability block diagram, Figure 14-2). Parts count and failure rates for these curcuits are given in Table 14-5. The reliability math model of the subassembly is:

$$R(PCU) \doteq R_O(2R_DR_C - R_D^2 R_C^2)^3 \; (2R_D - R_D^2)^3 \, R_U(R_C^2 \, R_\& + R_N R_O - R_O^3 R_\& R_N)$$

$$\times [(R_F R_A)^3 + 3(R_F R_A)^2 \, (1 - R_F R_A)] \;\; R_\&^3 \, R_A \, R_S^2$$

$$= .9546$$

14.1.4.3 Power Converter

No complete design of the equipment power converter is available at this time. However, it is expected that the converter used on this satellite will be quite similar to that used on the Intelsat III or ISIS program. The five-year mission reliability of the Intelsat III converter has been estimated at 0.9951.

14.1.4.4 Solar Arrays

The solar cells are arranged in a cross-strapped redundancy configuration conducive to high reliability. Many previous computer analyses of similar solar arrays on Intelsat and other spacecraft indicate that, considering this satellite's array size, power margins, cell failure modes, micrometeorite sensitivity, radiation, cover losses, etc., a realistic reliability estimate of the solar arrays is

$$R = .9985$$

14.1.4.5 Subsystem Reliability

The subsystem reliability is:

$$R(EDS) = R(BATT) \times R(PCU) \times R(CONV) \times R(ARRAYS)$$

$$= .9684 \times .9546 \times .9951 \times .9985$$

$$= .9166$$

14.1.5 Electrical Integration Assembly Subsystem (EIA)

The reliability block diagram of the EIA Subsyssem is presented in Figure 14-5. Although cross-strapping of the redundant TT & C decoders is provided in the EIA, no EIA circuitry is redundant. Parts counts and failure

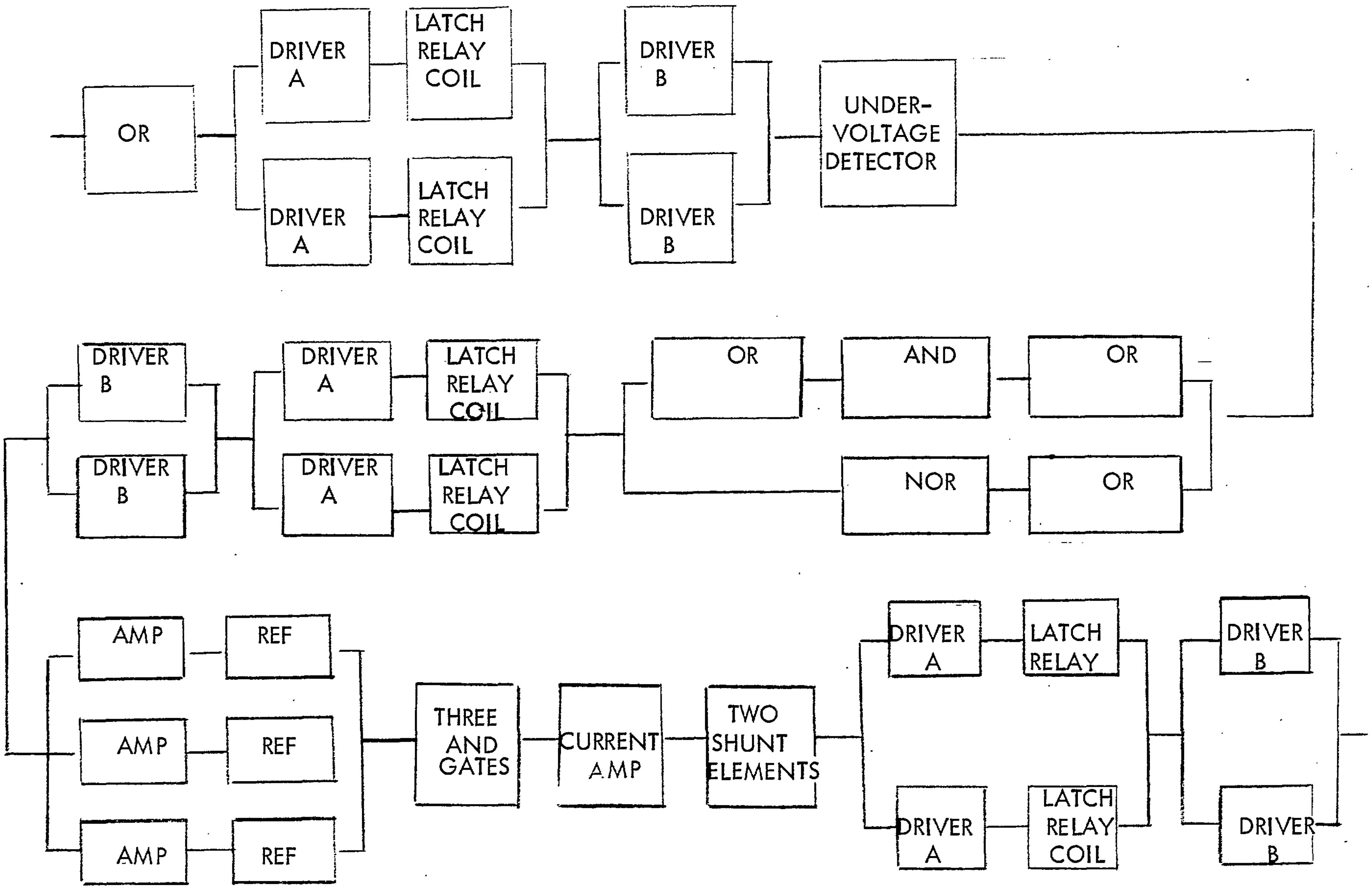

FIGURE 14-3. RELIABILITY BLOCK DIAGRAM OF EPS PCU SUBASSEMBLY

Part	F.R.	NOR		OR		Driver AorB		UV Detector		Amp/Ref		I-Amp		SEA		AND	
Composition Resistor	5	6	30	2	10	9	45	17	85	17	85	17	85	2	10	14	70
G.P.Diodes	10	13	130	12	120	3	30	3	30	2	20	2	20	2	20	4	40
Transistors GP	10	2	20			4	40	8	80	4	40	4	40	4	40	6	60
Zener V.R. Diode	50							2	100	1	50	1	50		–		
Ceramic Capacitor	3							1	3	2	6	2	6				
Power Transistors	50													4	200		
			180		130		115		298		201		201		270		170
		R_n=.9921		R_o=.9943		R_D-.9950		R_U=.9870		R_a=.9912		R_a=.9912		R_S=.9982		$R_\&$=.9926	

R_C= Reliability of Latching Relay Coil = $e^{-10 \times 10^{-9} \times 43830}$ = .99956

Table 14-5. Parts Count and Failure Rate (failures/10^9 hours) of PCU Circuits.

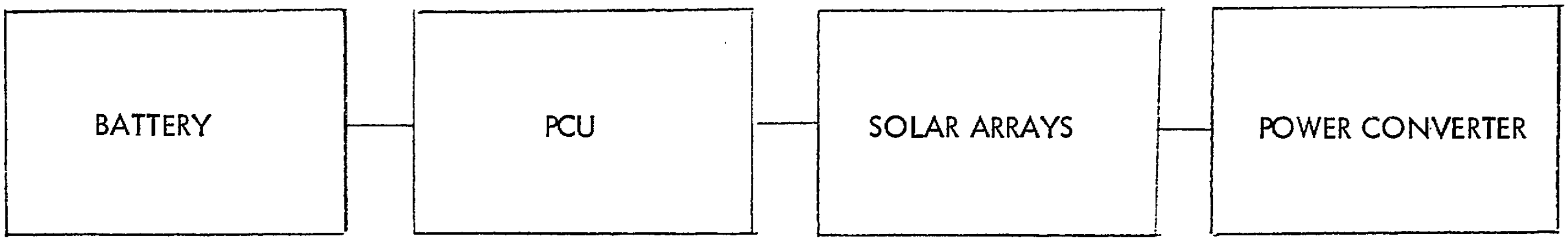

FIGURE 14-4. RELIABILITY BLOCK DIAGRAM OF ELECTRICAL POWER SUBSYSTEM

rates of EIA circuitry are given in Table 14-6. It is estimated that the average duty - cycle of any one circuit is 20%. Further, 15% of EIA circuitry could be lost without significant mission effect. Therefore,

$$R(EIA) = (.998)\left(e^{-40 \times 10^{-9} \times 43830 \times .85 \times .20}\right)^{32}$$

$$\times \left(\left(e^{-90 \times 10^{-9} \times .85 \times 43830}\right)^{13} \left(e^{-165 \times 10^{-9} \times 2.5}\right)\right.$$

$$= .9819$$

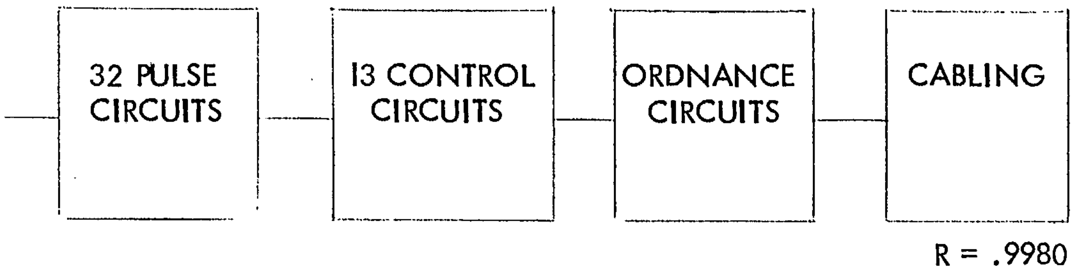

FIGURE 14-5. Reliability Block Diagram of Electrical Integration Subassembly

	F.R.	One Pulse Circuit		One Control Circuit		Ordnance Circuits	
I.C.'s	10	2	20	5	50	8	80
Transistor	10	1	10	2	20		
Resistor	5	2	10	4	20	2	10
Latching Relays	25					1	25
Non Latching Relays	25					2	50
Total			40		90		165
Mission Time			43830 hours		43830 hours		2.5 hours
Stress Factor			.20		.20		1.0

Table 14-6. Parts Count and Failure Rate (failures/10^9 hours) of EIA circuits.

14.1.6 Communications Subsystem (COMM)

14.1.6.1 High Level TWTA's

The Communications Subsystem features nine high-level TWTA's. Six TWTA's are active and are reliability-configured in pairs. Each of the remaining three TWTA's are in standby, parallel to one of the active pairs. The reliability block diagram of the high-level TWTA's is given in Figure 14-6. At most, only two channels operate simultaneously in each triplet of TWTA's. The probability that there is one (and only one) transmission path through one triplet is expressed as

$$P_1=2\left[\frac{\lambda_1}{\lambda_2} e^{-(2\lambda_1+\lambda_2)t}+e^{-\lambda_1 t}-\frac{\lambda_1+\lambda_2}{\lambda_2} e^{-2\lambda_1 t}\right.$$

$$\left.+\frac{\lambda_1^2}{\lambda_2(\lambda_1+\lambda_2)} e^{-(2\lambda_1+\lambda_2)t}+\frac{\lambda_1}{\lambda_1+\lambda_2} e^{-\lambda_1 t}-\frac{\lambda_1}{\lambda_2} e^{-2\lambda_1 t}\right]$$

where λ_1 = active faulure rate of one TWTA ($=3000 \times 10^{-9}$ failures/hour)

λ_2 = standby failure rate of one TWTA ($=.10 \times \lambda_1 = 300 \times 10^{-9}$ failures/hour)

$$P_1=0.0288$$

The probability that there are two transmission paths through a triplet is

$$P_2=e^{-2\lambda_1 t}+\frac{2\lambda_1}{\lambda_2}\left(e^{-2\lambda_1 t}-e^{-(2\lambda_1+\lambda_2)t}\right)$$

$$P_2=.9696$$

The probability that there are no transmission paths is

$$P_o=1-(P_1+P_2)$$

$$P_o=.0016$$

P_2, P_1, and P_o are identical for each triplet. Switching is accomplished by RF switches, whose failure rate is considered negligible compared to that of the TWTA's.

Of interest is the probability of having four or more, five or more, or six transmission paths available during the five-year mission, while six channels are desirable, degraded utility of the spacecraft can be achieved with four or more TWTA's.

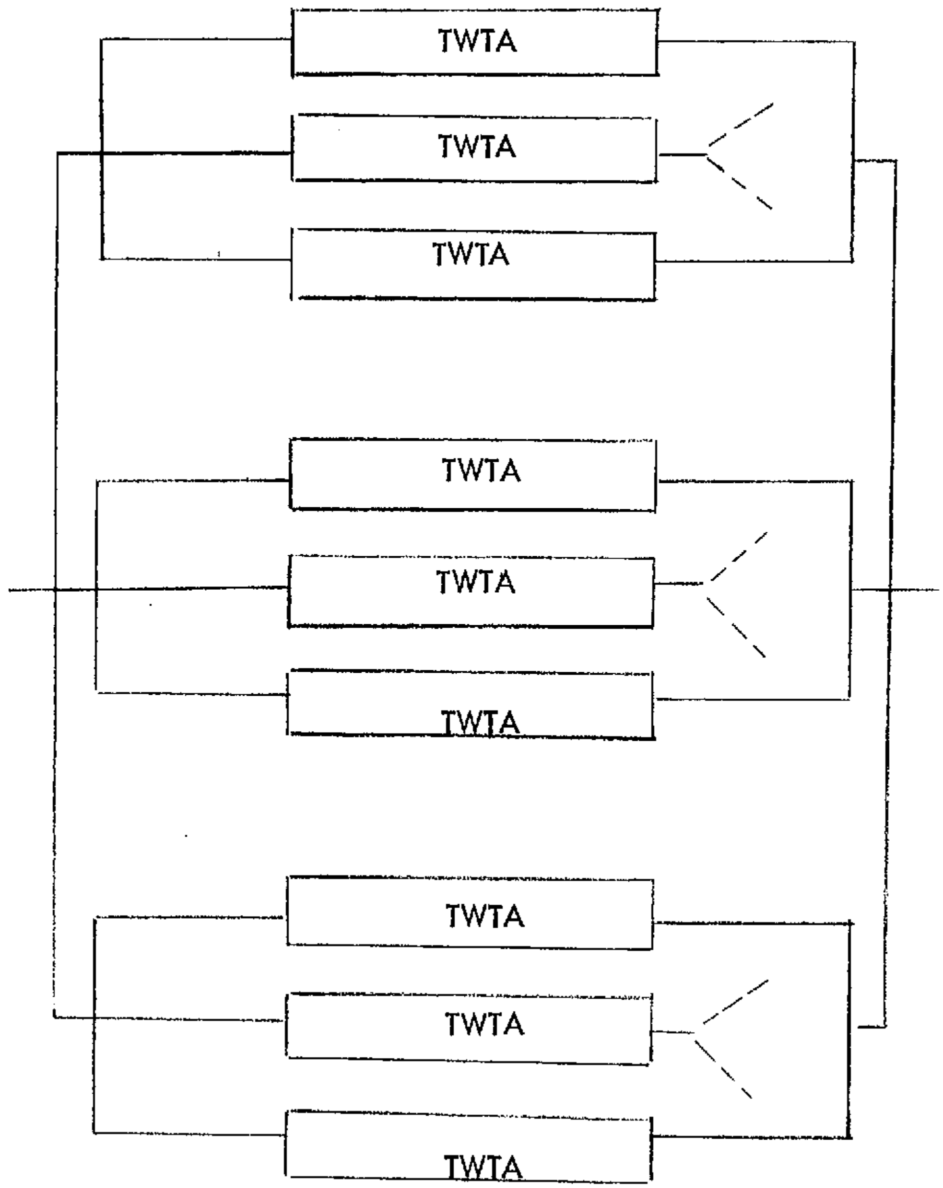

Figure 14-6. Reliability Block Diagram of TWTA Configuration

- Six transmission paths. Since only two channels in each triplet may be used at one time, all three triplets must have two channels operable; therefore

$$R = P_2^3 = (.9696)^3 = .9115$$

- Five or more transmission paths. Two triplets must have two channels operable, while the other triplet has either one or two channels operable; therefore

$$R_5 = P_2^3 + 3(P_2 \cdot P_2 \cdot P_1)$$
$$= .9927$$

- Four or more transmission paths. If two triplets have two channels available, the third can have zero, one or two channels operable; if only one triplet has two channels available, each other triplet must have two operable therefore,

$$R = 3 \cdot P_o \cdot P_2 \cdot P_2 + 3 \cdot P_1 \cdot P_2 \cdot P_2 + 3 \cdot P_1 \cdot P_1 \cdot P_2$$
$$+ P_2 \cdot P_2 \cdot P_2$$
$$= .99965$$

The results are tabulated in Table 11-7.

Success Criteria	Probability of Success after Five Years
6 transmission paths	.9115
5 or more transmission paths	.9927
4 or more transmission paths	.99965

Table 11 - 7. Reliability of TWTA Configuration for Various Success Criteria

14.1.6.2 Low Level TWTA's and Frequency Mixing

Standby-redundant low level pre-amp TWTA stages and standby-redundant frequency mixing devices are incorporated in the Communication Subsystem. The reliability block diagram is given in Figure 14-7. The reliability model does not include bandpass and noise filters, multi-plexers, attenuators or microwave cavities which are passive. Parts counts and failure rates of the active elements are shown in Table 14-8. These parts counts are based on probable circuit design; no firm design is available for the analysis.

The reliability math model (applicable to both the low-level TWTA and the frequency mixing configurations) is

$$R = e^{-\lambda A t} + \frac{\lambda A}{2\lambda_A + \lambda_I - \lambda_s}\left[e^{-st} - e^{(2\lambda A + \lambda I)t}\right]$$

where λ_A = failure rate of active elements
λ_I = failure rate of inactive elements
λ_S = failure rate of switch

The reliability of the frequency mixing configuration of Figure 14-8 is,

$$\lambda_A = (704 + 15 + 704 + 1010) \times 10^{-9} = 2433 \times 10^{-9}$$

$$\lambda_I = .1\lambda_A = 243 \times 10^{-9}$$

$$\lambda S = 2 \times 100 \times 10^{-9} = 200 \times 10^{-9}$$

$$R_m = e^{-2433 \times 10^{-9}t} + \frac{2433}{4909}\left[e^{-200 \times 10^{-9}t} - e^{-5109 \times 10^{-9}t}\right]$$

$= 0.9938$ for $t=5$ years

The reliability of the low-level TWTA configuration is

$$\lambda_A = 2000 \times 10^{-9}$$

$$\lambda_B = .1\lambda_A = 200 \times 10^{-9}$$

$$\lambda_S = 2 \times 100 \times 10^{-9} = 200 \times 10^{-9}$$

$$R_L = e^{-2000 \times 10^{-9}t} + \frac{2000}{4000}\left[e^{-200 \times 10^{-9}t} - e^{-4200 \times 10^{-9}t}\right]$$

$= 0.9958$ for $t=5$ years.

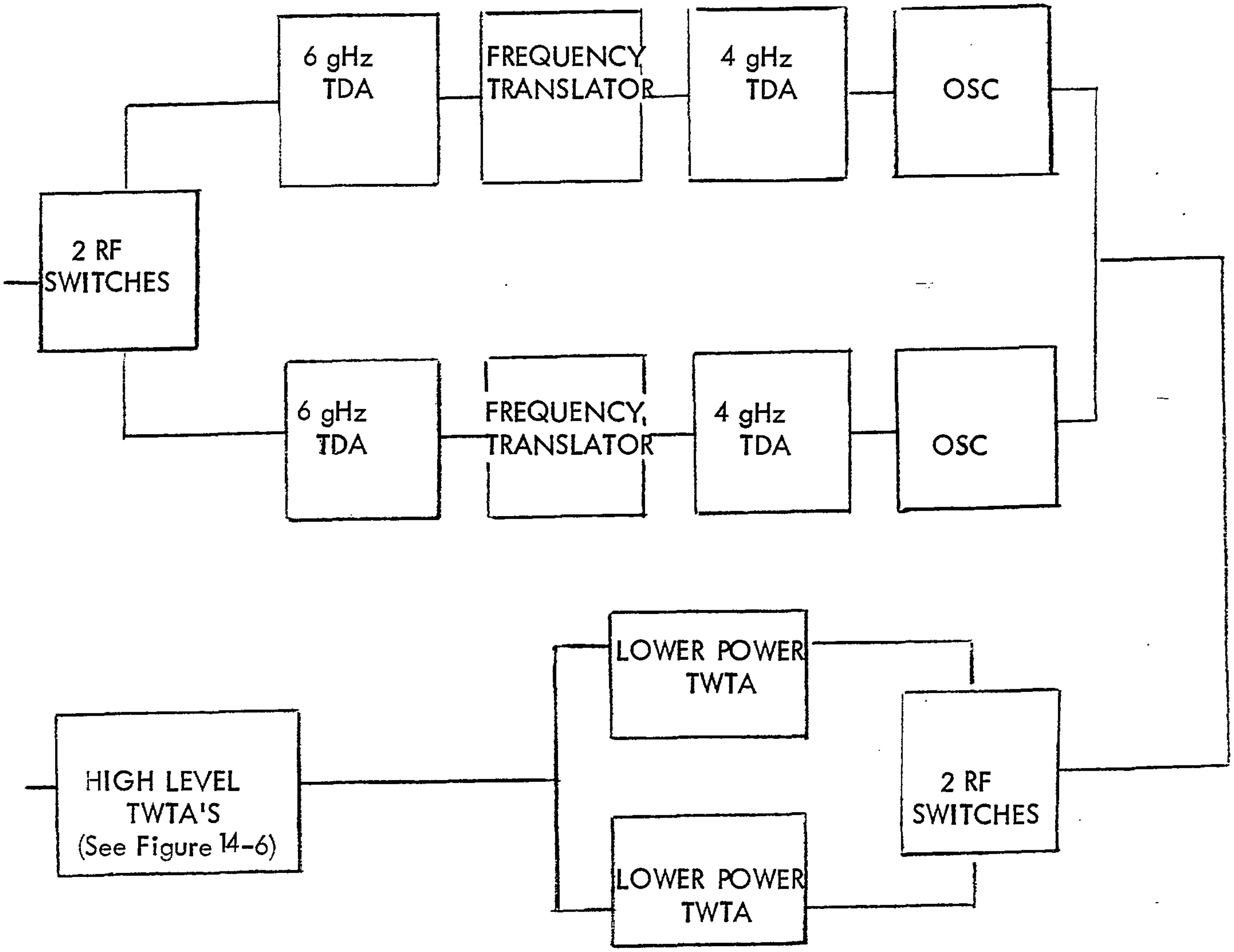

Figure 14-7. Reliability Block Diagram of Communications Subsystem

	Failure Rate	TDA		Mixer		Oscillator	
Diodes	10					20	200
Transistor	10					8	80
Composition Resistor	5	16	80	3	15	56	280
Capacitors	3	8	24			50	150
Coils	10					20	200
Zener Diodes	50	4	200				
Tunnel Diodes	100	4	400				
Total			704		15		1010

Table 14-8. Parts Count and Failure Rate of (failures/10^{6} hours) of Communications Subsystem

14.1.6.3 Subsystem Reliability

The Subsystem reliability block diagram is given in Figure 14-8.

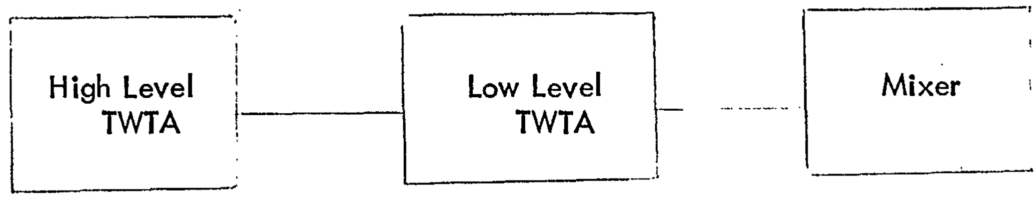

Figure 14-8. Communications Subsystem Reliability Block Diagram and the reliability of the subsystem reliability is given in Table 14-9.

Success Criteria	Subsystem Reliability $R_H \times R_L \times R_M$
6 transmission paths	.9020
5 or more transmission paths	.9824
4 or more transmission paths	.9892

Table 14-9. Communications Subsystem Reliability

14.1.7 Telemetry, Tracking and Control Subsystems (TT&C)

The reliability block diagram of the TT&C subsystem is given in Figure 14-9. The beacon circuitry is considered non-essential after acquisition of orbit (approximately 48 hours). Parts counts and failure rates of this equipment is given in Table 14-10. The reliability mathematical model for each reliability-parallel subassembly in standby configuration is

$$R_X = e^{-\lambda_{a_x} t} \times \left(1 + \frac{\lambda_{a_x}}{\lambda_{i_x}} \left(1 - e^{-\lambda_{i_x} t}\right)\right)$$

where λ_a = active failure rate of the x-th equipment

λ_i = standby failure rate = $.1 \lambda_a$

This model is applicable to the encoders, transmitters, receivers and decoders. It is estimated that 75% of all parts in each encoder subassembly may fail without loss of essential TT&C functions. This factor has been incorporated into subassembly and subsystem reliability. The TT&C subsystem reliability mathematical model of the subsystem is

$$R(TT\&C) = R_E \cdot R_T \cdot R_P^2 \cdot R_R \cdot R_D \cdot e^{-\lambda_{Beacon} \times 46}$$

$$= .9497$$

14.1.8 Attitude Control Subsystem (ACS)

The reliability block diagram of the Attitude Control Subsystem is given in Figure 14-10. The subassemblies of this subsystem are expected to be identical with those of the Intelsat III program. The 5-year mission reliability of each subassembly, determined from Intelsat III analyses is given in Table 14-11.

The subsystem reliability is

$$R(ACS) = (2R_E - R_E^2)\ (2R_V - R_V^2)\ R_S$$

$$= .9982$$

14.1.9 Mechanically Despun Antenna Subsystem

The mechanically despun antenna system presently being considered in this analysis is being provided by Philco-Ford. Redundancy is provided in the electronic control circuitry. The reliability of this subsystem is determined by Philco-Ford to be

$$R = .9467$$

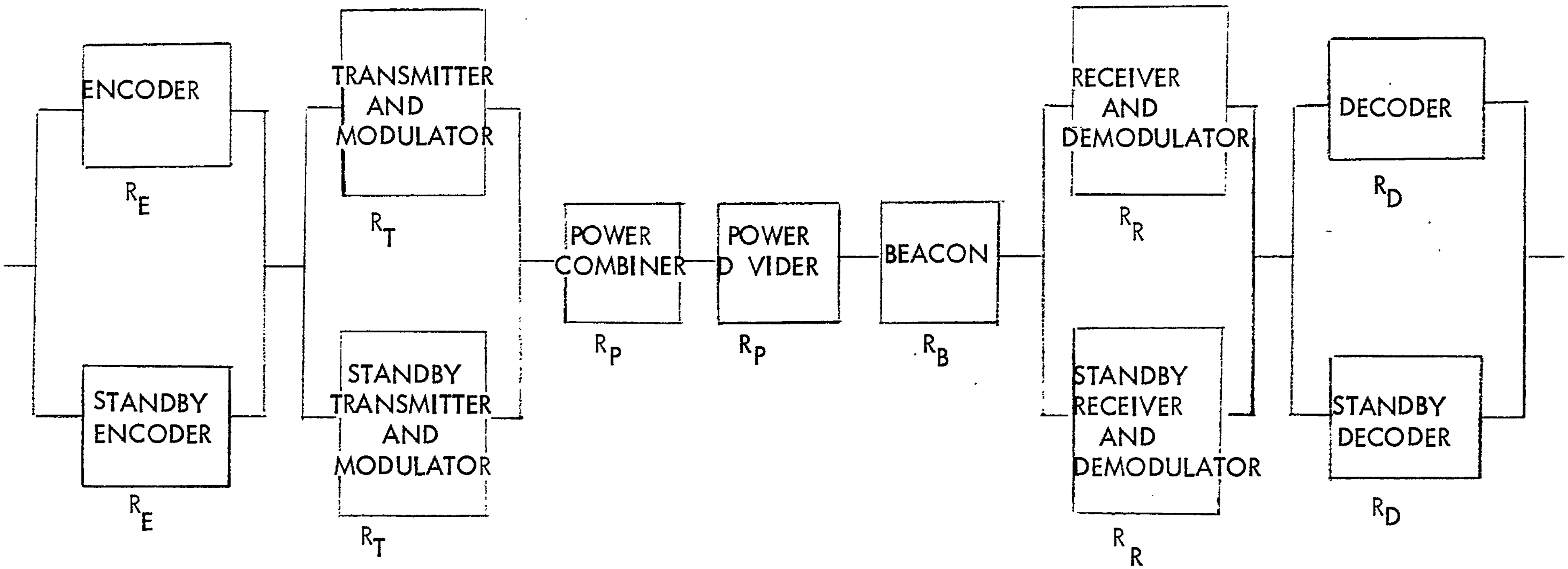

FIGURE 14-9 RELIABILITY BLOCK DIAGRAM OF TELEMETRY TRACKING AND COMMAND (TT&C) SUBSYSTEM. THE BEACON TRANSMITTER IS CONSIDERED NON-ESSENTIAL TO MISSION SUCCESS AFTER ORBIT IS ACQUIRED.

PART	F. RATE ($X10^9$)	RECEIVER NO.	RECEIVER F.R.	DECODER NO.	DECODER F.R.	ENCODER NO.	ENCODER F.R.	XMTR NO.	XMTR F.R.	POWER DIVIDER NO.	POWER DIVIDER F.R.
RESISTORS	5	87	435	40	200	40	200	41	205	5	25
CAPACITORS	3	102	306	70	210	35	105	92	186		
DIODES											
General purpose	10	14	140	190	1900	25	250	17	170		
TRANSISTORS											
RF	20	22	440	15	300	15	300	9	180		
I.C.'S											
Digital	10			70	700	265	2650				
TRANSFORMERS											
Signal	10	14	140	4	40	4	50	12	120		
Inductors	100	24	2400	6	600	5	500	37	3700		
Crystals	80	1	80			1	80	1	80		
SUM OF FAILURE RATE			3941		3950		4135		4641		25
CORRECTION FACTOR			1.0		1.0		.25		1.0		1.0
ADJUSTED FAILURE RATE			3941		3950		1036		4641		25

TABLE 14-10. PROJECTED PARTS COUNT, FAILURE RATE, AND RELIABILITY OF TT&C SUBASSEMBLIES

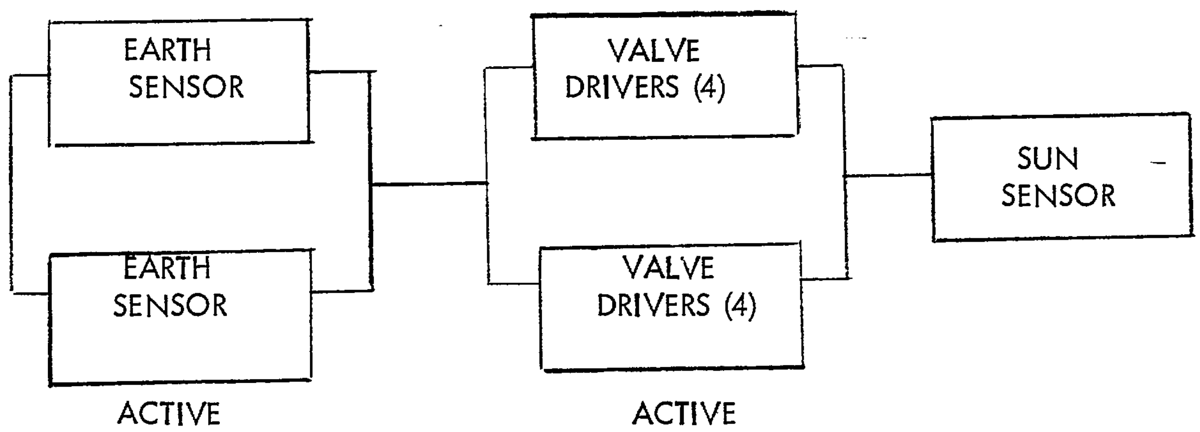

FIGURE 14-10. Reliability Block Diagram of Attitude Control Subsystem

SUBASSEMBLY	R (5 YEARS)
Earth Sensor	$R_E = .9653$
Valve Driver	$R_V = .9777$
Sun Sensor	$R_S = .99996$

TABLE 14-II. ACS SUBASSEMBLY RELIABILITY

14.2 SYSTEM RELIABILITY

14.2.1 Reliability Assessment

The reliability block diagram of the spacecraft is given in Figure 14-11. Subsystem reliabilities are discussed and developed in detail in Paragraphs 14.1.1 - 14.1.9. The total system reliability is

$$R(SYSTEM) = R(STR,THERM) \times R(POS) \times R(INJ) \times R(EPS) \times R(EIA) \times R(COMM) \times R(TTC) \times R(ACS) \times R(MDSA)$$

$$= (.9995) \times (.9686) \times (.9931) \times (.9166) \times (.9819) \times (.9022) \times (.9497) \times (.9982) \times (.9467)$$

$$= 0.7005$$

Of additional interest is the system reliability with the success criteria that four (five) or more TWTA channels are required (Paragraph 14.1.6.1), which is given in Table 14-12.

Subsystem MTTF has been computer - calculated; MTTF = 50.6 months, for the six TWTA channel criteria.

SUCCESS CRITERIA	SYSTEM RELIABILITY
6 CHANNELS OPERATIONAL	.7005
5 OR MORE CHANNELS OPERATIONAL	.7629
4 OR MORE CHANNELS OPERATIONAL	.7682

TABLE 14 - 12. SYSTEM RELIABILITY WITH VARIOUS SUCCESS CRITERIA IMPOSED ON THE HIGH - LEVEL TWTA'S IN THE COMMUNUCATIONS SUBSYSTEM.

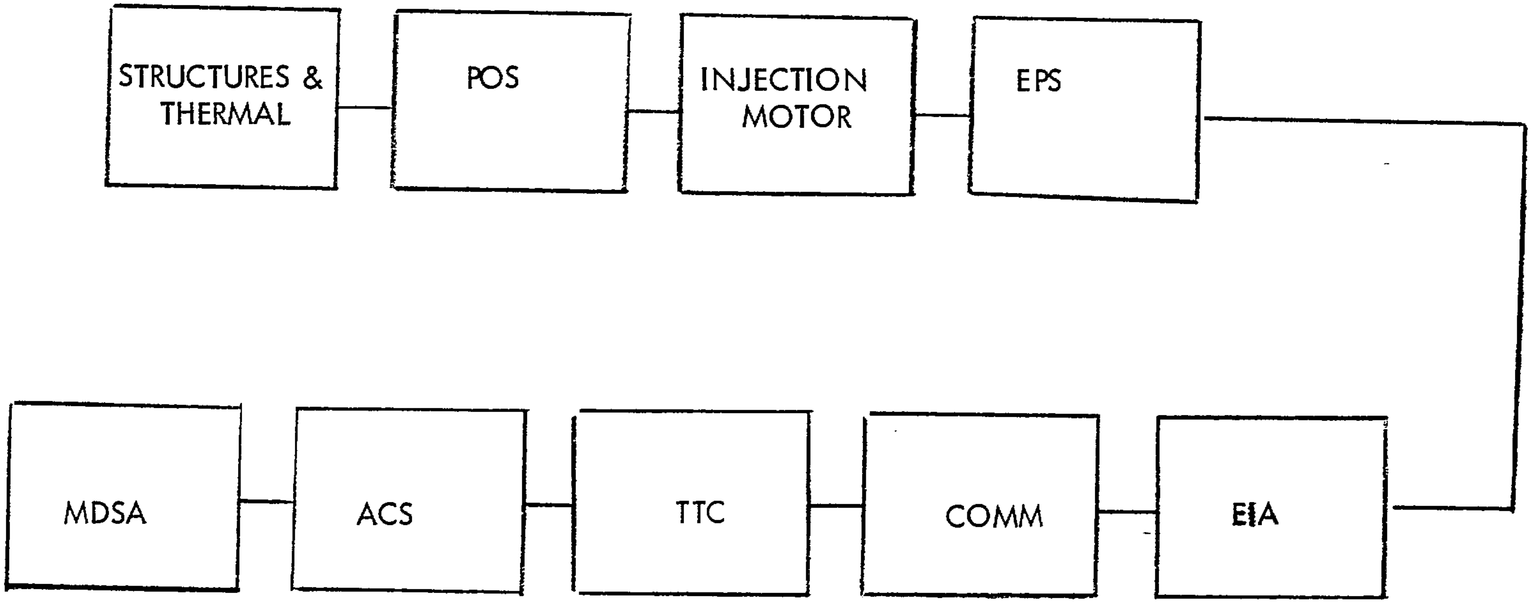

FIGURE 14-11. Reliability Block Diagram of the Spacecraft

A computer program has been written to generate the system reliability versus time characteristic curve which is shown in Figure 14-12, along with the system reliability curve if no reliavility redundancy were incorporated. A substantial improvement in reliability is shown with the proposed design.

14.2.2 Failure Mode and Contingency Analysis

This satellite design employs a highly redundant approach to achieve high reliability for the five-year mission. Nearly every spacecraft function is provided with some alternate means of accomplishing non-degraded performance in the event of primary system failure. Table 14-13 is a subsystem list of redundant backup provisions which currently exist.

14.2.3 Mathematical Models

Ample discussion of the mathematical models applicable in each subsystem analysis is given in the appropriate subsystem discussion (Paragraph 14.1.1 - 14.1.9).

14.2.4 Failure Rate, Mission Time, and Duty Cycles

Most failure rates utilized in this analysis were negotiated with COMSAT Corporation for use on the Intelsat programs. Those failure rates are given in Table 14 - 14. TWTA failure rates are established at 3000 x 10^{-9} failures/hour for high-level TWTA's, and 2000 x 10^{-9} failures/hour for low-level TWTA's. Propulsion equipment failure rates were established by TRW for use on the Intelsat programs (Table 14-1). Standby failure rates for electronic equipment is taken as 10% of the active failure rate of that equipment.

Mission time of most equipment is five years (43,800 hours), plus 30 additional hours to account for launch stresses (43,830 hours, total). The apogee motor and beacon mission times are taken as 48 hours (until acquisition). Some propulsion equipment mission time is quoted in cycles, based on design engineering analysis of the mission profile and performance capabilities of the POS subsystem (Table 14-1).

The only duty cycle imposed is on the electrical integration assembly, where 20% average duty cycle is used, to account for the fact that most of the circuitry is electrically standby status most of the time.

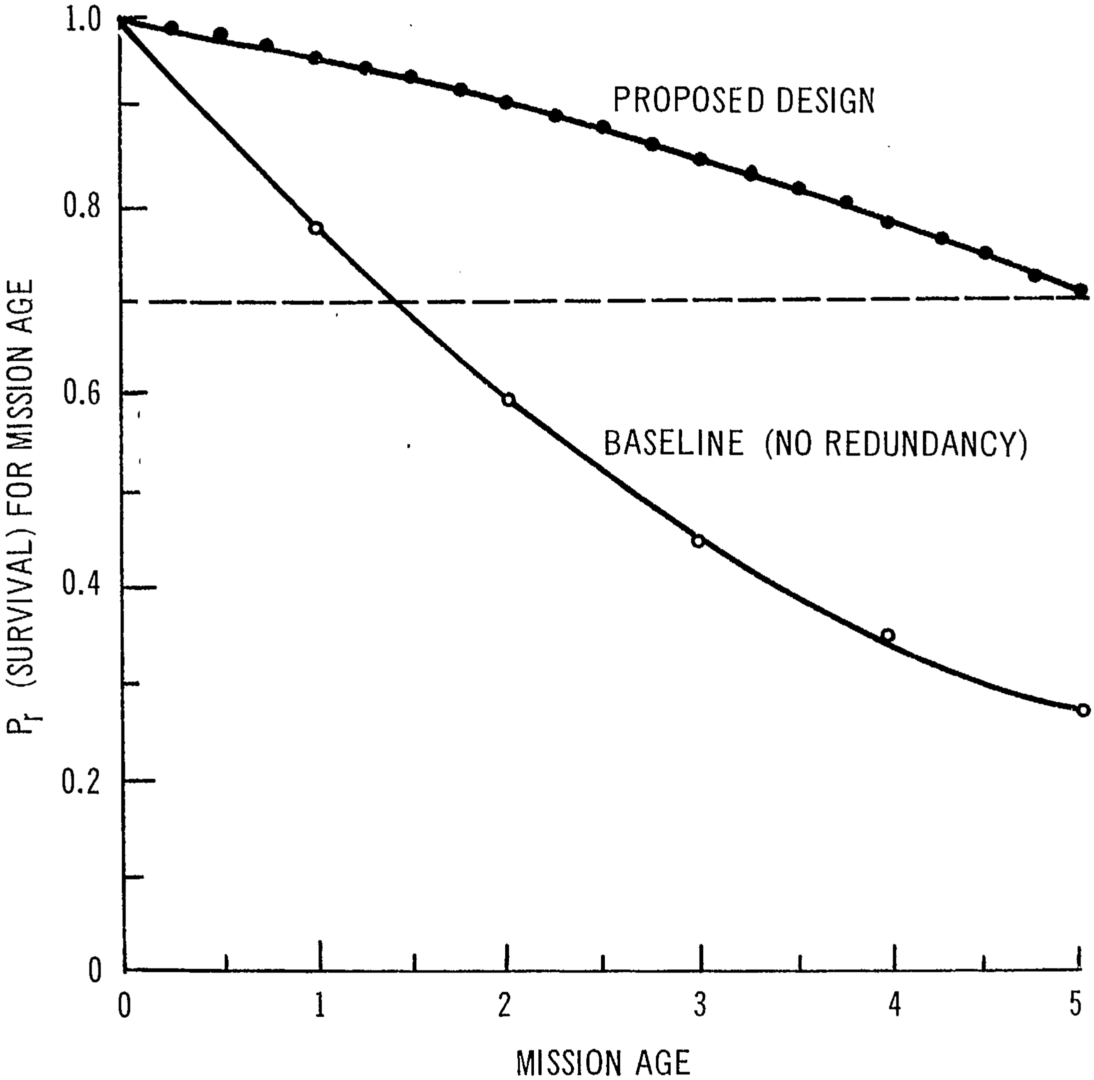

Figure 14–12 Reliability versus Time

Subsystem	System Protection
Positioning and Orientation	Redundant thrusters are available to provide back up if one or both primary thrusters fail closed. Explosive valve is used to route hydrazine from primary to back up thrusters. If one valve fails open, only the fuel remaining in the tanks for that valve is lost.
Electrical Power	Battery is so sized that one of its twenty cells can fail without mission degradation. Battery is protected by special charge monitoring circuits to prevent over-charging. Voting redundancy is provided in charge control and shunting controls. Redundant relay drivers and coils are used. Solar cells are multiply redundantly wired.
EIA	Diodes are used to prevent loss of EIA in the event of failure of either TT&C Decoder.
Communications	A redundant high-level TWTA backs up every pair of active TWTA's to assure as many operating channels as possible at the end of the mission. Redundant low-level TWTA's and mixing circuits are provided.
Telemetry, Tracking and Control	Redundant decoders, receivers, transmitters and encoders are employed. Any configuration of these items may be switched into operation.
Attitude Control	Redundant Earth Sensors are provided. Redundant valve drivers for the POS thruster valves are provided.
Mechanically Despun Antenna	Redundant control electronics is provided.

Table 14 - 13. Failure Mode and Contingency Analysis

PART	FAIL RATE ($X10^9$)
RESISTORS	
Carbon Composition	5
Metal Film	5
Wirewound	10
Thermistor	10
CAPACITORS	
Ceramic	3
Glass	3
Solid Tantalum	20
Trimmer	20
Varicap	10
Feed-Thru	10
DIODES	
Switching	4
General Purpose	10
Zener	50
Varactors	50
Step Recovery	50
Detector / Mixer	100
FILTERS-BANDPASS	10
COUPLERS & CIRCULATORS	10
PLUG & RECEPTACLE CONNECTIONS	2
TRANSISTORS	
Si-General	10
RF	20
Power	50
I.C. 'S	
Analog	20
Digital	10
Insulated (1-10 Gates)	100
TRANSFORMERS	
Signal	10
Inductors	100
Crystals	80

TABLE 14 - 14. PARTS FAILURE RATES

14.2.5 Reliability Versus Weight Tradeoff

To aid in further design optimization of reliability at the minimum weight penalty, a reliability versus weight tradeoff has been performed, the implications of which will be studied and incorporated in succeeding design efforts. For each subsystem, alternate design configurations were generated, including different redundancy schemes and combinations of units. The reliabilities and weights for each configuration were calculated (Table 14-15) and fed to a computerized program; Figure 14-13 is the curve generated from the computer output, which selects the optimum reliability configuration for each weight increment, on the basis of which the optimum configuration may be selected for a given weight constraint.

In this analysis, two optimized system configurations are of particular interest:

- The minimum system weight which meets the minimum reliability goal.

- The maximum system reliability acheivable within a given maximum weight constraint.

The subsystem alternates which yield these system configurations are shown in Table 14-16.

II 15
CONFIGURATION
& LAYOUTS

Communications		Reliability	Weight	Δwt. of Alternative
1.	Non-redundant	.3711	47.6	
2.	Frequency Mixer Redundant	.4107		3.4
3.	One TWTA backing up every two	.7439		14.4
4.	(Alternative 2 & 3 combined)	.8233		17.8
*5.	(Alternative 2 & 3) plus LLTWTA redundant	.9020		20.8
6.	Frequency Mixer Redundant One TWTA backing up every active TWTA LLTWTA redundant	.9368		35.2

TT & C		Reliability	Weight	Δwt. of Alternative
1.	Non-redundant	.5522	11.2	
2.	Decoder redundant	.6400		1.0
3.	Transmitter redundant	.6646		1.6
4.	(Alternative 2 & 3 combined)	.7703		2.6
5.	(Alternative 2 & 3) plus Receiver redundant	.8903		4.2
*6.	(Alternative 5) plus Encoder redundant	.9308		7.8

Electrical Power

Battery & Aux. Electrode Control		Reliability	Weight	Δwt. of Alternative
*1.	Non-redundant	.9652	86	
2.	Electrode Control redundant	.9669		3.1
3.	Battery redundant	.9719		25.9
4.	(alternative 1 & 3)	.9738		29.0

PCU - Converter		Reliability	Weight	Δwt. of Alternative
*1.	Non-redundant	.9325	13.8	
2.	PCU redundant	.9446		.4
3.	Under voltage sensor	.9749		3.8
4.	(alternative 2 & 3)	.9886		4.2

Table 14 - 15. Alternative Designs Considered for Reliability vs. Weight Tradeoff. The Configuration Marked (*) is that adopted in this design.

Table 14-15 - continued

P & O		Reliability	Weight	Alternative
1.	Non-redundant	.9605	91.3	
*2.	Thrusters redundant	.9730		3.6
3.	Leakage Valve added	.9732		4.2
EIA				
*1.	Non-redundant	.9820	19.0	
2.	Active Parallel EIA	.9977		3.0
Despin Antenna				
1.	No redundancy	.8926	19.5	
*2.	Redundant Electronics	.9465		4.5
ACS				
1.	Non-redundant	.9648	3.0	
*2.	Redundant ESA	.9982		1.2
3.	Two redundant ESA's	.9991		2.4
Struct., Thermal, Apogee Motor				
*1.	Non-redundant	.9926	594.3	

Table 14 - 15. Alternate Designs Considered for Reliability vs. Weight Tradeoff. The Configuration Marked (*) is that Adopted in this Design.

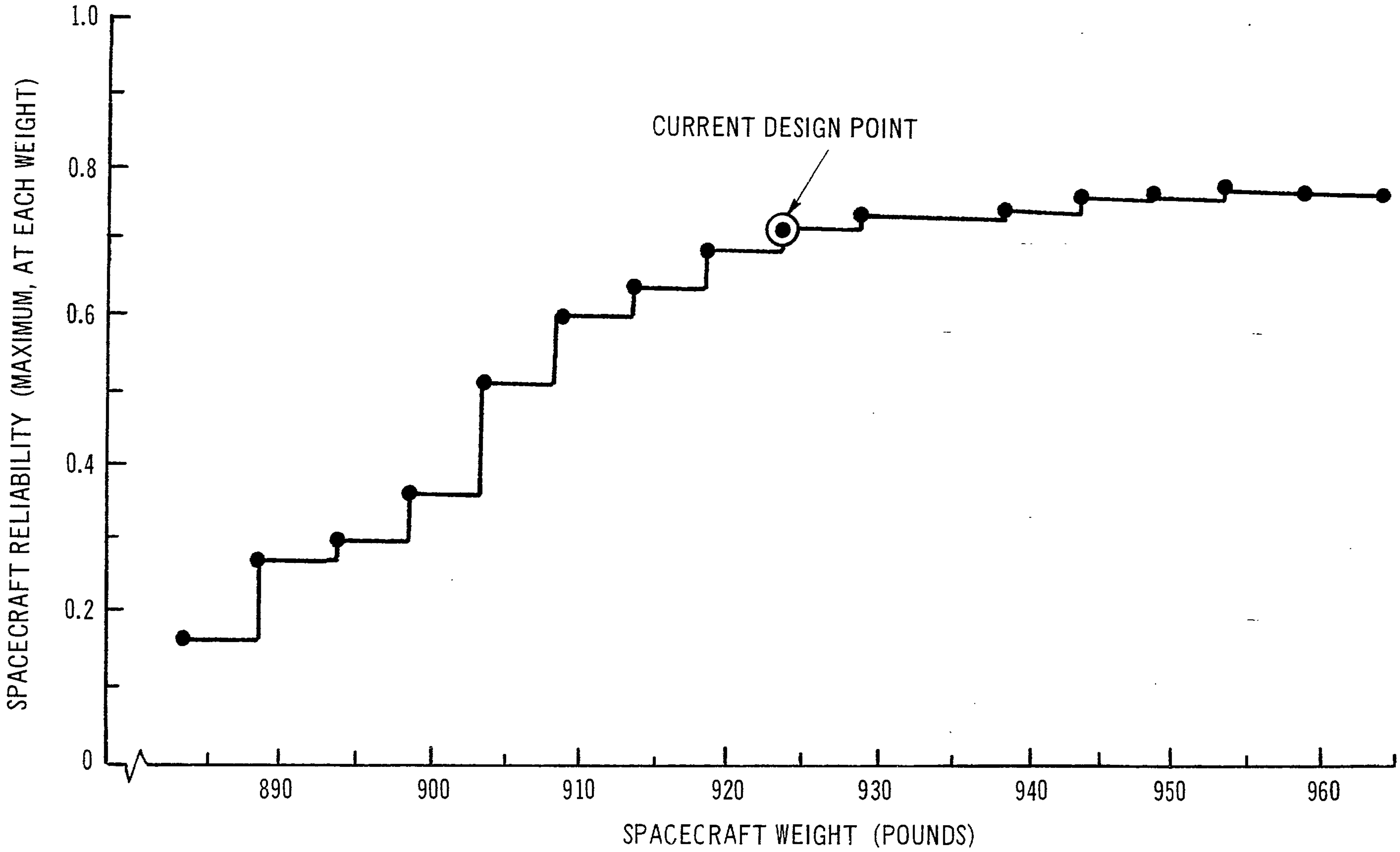

Figure 14-13 Maximum Reliability versus Weight Curve

Subsystem	Proposed Configuration Config. No.	Proposed Configuration Weight	Max. Reliability with Weight Constraint=965# Config. No.	Max. Reliability with Weight Constraint=965# Weight	Minimum Weight Meeting R = .70 Config. No.	Minimum Weight Meeting R = .70 Weight
Communications	5	68.4	6	82.8	5	68.4
TT&C	6	19.0	6	19.0	6	19.0
Battery & Aux. Electrode Control	1	86.0	2	89.1	1	86.0
PCU-Converter	1	13.8	4	18.0	4	18.0
Pos. & Orientation	2	94.9	3	95.5	1	91.3
EIA	1	19.0	2	22.0	1	19.0
Despin Antenna	2	24.0	2	24.0	2	24.0
ACS	2	4.2	3	5.4	1	3.0
Structures, Thermal, etc.	1	597.7	1	597.7	1	597.7
Total		927.0		953.5		926.4
Reliability		0.7005		0.7796		0.7000

Note that, although the proposed configuration is slightly different than the optimum one for achieving reliability of 0.7 for the five-year mission, only a very slight weight penalty is imposed (.6 pounds). Reliability of .7 cannot be obtained with less weight than 926.4 pounds. No additional reliability can be obtained from the alternative configurations chosen for the study by increasing the weight of the spacecraft above 953.5 pounds (but staying within the 965 pound maximum weight.)

Figure 14-16. Optimum reliability vs. weight tradeoff.

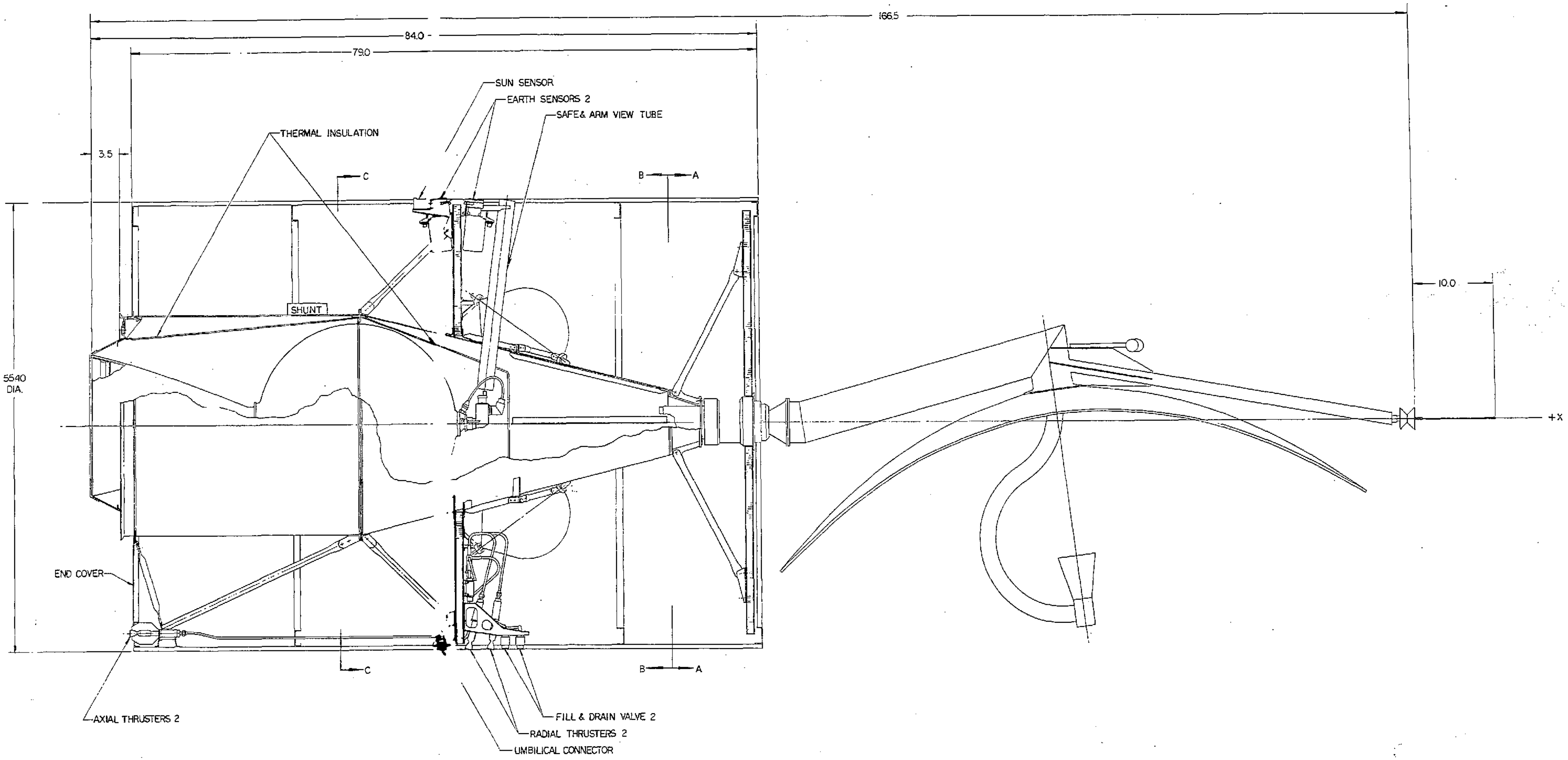

Figure 15-1 General arrangement of Spacecraft

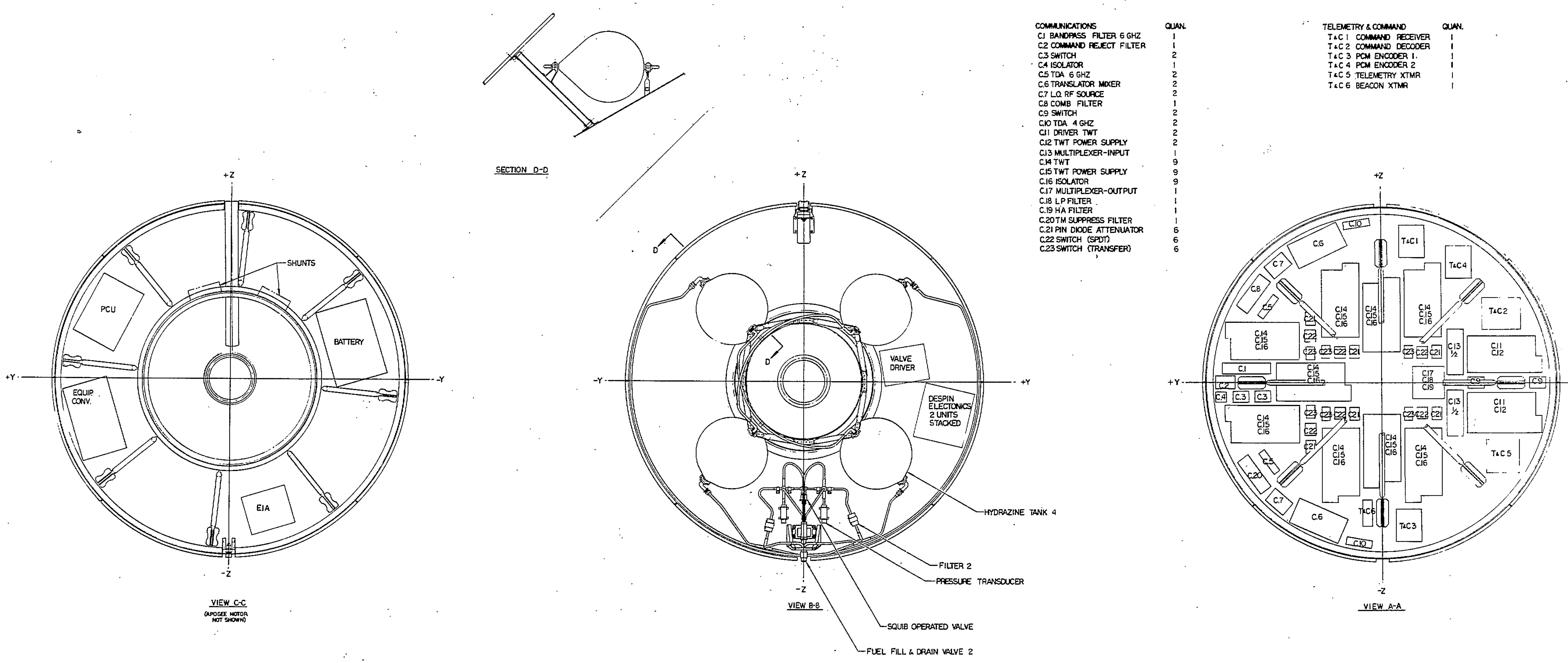

COMMUNICATIONS	QUAN.
C.1 BANDPASS FILTER 6 GHZ	1
C.2 COMMAND REJECT FILTER	1
C.3 SWITCH	2
C.4 ISOLATOR	1
C.5 TDA 6 GHZ	2
C.6 TRANSLATOR MIXER	2
C.7 L.O. RF SOURCE	2
C.8 COMB FILTER	1
C.9 SWITCH	2
C.10 TDA 4 GHZ	2
C.11 DRIVER TWT	2
C.12 TWT POWER SUPPLY	2
C.13 MULTIPLEXER-INPUT	1
C.14 TWT	9
C.15 TWT POWER SUPPLY	9
C.16 ISOLATOR	9
C.17 MULTIPLEXER-OUTPUT	1
C.18 L.P FILTER	1
C.19 H.A FILTER	1
C.20 TM SUPPRESS FILTER	1
C.21 PIN DIODE ATTENUATOR	6
C.22 SWITCH (SPDT)	6
C.23 SWITCH (TRANSFER)	6

TELEMETRY & COMMAND	QUAN.
T&C 1 COMMAND RECEIVER	1
T&C 2 COMMAND DECODER	1
T&C 3 PCM ENCODER 1	1
T&C 4 PCM ENCODER 2	1
T&C 5 TELEMETRY XTMR	1
T&C 6 BEACON XTMR	1

Figure 15-2 General Deck Arrangement of Spacecraft

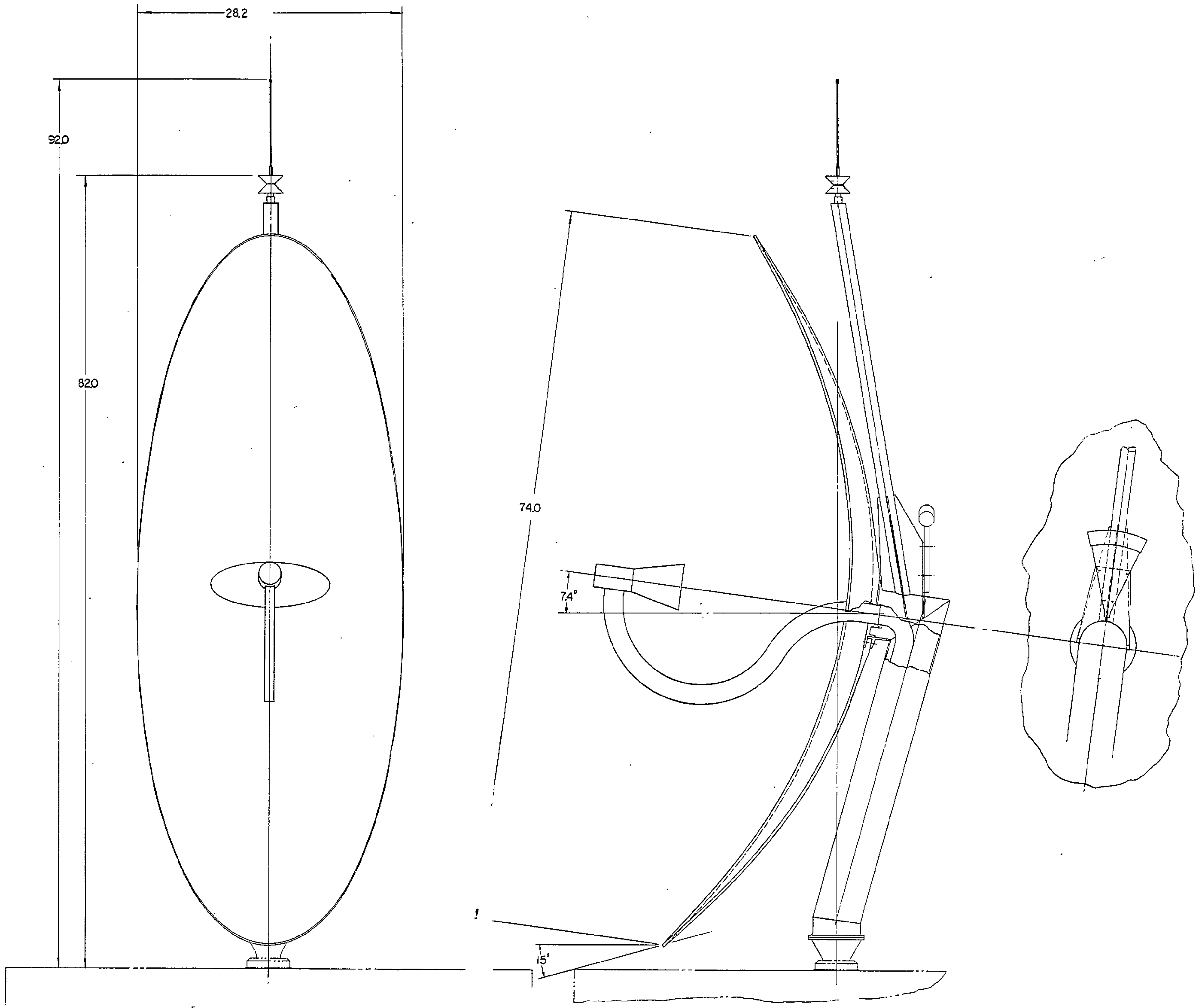

Figure 15-3 Spacecraft Antenna Arrangement

16

GROUND SUPPORT

16. GROUND SUPPORT EQUIPMENT

16.1 INTRODUCTION

The purpose of the ground support equipment is to provide suitable power and test signals, displays, and mechanical handling as are necessary to integrate and test subsystems as well as a complete spacecraft. To achieve this the equipment is broken down into segments which correspond to the major subsystems of the spacecraft which may be built and tested at widely separated locations. These segments may be duplicated in part or whole to make up an integrated system test set (ISTS) which will be used to check out the complete spacecraft during integration and environmental testing. It is expected that two ISTS will be required for the program because of schedule and location requirements. For the lower equipment deck and the solar panels, an arrangement of test equipment called the Hardline Test Station (HLTS) will be used. For the upper equipment deck and antenna two arrangements of test equipment called the Communications Test Set (CTS) and the Telemetry and Command Test Set (TCTS) will be used.

16.2 HARDLINE TEST STATION

16.2.1 GeneralDescription of Hardline Test Station (HLTS)

The Hardline Test Station (HLTS) provides a "stand-alone" capability to support integration and functional system test of the TRW furnished equipment for this program. The HLTS is comprised of a double-bay, dolly-mounted electronic enclosure housing rackmounted electronic drawers, (figure 16-1, Front Rack Layout) which will be custom designed to permit complete test and evaluation of the TRW "spacecraft." The HLTS will become part of the total system test set when combined with the RCA furnished communications, telemetry, tracking and command and antenna test sets, during spacecraft integration.

The HLTS uses design concepts from INTELSAT III and other spacecraft programs. Equipment selection is based on prior experience and proven design standards to assure meeting requirements in transportability, reliability, electromagnetic compatibility, maintainability, environmental control, and human factor considerations.

Two complete sets of the HLTS are required to satisfy schedule constraints as well as provide some spares coverage. The Equipment List, Table 16-1, shows equipment design status, derivation and required quantities.

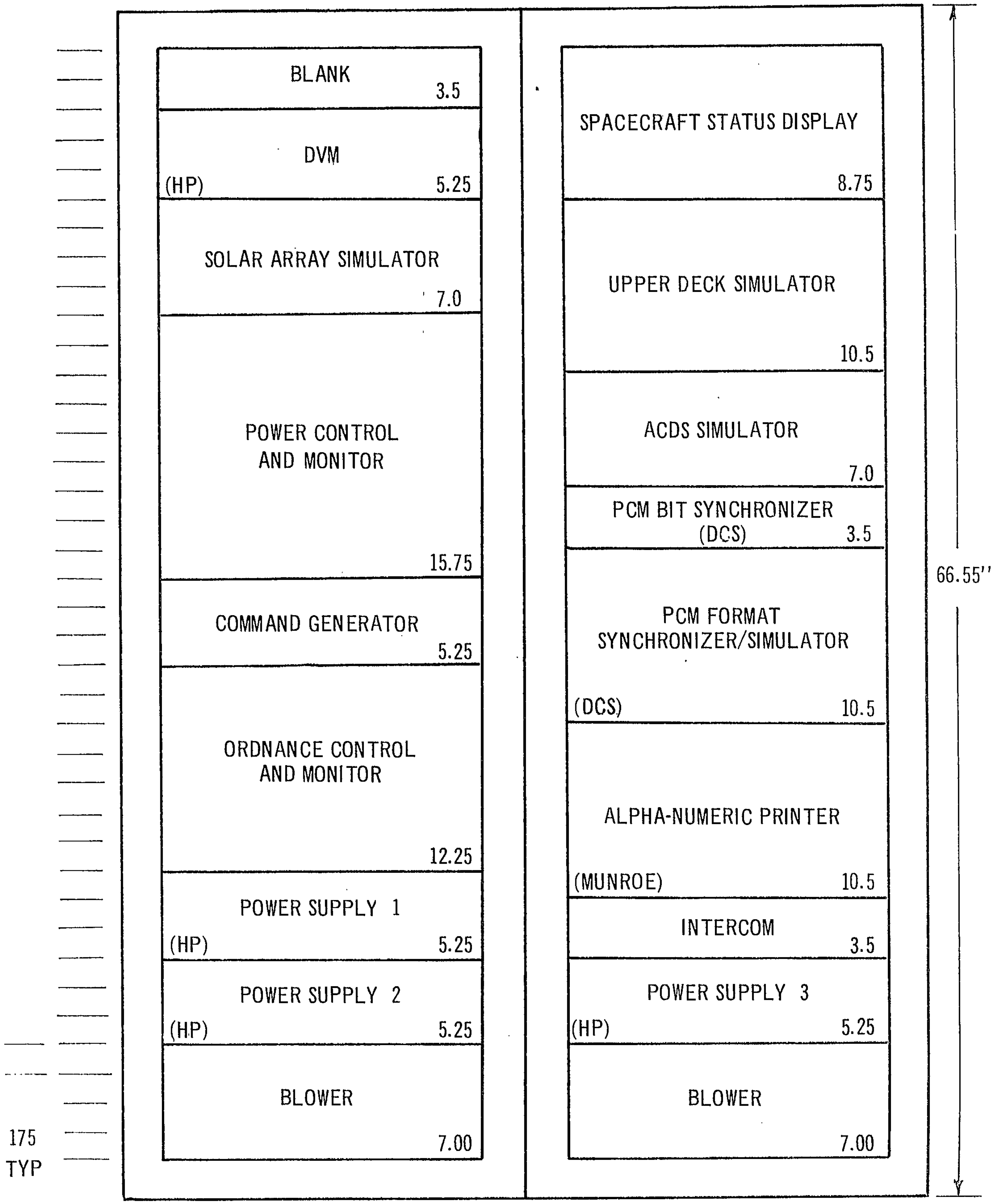

Figure 16–1 Hardline Test Station Front Rack Layout

Table 16-1 Hard Line Test Set Equipment List

1. DVM - Hewlett Packard
2. Solar Array Simulator
3. Power Control and Monitor
4. Command Generator
5. Ordnance Control and Monitor
6. Power Supply 1
7. Power Supply 2
8. Spacecraft Status Display
9. Upper Deck Simulator
10. ADCS Simulator
11. PCM Bit Synchronizer - DCS
12. PCM Format Sync/Sim - DCS
13. Printer - Monroe
14. Ordnance Load Simulator
15. In-Flight Jumper Simulator
16. Cable Subset
17. Series Fuse Box
18. Sun Sensor Stimulus
19. Earth Sensor Stimulus

16.2.2 Detailed Description

16.2.2.1 Power Subsystem Test Equipment

The HLTS provides a means of operating the power subsystem in all preflight and flight modes. The three basic modes are:

- o Solar Array Simulation, which permits exercise of the power subsystem in all flight modes.
- o External Power, which permits powering the S/C primary bus from a regulated power supply to permit over/under voltage and power profile testing.
- o Battery Charging, which permits charging the S/C battery from the test set during battery discharge tests and prelaunch operations.

The Test Set Block Diagram, Figure 16-2, shows the manner in which these power modes are implemented. The Power Control and Monitor Drawer contains switching, metering and controls for power supplies No. 1, 2 and 3, as well as analog metering for S/C bus and battery voltage, current and temperature. The supplies can be configured as follows:

In the Solar Array Simulator Mode, PS-1 operates in constant voltage to simulate the upper half of the Solar Array, while PS-2 operates in constant current, conditioned by circuitry in the Solar Array Simulator Drawer to simulate the bottom (shunt regulated) half of the Solar Array.

In the External Power Mode, PS-1 supplies power to the S/C primary bus in a constant voltage mode.

In the Battery Charge Mode, PS-3 supplies current to the S/C battery in either constant current (trickle) or constant voltage.

The Power Control and Monitor Drawer also contains discrete status indicators for monitoring power subsystem status.

The In-flight Jumper (IFJ) Simulator is a peripheral equipment item which relays power functions to the spacecraft in lieu of the flight jumper which is a connector. Controls for the IFJ Simulator are located in the Power Control and Monitor Drawer.

Lastly, a Digital Voltmeter (DVM) is provided for precise monitoring of critical power subsystem parameters; e.g., battery terminal voltage, trickle charge current, etc.

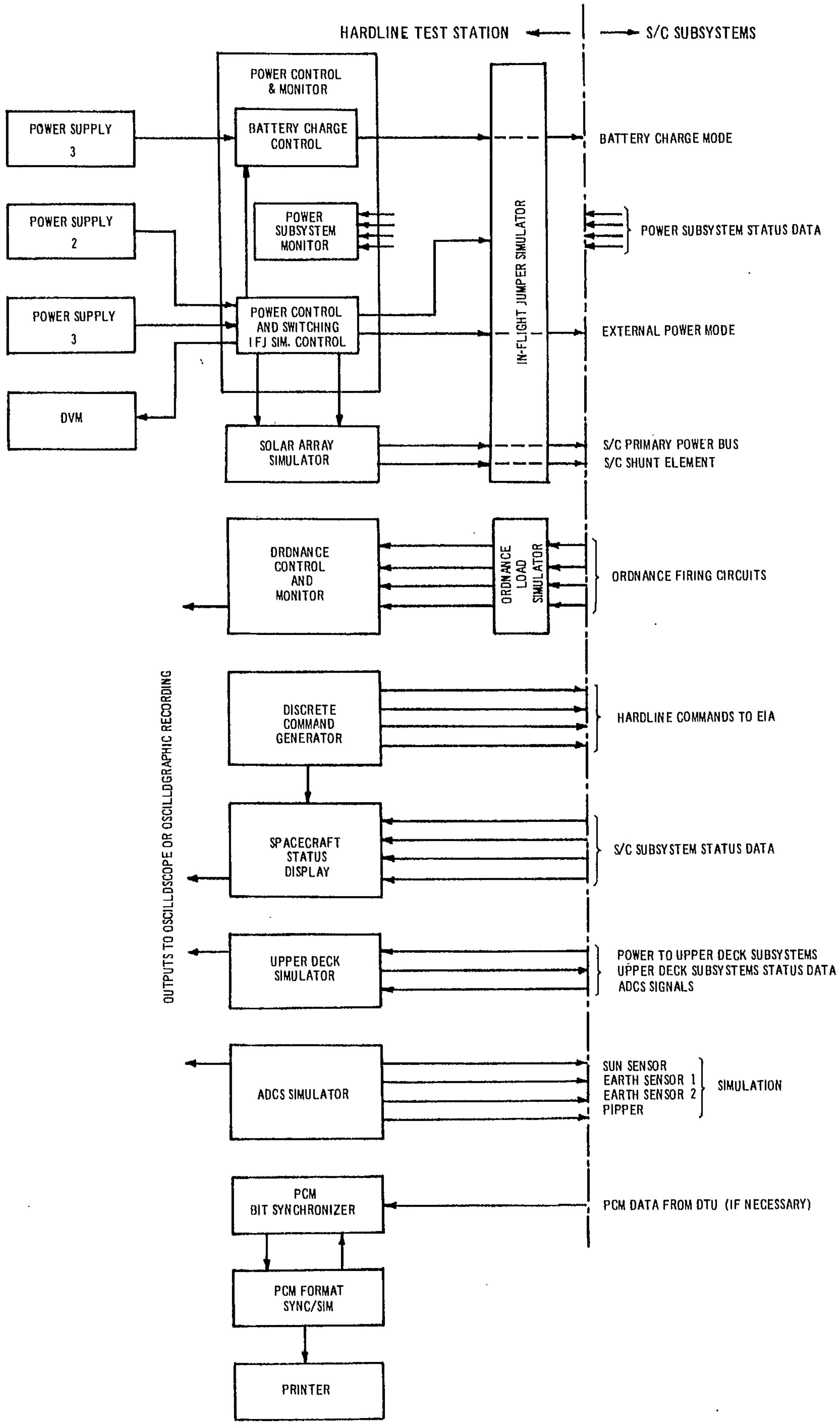

Figure 16-2 Block Diagram Hardline Test Switch

16.2.2.2 Ordnance Control and Monitor

The Ordnance Control and Monitor together with the Ordnance Load Simulator permits measurement of ordnance current pulses, both amplitude and duration, into a simulated squib load, to verify:

- The presence of an "all-fire" pulse when S/C ordnance circuits are activated or --
- The presence of a "no-fire" pulse occurring during all or any other S/C subsystem testing.

The Ordnance Load Simulator, is a peripheral equipment item containing resistive loads which are connected to the S/C ordnance circuits in place of live ordnance. When an ordnance pulse occurs, the voltage across this simulated squib is sensed for both magnitude and duration. Some short time (5-10 ms) after initiation of the firing pulse, a "clear" relay in the ordnance load simulator opens the load on the S/C ordnance relay so as to relieve it from switching ordnance firing currents and arcing contacts. The Ordnance Control and Monitor contains go-no-go indicators which "go" when the conditions for all-fire ordnance currents are satisfied. The thresholds for both pulse amplitude and duration are variable to permit monitoring both all-fire and no-fire currents.

16.2.2.3 Command Generator

Since the command decoders are located on the upper deck, it is necessary to provide a hardline capability to command the TRW furnished subsystems and the upper deck simulator prior to satellite integration. The Command Generator Drawer develops the required hardline commands for injection into the EIA at the decoder interface. Since it is necessary to provide a complete command capability; e.g., power, ordnance, mode and unit select, it will be cost effective to utilize a common design for both the HLTS and the EIA factory support equipment.

16.2.2.4 Spacecraft Status Display

The Spacecraft Status Display Drawer provides continuously updated status data of the spacecraft command configuration, and other operating modes. The unit will receive status data from two sources:

- A command matrix monitor will accept output data from the command generator, in parallel with the spacecraft.
- A spacecraft status monitor will accept discrete output data from the EIA which indicates command receipt and execution, and also status data which is non-command oriented; i.e., ACS mode, redundant mode, etc.

16.2.2.5 Upper Deck Simulator

During integration and functional system test of the TRW portion of the satellite, it is necessary to exactly simulate the electrical interface of the upper deck. The Upper Deck Simulator (UDS) Drawer will contain:

- Loads for all power lines to the UDS
- Loads for all commands to the UDS
- Loads for all ADCS signals to the UDS
- Loads for all telemetry outputs from the lower deck to the upper deck, if the satellite DTU is located on the upper deck.

16.2.2.6 Attitude Determination & Control Subsystem (ADCS) Simulator

The ADCS Simulator Drawer provides capability to:

- Simulate earth (2) and sun sensor electrical outputs
- Simulate earth reference pipper signal
- Stimulate earth (2) and sun sensors

Simulators

Simulation of the earth sensor signals is performed by applying the simulator signals at the earth sensor/attitude determination and control interface. Similarly sun sensor and earth reference pipper simulation signals are applied at the sun sensor and pipper interfaces with the attitude determination and control interfaces.

The various simulations required are controlled in the drawer by:

- A basic variable clock where the clock provides the timing trigger for all simulation signals.
- Positioning signals which are adjustable delays from the basic clock pulse.
- One-shot pulse generators, which have controllable widths.

In a typical sequence the clock pulse triggers the positioning circuit and after the preset delay period the one-shot circuit is triggered to form a pulse with the preset width.

Different spin rates are simulated by changing the frequency of the clock. Simulation of the earth sensor pulse pairs is accomplished by adjusting variable pulse width, one-shot circuits. The differentiated output of these pulses is the required pulse pairs. The pulses are positioned by delay circuits.

The three pulse outputs of the sun sensor (reference pulse, measurement pulse, and polarity pulse) which vary in relative position and width as a function of angular position of the spacecraft with respect to the sun are simulated by adjusting a delay circuit between the reference pulse, which is the first pulse in the group, and the measurement pulse, and between the reference pulse and the polarity pulse. Pulse widths are controlled by variable width, one-shot circuits The polarity pulse either exists or is deleted to simulate polarity. Again the pulse group is positioned by a delay circuit.

The earth reference pipper output, which is variable as a function of the spacecraft azimuth angle with respect to the earth, is simulated by positioning the pulse with the delay circuit and adjusting pulse width with a one-shot circuit.

Stimulators

The sun sensor stimulator is a gun with a high intensity, high temperature tungsten filament source. The earth sensor stimulators, fastening directly on the sensor, are infrared sources with a rotating disc assembly to simulate the earth-body and spin of the spacecraft. The output of the stimulator is collimated to the earth sensor with collimating mirrors.

16.2.2.7 PCM Decommutator

This item is proposed as an option, if it is decided to locate a digital telemetry unit (DTU) on the lower deck with the TRW furnished equipment. It is extremely desirable from a test point of view to have telemetry data as well as hardline data available during integration and test.

The PCM Bit Synchronizer would receive baseband PCM data from the output of the DTU, establish synchronization and extract serial clock and data. The PCM Format Synchronizer will format and serial to parallel convert the telemetry data for compatibility with the output printer. Both units are commercially available items, off-the-shelf.

16.2.2.8 Alpha-Numeric Printer

If the PCM Decommutator is utilized, a high-speed alpha numeric printer is proposed to output the telemetry data. The proposed unit will print 6000 lines of 32 alpha numeric characters per minute which will enable printout of 100% of telemetry data if desired. This unit, too, is commercial and off-the-shelf.

16.2.2.9 Integration Equipment

A cable set will be provided to permit interconnection of the HLTS with primary power and with the spacecraft. The cables are the heavy-duty rubber-molded type for maximum reliability.

Two series fuse boxes with cable adapters will be provided with each HLTS to provide capability for test points and fusing S/C circuits during integration.

16.3 COMMUNICATION TEST-SET

16.3.1 Description of Communication Test-Set

The integrated system tests cover a series of RF tests and baseband measurements. The effort is to ensure satisfactory performance of the satellite when in operation.

The transmission characteristics which will be measured are;

- Input VSWR - Output VSWR

  Measurements of the Return loss level at the input and at the output of the transponder. Frequency markers give the exact channel bandwidths.

- Gain and Isolation Characteristics

  The relative RF amplitude response is recorded to give the transfer characteristics. Each channel is marked with frequency markers giving individual channel bandwidths and centre frequencies.

- Group Delay

  Individual channel responses are recorded using an RF Network Analyzer. The linear,parabolic,and ripple components are checked using a FM Measuring test set.

- RF Noise Loading

  The crosstalk and intermodulation is evaluated using RF noise equipment.

- Intelligible Crosstalk and AM-to-PM Conversion

  The AM/PM transfer coefficient and crosstalk characteristics of the transponder is measured.

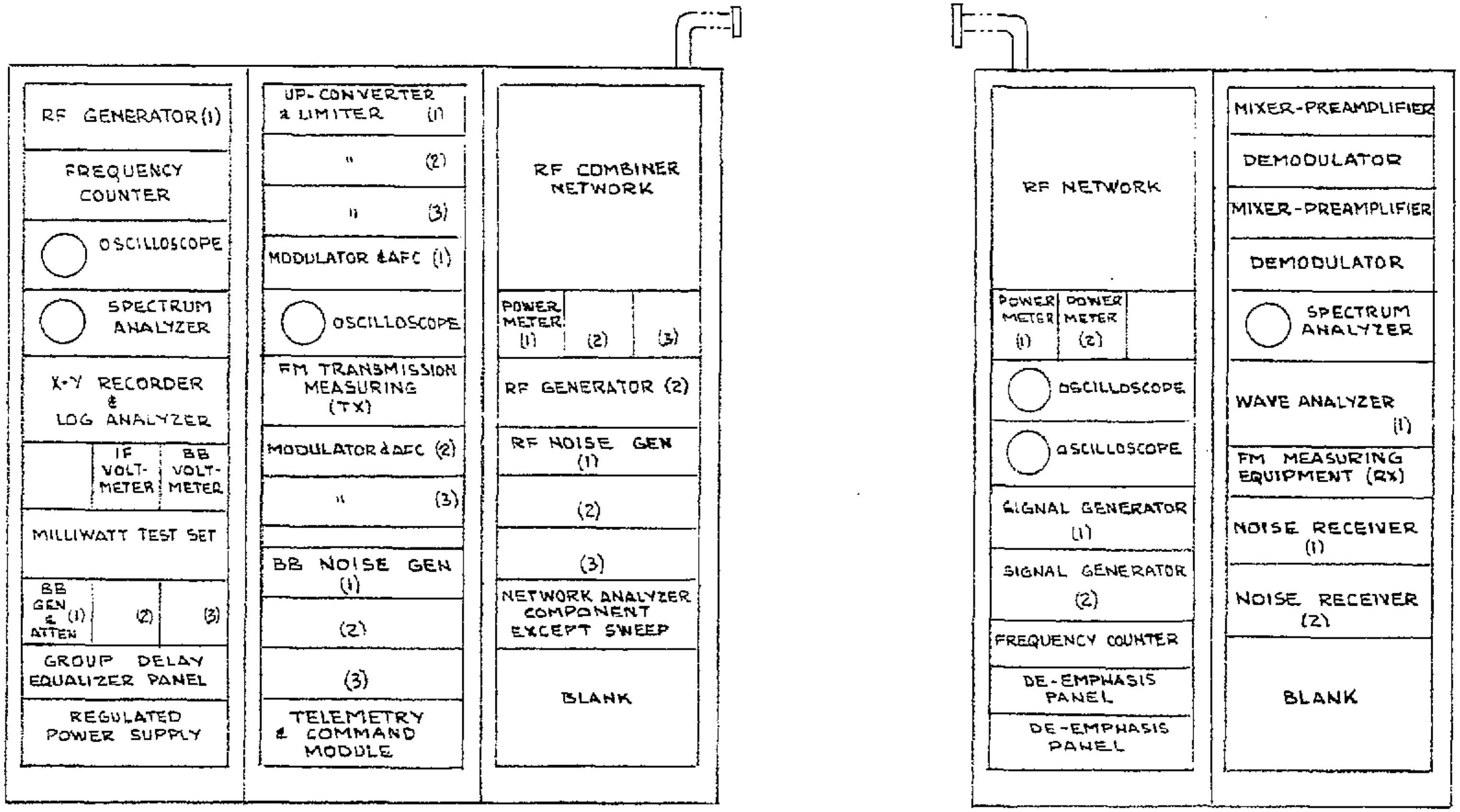

TEST BAYS: TRANSMITTER; CAPABLE OF SIMULATING 3 TRANSMITTER SIMULTANEOUSLY.
(ALL 6 CHANNELS IF 3 CHANNELS ARE LOADED WITH NOISE)

RECEIVER; CAN MONITOR 2 CHANNELS SIMULTANEOUSLY.

NOTE: TO EASE MEASUREMENTS A FURTHER RACK MAY BE ADDED TO BOTH TEST BAYS.

Figure 16-3 Communications Test Set Rack Layout o **Receive Sensitivity**

The carrier to noise density is measured.

o **NPR**

Measurements to determine the NPR are performed.

A checkout of a simulated failure plus the exercise of switching operations concludes the communication tests.

16.3.2 Test Equipment List

This equipment can simulate up to 3 RF Channels simultaneously.

Table 16.2

Transmitter Test Bay Equipment

Qty	Name or Function
1	Spectrum Analyzer
1	Frequency Counter
2	RF Sweep Generators
1	X-Y Recorder and Log Converter
1	RF Attenuator and IF Att. Panel
1	Milliwatt Test Set
3	Power Meters
3	RF Noise Generators
3	BB Noise Generators
1	FM Transmission Measuring Equipment
3	Modulators and AFC Panels
3	Upconverters and Limiters
1	BB Voltmeters
3	Group Delay Equalizer panel
1	IF Voltmeter
3	BB Attenuators and Generators
3	Oscilloscopes
1	RF Network Analyzer Set-Up (Sweep Gen. PIN Modulator Mod. Generator 1-10 MHz Vector Voltmeter X-Y Recorder Test Atten. pads
1	RF Combining Network
1	Telemetry and Command Simulator
Misc.	IF, RF detectors and coaxial attenuators, polaroid camera, frequency meters.

Power supplies for operation of all active components in the transponder are assumed supplied.

Receiver Test Bay Equipment

Qty	Name
1	Spectrum Analyzer
1	X-Y Recorder
1	Frequency Counter
2	Power Meters
1	IF Voltmeter
1	FM Transmission Measuring Equipment (Rx)
1	Wave Analyzer
2	4 GHz demodulators
2	4 GHz De-emphasis Panels
2	Mixer Pre-amp 4 GHz
2	Oscilloscopes
2	L.O. Signal Generators
2	Noise Receivers

Other Miscellaneous Items

IF and RF Detectors
Coaxial Attenuators
Coaxial cables
RF Variable Attenuator
IF Variable Attenuator
RF Filter Panels
Group Delay Equalizer Panels
Regulated Power Supply
Polaroid Camera
RF Wavemeters

This equipment is sufficient to monitor two channels simultaneously at RF, IF or baseband frequencies.

16.4 TELEMETRY AND COMMAND TEST-SET

16.4.1 General

The Telemetry and Command Test Set portion of the Ground Support Equipment would require about 8 racks of equipment to provide the check-out capability for the spacecraft. Basically, this equipment* would consist of;

a) Command Generator
b) Range Tone Generator
c) Command Transmitter
d) Telemetry Receiver
e) Telemetry Baseband Processing
f) PCM Processing
g) Displays
h) Computer
i) Patching
j) Tape Recorder and Miscellaneous Equipment

A typical block diagram of the equipment is shown in Figure 16-4 whilst a possible rack layout is shown in Figure 16-5. A more detailed requirement of the equipment now follows.

a) Command Generator

This unit would generate all spacecraft commands and execute tones, including the address code, in the proper format. It should be capable of either "manual" or "automatic" operation.

In "manual" operation, each command would be entered into the input register of the generator by the operator using push buttons, toggle switches, or other suitable means. Commands would be transmitted and verified and then executed, each step requiring a definite operator action.

In "automatic", a series of commands would be stored in a computer or on punch card or tape. The operator would start the sequence and thereafter the sequence of events would be automatic. In a typical sequence, a command would be transferred from the computer (or punched medium) to the input register of the command generator and transmitted to the spacecraft. The verified command would be received and entered into the verify register and compared with the input register. If the two agree, the execute command would be transmitted. When the execute verify is received, the next command would be entered into the input register and the process repeated.

If command verification were not received within a predetermined period, the command would be sent again. If no verification is received after a certain number of attempts (say, three), then the sequence would be terminated and an alarm sounded to summon the operator.

* Sensor pulse simulators, attitude processing equipment and artificial earth pulse generators are described in Section 16.2. However, they are shown in the telemetry and command GSE block diagram and rack layouts for completeness and to illustrate interface.

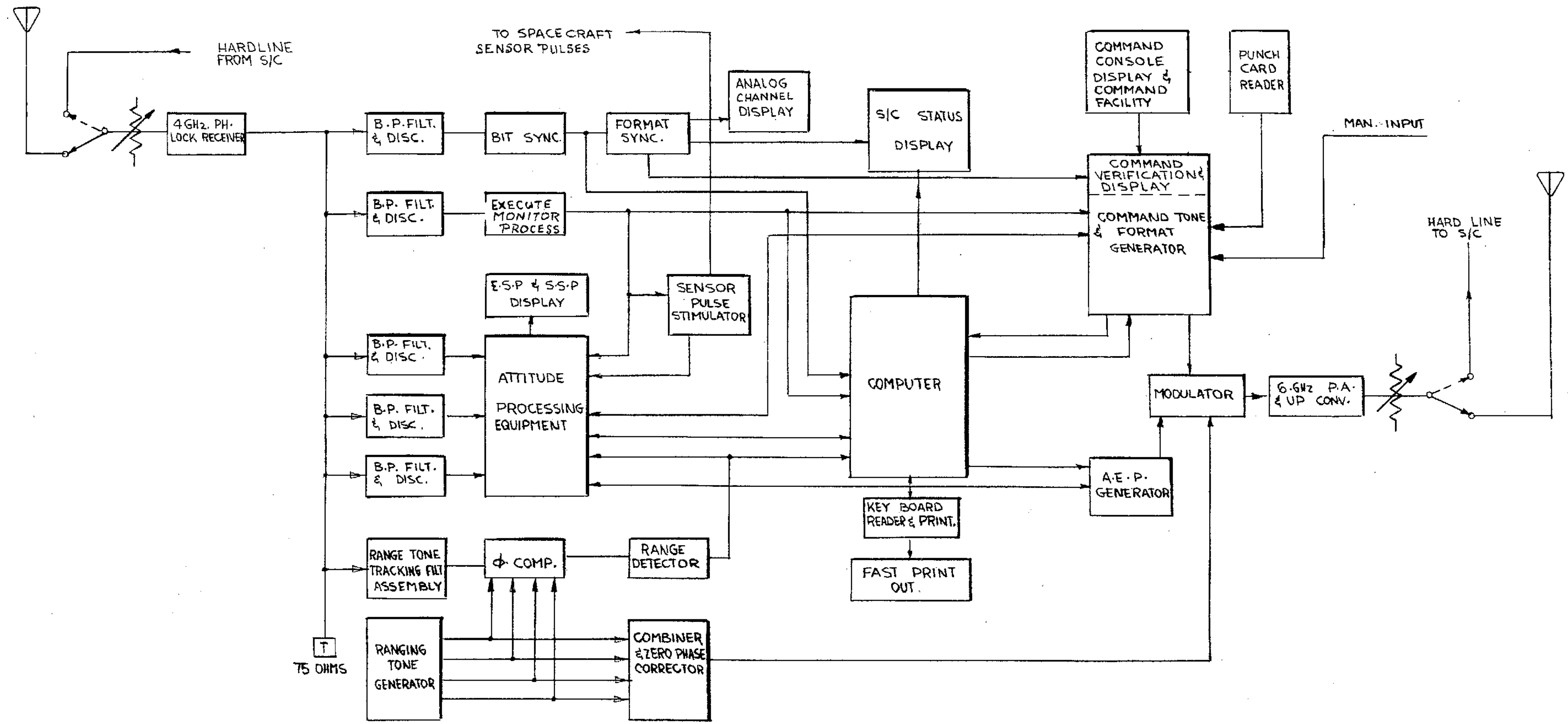

T – TERMINATION
E.S.P. – EARTH SENSOR PULSE
S.S.P – SUN SENSOR PULSE

Figure 16.4
Telemetry & Command Test Set Block Diagram
Ground Support

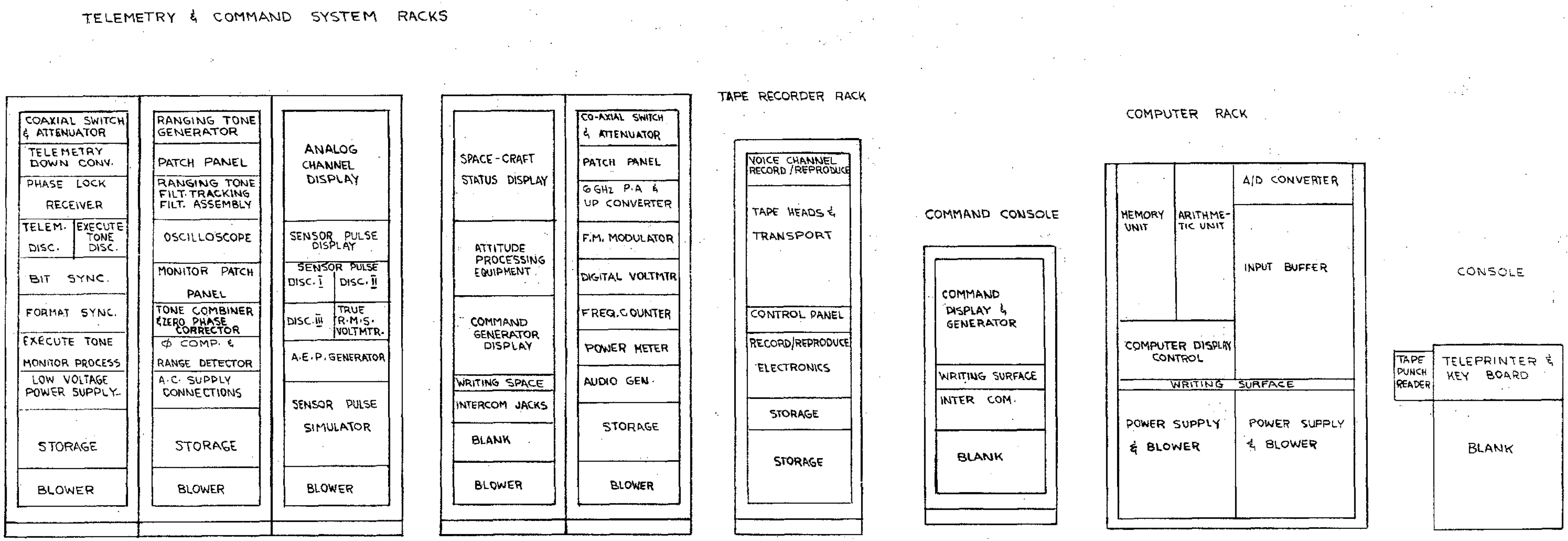

Figure 16.5
Typical GSE Rack Layout for the Telemetry and Command Subsystem

b) Range Tone Generator

This unit would generate the four ranging tones. Phasing and amplitude adjustments would be provided for calibration.

c) Command Transmitter

This unit would receive the command and execute signals, ranging tones, and the artificial earth pulse sub-carrier. These would be combined into a single baseband which would frequency modulate an IF carrier. The IF carrier would then be up-converted to the 6 GHz command frequency authorized, and amplified to a suitable level* for either hard line connection or radiation to the satellite. RF attenuators and switches would be provided in the output circuitry for control of carrier level.

d) Telemetry Receiver

The 4 GHz telemetry signals would be received either by hard line connection from the spacecraft or "off-air" from an antenna. RF attenuators and switches in the antenna line would permit adjustment of the received carrier level.

The received signal would be first down converted to the 136 MHz band after amplification by either a parametric amplifier or a tunnel diode amplifier. The use of either of these low noise microwave devices would permit use of the receiving equipment during the initial orbital passes of the spacecraft after launch.

A conventional "off-the-shelf" 136 MHz telemetry receiver would be used for recovery of the telemetry baseband signal. The receiver would be fitted with a carrier phase lock demodulator.

The receiver baseband output would consist of a telemetry sub-carrier, three sensor pulse sub-carriers, four ranging tones, and (intermittently) the execute verification tone.

e) Telemetry Baseband Processing

This equipment would be used to separate the component signals in the baseband and to demodulate the sub-carriers.

Separation of the signals would be accomplished using bandpass filters buffered at the input and the output by amplifiers. The impendance of the

* A nominal 10 watt RF output level from the transmitter would provide ample range for all checkout requirements before launch.

input buffer amplifier would be much higher than the receiver output impedance to prevent loading changes of the receiver output whenever filters are removed or replaced.

The extracted telemetry sub-carrier would be demodulated using either a FSK or PSK demodulator. If FSK demodulation were used, some de-emphasis would have to be added. The output telemetry signal would be raw PCM data to be further processed.

The sensor sub-carriers are modulated in accordance with IRIG recommendations, hence conventional "off-the-shelf" IRIG demodulators can be used to recover the sensor signals. Three separate demodulators are required, and the recovered sensor signals are now sent to the attitude control equipment for further processing.

The ranging tones are recovered using 1 Hz bandpass phase lock demodulators. The recovered ranging tones are sent to the range processor.

f) <u>PCM Processing</u>

The raw PCM signal from the telemetry sub-carrier discriminator is first "cleaned up" with a bit synchronizer, where the signal is reshaped and a bit rate clock signal derived. The reshaped signal is then applied to a format synchronizer where the synchronizing code is recognized and from this the PCM data can be re-constructed properly. At this point, the sub-frame can be identified, the spacecraft signature can be obtained, and the command verification signal can be extracted and sent to the command generator. All PCM data can be sent to the computer for processing and storage, or printed out as required for record and examination.

g) <u>Displays</u>

There are three display drawers provided for. During manual operation they receive signals from the format synchronizer and attitude processing equipment while during automatic operation the computer provides the required signals.

The analogue display selects any ten of the analogue channels and presents the telemetered data in digital form. This data is updated at the analogue channel rate.

The spacecraft status display decodes the telemetry flags and displays the continuously updated status of the various spacecraft systems together with the spacecraft signature.

The command and verification display is duplicated in command generator rack and in the command console for convenience. It displays the text of the command transmitted in coded form. When the verified text is received from the spacecraft via telemetry, it too is displayed. The two texts are compared and, if they agree, the 'execute ready' sign is displayed and the command generator can then transmit the execute part of the command.

h) Computer

The computer rack with its teleprinter console is self-sufficient. It is mainly used for the automatic checkout of the spacecraft, however it may also be used for some signal processing or error rate evaluation.

In automatic operation, it will interface with the command generator and will command spacecraft through some predetermined sequence of commands. During this sequence it will accept processed data which will continuously update the displays and will be available in memory for fast printout.

i) Patch Panels

These are provided to interconnect the equipment in various racks and to permit test points. There are separate monitor patch panels for monitoring during test as well.

j) Tape Recorder and Other Support Equipment

The tape recorder will have the capability of analogue recording, frequency modulated recording (for video signals) and a voice track. It will be mainly required when the real time analysis of the signals is not practical as during automatic checkouts.

Some of the support equipment required during tests is shown in the racks. These are a few most often required, however it is expected that other equipment like signal generators, distortion analysers, vector voltmeter etc. will be available as required.

16.5 MECHANICAL GROUND SUPPORT EQUIPMENT (MGSE)

16.5.1 Summary

The mechanical ground support equipment (MGSE) provides the capability for (1) lifting, holding, positioning, aligning, and protecting the spacecraft and subassemblies during assembly and test; (2) simulation and measurement during mechanical tests; (3) transporting the spacecraft and its subassemblies during assembly and test; (4) supplying gases and liquids to the spacecraft. It is noted that MGSE is defined to include only those items of subsystem MGSE, e.g., propellant loading equipment, that are required for system assembly and checkout. The subsystem level equipment that is peculiar to individual subsystem development, test and fabrication, e.g., black box vibration fixture, is included in the individual subsystem design and development equipment. The MGSE equipment described herein supports the integration operations, the system level environmental tests at the shipment to the launch site and the launch cycle up to and including mating to the launch vehicle. Design verification testing, i.e., structural and thermal model testing, are supported by the MGSE.

16.5.2 Equipment Use

This section identifies and describes the use of the MGSE. For convenience, the equipment has been categorized into the following groups:

- Propellant and Pressurization Unit - This equipment is provided to supply fluids and gases to the spacecraft P and O subsystems; flush, purge, and dry the spacecraft.

- Lifting and Handling Equipment - This equipment includes all handling dollies, hoisting slings, handling fixtures, and protective covers.

- Shipping Containers - This equipment consists of the items used in the transportation of the spacecraft (less antenna), antenna, solar arrays, and system test equipment between the various sites, and to the launch site.

- Measurement Equipment - Mechanical - This equipment includes the items required to verify weight, center of gravity and alignments on the spacecraft. In general, this equipment does not leave the contractor's facility.

- Environmental Test Equipment - This equipment includes the test fixtures, (e.g., thermal vacuum, vibration) required to support spacecraft level assembly and testing.

Table 16.3 summarizes the MGSE and the usage of the equipment planned for this program.

Table 16.3 List of MGSE and Use

MGSE No.	Item	Use
1	Propellant and Pressurization Loading Unit	Required for in-plant (TRW) and at the launch site to check out the positioning and orientation propulsion subsystem; to fill, bleed and drain the subsystem of N_2H_4 and GN_2.
	Lifting and Handling Equipment	
2	Spacecraft Handling Dolly	Used to transport spacecraft.
3	Spacecraft Handling Ring and Sling	Used to lift and rotate the spacecraft; the handling ring interfaces with the spacecraft platform.
4	Spacecraft Rotation Fixture	Used in conjunction with the spacecraft handling ring to pick up the spacecraft and rotate it end over end. Rotations are required for apogee motor installation, mass property measurements and the thermal vacuum test.
5	Spacecraft Aft Adapter	Interfaces between the spacecraft separation interface and various test fixtures, e.g., spacecraft shipping container, spacecraft handling dolly, balance adapter.
6	Spacecraft Ring Clamp	Used to clamp the spacecraft at the separation interface to the spacecraft aft adapter.
7	Apogee Motor Dolly	Used to support and transport the apogee motor.
8	Apogee Motor Hoist Sling	Attaches to the apogee motor flange for hoisting and installing the motor into the spacecraft.
9	Solar Array Protective Covers	Form protective shells for individual solar array panels; attached to the solar array substrate through inserts. Two sets of covers are transparent for test purposes. Since plastic covers may cause static electricity, two sets of metal covers are required.

Table 16.3 List of MGSE and Use (Continued)

MGSE No.	Item	Use
	<u>Lifting and Handling Equipment</u>	
10	Propulsion Equipment Handling Fixture	Used to support the propulsion equipment, e.g., bottles, lines, thrusters, transducer, during installation onto the spacecraft structure.
	<u>Shipping Equipment</u>	
11	Spacecraft Shipping Container	Used to enclose, protect and transport the spacecraft (less antenna) between plant and to the launch site. The metal container will contain pressure relief valves, desicant bags for humidity control, and a 3 axis "g" level recorder.
12	Antenna Shipping Container	Same requirements as spacecraft shipping container.
13	Solar Array Shipping Container	Used to enclose, protect and ship the individual solar arrays with their protective covers. The container will contain pressure relief valves and desicant bags for humidity control.
14	MGSE and EGSE Shipping Containers	Used to enclose and protect system test equipment for shipment to the launch site.
	<u>Measurement Equipment</u>	
15	Spacecraft Weight and C. G. Fixture	Supports the spacecraft in a horizontal position and adapts it to a center-of-gravity determination machine. Roll moment of inertia is also measured during this test.
16	Spacecraft Dynamic Balance Fixture	Adapts the spacecraft to a dynamic balance machine.

Table 16.3 List of MGSE and Use (Continued)

MGSE No.	Item	Use
17	Spacecraft Inertia Measurement Fixture	Adapts the vertically oriented spacecraft to a roll inertia test fixture.
	<u>Measurement Equipment</u>	
18	Alignment Fixtures	The fixtures consist of devices to hold alignment targets, mirrors and support levels; adapt to the spacecraft components such as thruster nozzles, sensors and antennas.
	<u>Environmental Test Equipment</u>	
19	Thermal Vacuum Fixtures	Used to support and spin an inverted spacecraft at flight rpm during thermal vacuum tests in a 30' diameter chamber.
20	Spacecraft Vibration Fixture	Used to rigidly support and adapt the spacecraft to the vibration shaker.

II-17

CONTROL STATION

17. CONTROL STATION

17.1 INTRODUCTION

In this section we will very briefly discuss some of the requirements and practices necessary for operational control and maintenance of the spacecraft by ground personnel. A detailed discussion is beyond the scope of this study but we would hope that, when a detailed study is launched, it might be guided by the comments made in this section. We will also note that the communications requirements are not covered, since we are purely interested in command and telemetry.

17.2 GENERAL

Control stations will be defined as those earth stations in the satellite system grid which would be equipped with full telemetry, tracking and command capability. For security and operational control, the number of these stations would be limited. We should think that two stations would be sufficient: a main control station and a standby.

The control stations are required to perform the following tasks:

1) Track the spacecraft during all orbital manoeuvers

2) Receive and process all telemetry data

3) Orient the spacecraft into the correct position for the apogee motor firing

4) Command the spacecraft to fire the apogee motor

5) Track the spacecraft during the orbital drift period following apogee motor firing

6) Command the spacecraft to orient its axis parallel to the earth's axis

7) Command the spacecraft antenna to "lock-on" to the earth

8) Check the spacecraft "drift" when it is "on-station"

9) Control the spacecraft's operational set-up

10) Perform all station-keeping duties during the operational lifetime of the spacecraft.

We may assume that, for reasons of sovereignty and national pride, control from a Canadian Earth Station is most desirable. At present, the only operational Canadian Earth Station is at Mill Village, Nova Scotia. This station is equipped with an 85 foot fully steerable parabolic antenna 4 GHz and 6 GHz communications capability and 4 GHz tracking capability. It is not equipped with command or 136 MHz tracking capability. A second 97 foot parabolic antenna structure is under construction and will shortly be commissioned into service.

17.3 POLARIZATION CONSIDERATIONS

We have visualized that, for a simplified spacecraft telemetry and command antenna structure, the RF emissions would be linearly polarized. However, because of the trajectories during the elliptical transfer orbit and the requirement for spacecraft orientations prior to and after apogee motor ignition, the sense of polarization as seen by an earth-based antenna would be variable. Thus the earth station antenna must be able to either vary the polarization angle of the feed, or be circularly polarized.

If the 3 dB polarization loss can be tolerated, the reception of linearly polarized signals using circularly polarized feeds is operationally simpler than alignments of polarization. Mill Village, with an 85' antenna and a system noise temperature of about 65°K (dry weather) is more than 7 dB better in performance than the assumed parameters in this study, therefore circular polarization of this earth station would be a practical and therefore preferred characteristic during the initial orbital manoeuvers.

However, when the spacecraft is oriented N-S in anticipation of operational use then the polarization variability disappears. The signals will always be linearly polarized essentially in a N-S direction. It would then be convenient to convert the feed to linear operation.

The communications signals are also linearly polarized but may have polarizations in the E-W direction.* Therefore we have the prospect of crossed polarization between telemetry and command signals on the one hand, and communications signal on the other. The ability to receive and transmit such combinations of signals places a heavy burden on feed design, but permits complete flexibility in channeling and system utilizations. We should therefore suggest that the control station include such polarization capability.

* This depends on channeling plans and the possible use of either N-S or E-W polarization. We assume the most pessimistic conditions here.

17.4 MILL VILLAGE EXPANSION

Equipping Mill Village for control service in the Domestic SatelliteSystem should not be a particularly difficult task, providing satisfactory scheduling arrangements between the requirements of the Domestic System and the International Service could be worked out. Since communications capabilities would not be required during the initial orbit manoeuvers (except, perhaps, for test) the 4 GHz and 6 GHz communications equipment would be available for control usage. **

However, the command signal generating and modulating equipment, the telemetry processing and demodulation signal would need to be added, and the feed system would have to be modified.

136 MHz tracking signal reception could be provided by a modification of the feed in the antenna, or even by addition of a separate telemetry antenna (9 element Yagi, say). Alternatively, arrangements may be made with NASA to obtain tracking data from their Minitrack or Stadan network to the precision necessary for aquisition by the 4 GHz telemetry system. Further discussion of this latter possibility is beyond the scope of this report as it would involve governmental negotiations and so forth. It is sufficient to acknowledge the possibility that it could be done.

In line with the comments on polarization the feed might have to be modified to provide crossed polarization capability, but this depends upon whether both communications and control service are required simultaneously.

17.5 TRACKING

The 4 GHz tracking equipment is more closely related to antenna control and drive systems than to telemetry except that the tracking receiver and the telemetry receiver are usually one and the same. This is because the tracking signal is actually the carrier component of the telemetry signal.

** However, it may be necessary to add oscillators, filters, and so forth to enable operation at the new carrier frequencies.

We would assume that the tracking requirements for the control station would be conventional,having probably the following modes:

a) manual
b) autotrack (monopulse system)
c) programmed track (computer control)

Since the specific requirements and equipments for providing these modes are heavily dependent upon the antenna system used and the operational requirements of the system we will not discuss them in detail here. Rather, they would be covered in earth station study portions.

However we might note that for autotrack, a sun channel and two error channel receiving systems would have to be provided. Each receiver channel would consist of a 4 GHz to 136 MHz down-converter, and a telemetry receiver. The error signals (azimuth and elevation) would be either used as the autotrack control signal, or would be fed to the computer for analysis and, if required, updating of programmed track prediction data.

For 136 MHz tracking, the received 136 MHz signals can be directly connected to the receiver,bypassing the 4 GHz to 136 MHz down converter.

17.6 OTHER STATIONS

At least one other station besides Mill Village with control capability is envisioned. This station may be assumed to have the same operating characteristics as the modified Mill Village station. Its location could be either near the major population cities of Montreal and Toronto or could be farther west, say in British Columbia. A far west station has the advantage that control capabilities could exist over a much larger range of longitudes and would greatly simplify command problems during apogee motor firing.

However, regardless of actual location, we can still define the requirements and the operational philosophy for the station.

17.7 OPERATING REQUIREMENTS

If the ground station is to provide an efficient data processing system it should be capable of performing the following tasks.

a) Generating, transmitting and verifying the spacecraft commands.

b) Receiving, demodulating, processing and displaying PCM telemetry data necessary for monitoring subsystem operational status and spacecraft performance parameters.

c) Performing station readiness tests, and station calibration using a spacecraft simulator.

d) Providing the necessary data to the computer, to allow computation and analysis of the spacecraft parameters and generation of commands necessary for in-orbit attitude control and antenna control functions.

17.8 OPERATIONAL PHILOSOPHY

The support and the operational requirements impose a ground station operational philosophy. We will broadly categorize the ground station operations in three modes and then the equipment required to perform these operational modes in the most efficient manner.

a) Normal Mode

This mode occurs when all the equipment is calibrated and is functioning normally. In general a prepared routine is followed.

After initial aquisition the data quality is assessed and logged, prepared commands are executed, and telemetry processing is accomplished confirming the normal operation of the spacecraft.

This mode will include the operations required to conserve battery power or change to alternate spacecraft configurations.

b) Emergency Mode

This occurs when the critical parameters are out of limit. This may dictate special data analysis, orbital manoeuver commands, the attitude and antenna pointing data analysis. Subsystem performance analysis will usually require analysis of spacecraft response to special commands.

This mode requires that the ground station equipment be flexible and capable of both automatic and manual control.

c) Test Mode

Periodic ground station equipment and system tests must be performed to assure operational readiness and calibration check. These tests will be scheduled on the non-interference basis with the normal mode operations, hence spacecraft signal simulators will need to be provided.

17.8 EQUIPMENT DESCRIPTION

A typical block diagram of the command and telemetry link associated with the spacecraft signal simulator is shown in Figure 17-1. The equipment discussion is divided into the command link, telemetry link, computer, spacecraft simulator and display sections.

a) Command Link

The command link, as the title suggests, will be capable of commanding the spacecraft in the required mode. The command generator will provide the required tone sequence and the format,' either automatically controlled by the computer or manually controlled by the operator. The command signal will frequency modulate a carrier in the V.H.F. band. When required, together with the command tones the modulator will also accept the ranging tones and the artificial earth pulses. The modulated carrier will be up converted in the 6 GHz band and amplified to the required power. The minimum power requirements are discussed in section 3.2.10.

The patch panels provided at the critical stages are to facilitate monitoring and calibration.

b) Telemetry Link

The signal received from the spacecraft is amplified and down converted to 136 MHz band; this allows the use of standard receivers. The demodulated output is processed in the following four ways.

1) Bit synchronizer and format synchronizer cleans up the PCM signal and generates the clocking signal required to distinguish the various channels. The data is supplied to computer and to spacecraft display board.

2) The sensor signal processing assembly recognizes the two earth sensor pulses, antenna sensor pulse and the sun sensor pulse. These sensor pulses determine the attitude of the spacecraft which is displayed on the spacecraft display board. Also the information is supplied to the computer where the requirement of artificial pulses and attitude correction are calculated.

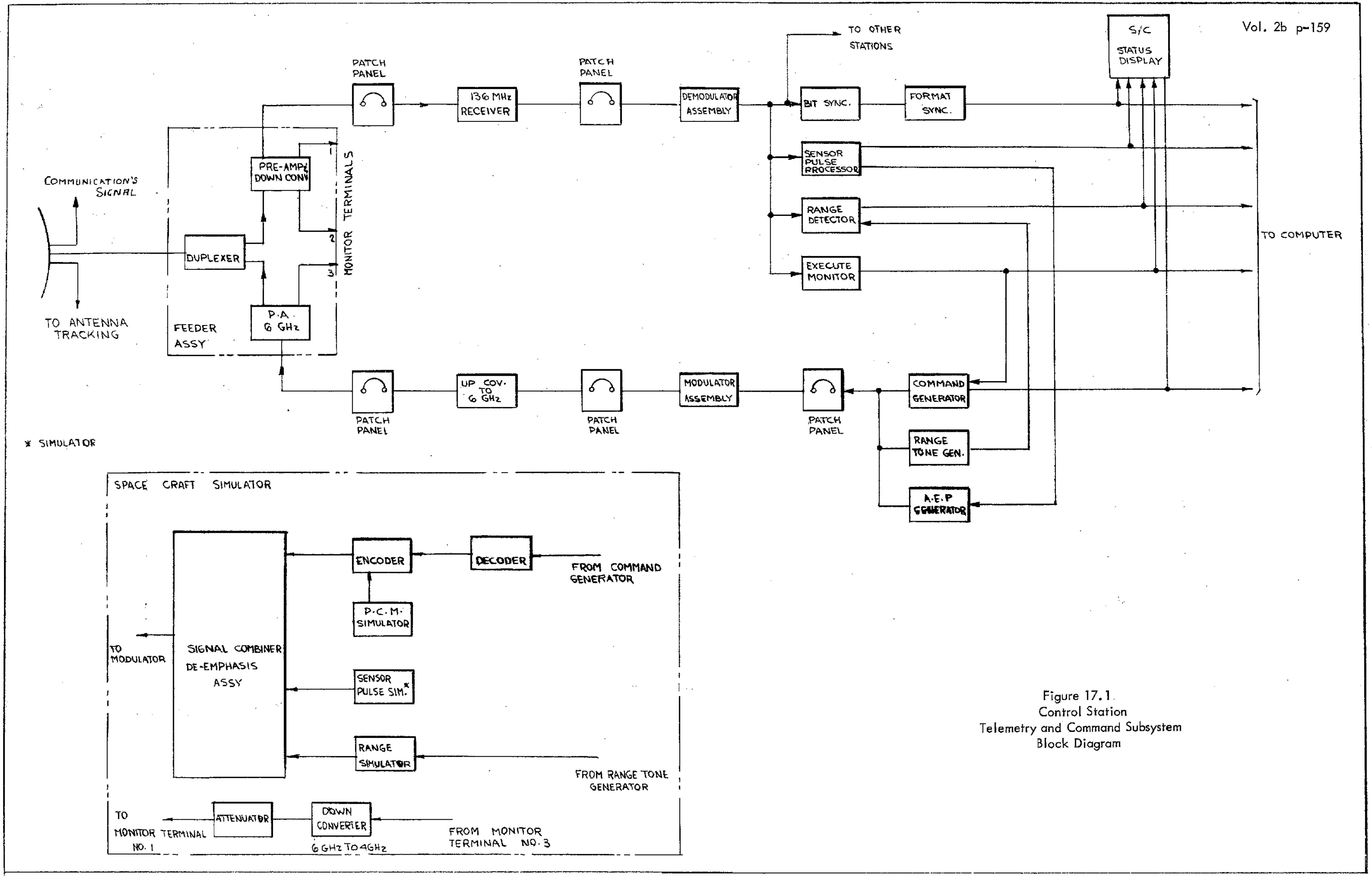

Figure 17.1
Control Station
Telemetry and Command Subsystem
Block Diagram

3) Range detector recognizes the four tones available in the base band and compares their phase with that of tones generated on the ground. Thus the range of the spacecraft is electronically computed, and the information is supplied to the computer and the spacecraft status display board.

4) The execute monitor tone is required for command verification. The signal allows the computer to initiate the next command in automatic mode and in the manual mode the signal is supplied directly to the command generator, resetting it to generate the next command.

c) The Computer

In the previous discussions we have made numerous references to the computer. In fact we have assigned to the computer the task of:

a) reducing all telemetered data

b) preparing orbital predictions

c) possible actual command of the spacecraft

d) predicting the amount and timing of station keeping correcting manoeuvers

e) updating status board

f) issuing warnings that out of tolerance conditions exist.

and many others. The extent to which these tasks are to be performed, and the general station operational philosophy have a particularly direct bearing on the required capabilities of the computer. Thus we cannot at this point specify the computer requirements. To do so would require much further research into operational requirements, programming and so forth, with respect to overall requirements.

d) Spacecraft Simulator

This facility will be required for ground station equipment and system tests and calibration. It will have the facility to simulate spacecraft, range, attitude and the PCM data. The simulated data will be fed to the modulator in the command link,and the output of the power amplifier instead of being transmitted will be converted to 4 GHz band and fed to the telemetry link. Thus the complete command and telemetry link can be tested and calibrated, independent of the spacecraft.

17.9 A SUGGESTION FOR CONSOLES AND STATUS DISPLAYS

The arrangement of equipment racks, consoles and displays in the control room of an earth station should be carefully considered using the principles of human engineering. Care should be taken to provide reasonable central control, adequate and easily visible monitor systems, and comfortable and clean surroundings. Careful attention to creature comforts can greatly reduce the possibility of operator error and its consequences.

The operating consoles should form a central location where antenna motion, communications and television monitoring, and command and telemetry activities can be properly controlled by one or perhaps two operators. Meters, monitors and controls should be selected in accordance with good human engineering practices.

In front of the consoles, we suggest would be several large status boards, one for each spacecraft and properly identified in accordance with the spacecraft address. We further suggest that the spacecraft status be shown in the form of a functional flow chart similar to those used in generating plants. The flow lines would be illuminated in accordance with the spacecraft status.

A color code for illumination is helpful. For example, we may establish that

a) no illumination means no connection

b) amber means that an instruction command has been sent but not executed

c) green means that the execution of a command has been verified by flag status

d) red means that a warning, that a particular subsystem is operating out of specification, has been sounded (via telemetry, or from the computer).

Thus, a complete set of green flow lines would show the signal path.

Each status board would be updated by the received telemetry data from the spacecraft which, for flags, means an update every 4 seconds. The spacecraft signature would automatically determine which status board to update. No updating would occur unless the spacecraft signature were properly received, and in the absence of signals, a memory in the status board would "remember" the last status report, unless manually cancelled.